

The application of magnetic moulding in casting of a ductile iron valve

E. Burger

 [orcid.org 0000-0002-6292-3383](https://orcid.org/0000-0002-6292-3383)

Dissertation submitted in partial fulfilment of the requirements
for the degree *Master of Engineering in Mechanical Engineering*
at the North-West University

Supervisor:

Prof J.A. Markgraaff

Graduation May 2018

Student number: 23375167

The application of magnetic moulding in casting of a ductile iron valve

Dissertation submitted in partial fulfilment of the requirements for the degree
Master of Engineering in Mechanical Engineering at the Potchefstroom campus of
the
North-West University

E. Burger

0000-0002-6292-3383

Supervisor: Prof. J.A. Markgraaff

November 2017

Declaration

I, Elizabeth Burger hereby declare that the dissertation entitled “The application of magnetic moulding in casting of a ductile iron valve” is my own original work and has not been submitted to any other university or institution for examination.



E. Burger

Student number: 23375167

Signed on the 20th day of November 2017 at Potchefstroom.

Acknowledgements

I want to thank the following members of the industry and academia for their generous contribution to this research project. Their experienced input, time and support made it possible to succeed.

- Mr. Paul Burger [Burg Refractories]
- Mr. Giep van Eck [High Temperature Engineering]
- Prof. Jan de Kock [NWU Faculty of Electrical Engineering]
- Mr. Wikus Williams [LH Marthinusen]
- Mr. Pierre Rossouw [CSIR Material Science and Manufacturing]
- Mr. Andrew Mc Farlane [Ametex]
- Prof. Deon de Beer [NWU Technology Transfer and Innovation Support]
- Mr. CP Kloppers [NWU Faculty of Mechanical Engineering]
- Mr. David Mauchline [VUT Department of Additive Manufacturing]

My study leaders, Prof. Markgraaff and Dr. Grobler, thank you for your time, guidance and shared knowledge. My parents, Piet and Amanda, your support, advice and prayers carried me to new heights. Quinton van Riet, your patience and support extends beyond measure and I am very grateful.

I thank God for his never ending grace and guidance.

Abstract

Impeding problems experienced in the valve manufacturing industry has resulted in the cost of locally manufactured valves to be up to 60% more expensive than imported products. The overall cost of manufactured products may be reduced by increasing the efficiency of manufacturing methods.

A review and investigation of various manufacturing methods have led to the selection of the magnetic moulding process for further investigation. It was determined that due to the traditional mould materials used for the casting of cast irons, variation and control of the microstructure, determined by cooling rate, is limited. If the thermal conductivity of the mould material can be varied or controlled, substantial microstructural variation becomes possible that can substantially improve the strength of the cast product and lower the overall cost of local valve manufacturing.

The feasibility of the magnetic moulding process on the casting of a ductile iron valve was tested by implementing this casting method. A casting was performed with an additive manufactured PMMA pattern and due to inconclusive results, a wire-cut EPS pattern with a square geometry was cast successfully with this method. The results of both castings were analysed by means of microstructural inspection and the testing of mechanical properties.

Ultimately, it was concluded that the magnetic moulding casting process is a feasible manufacturing method with the potential to increase the affordability of locally manufactured valves if a low-density pattern material, such as EPS, is used. Additionally, it is a viable method that offers a vast amount of opportunities to vary the microstructural properties of cast iron if it is to be further implemented in valve casting.

Keywords: *Magnetic Moulding, Ductile Iron, Valves*

Contents

List of Figures	viii
List of Tables	xiii
List of Acronyms	xv
List of Symbols & Subscripts	xvii
1 Introduction	1
1.1 Background	1
1.2 Problem Statement	5
1.3 Aim	5
2 Literature Study	6
2.1 Valves and Valve Material Selection	6
2.2 Cast Irons	11
2.2.1 Grey Iron	13
2.2.2 Ductile Iron	16
2.3 Valve Manufacturing Methods	19
2.3.1 Forging	19
2.3.2 Casting	22

2.4	Summary	36
3	Magnetic Moulding	38
3.1	Pattern Making	38
3.1.1	EPS	40
3.1.2	PMMA	41
3.1.3	PLA and ABS	42
3.2	Refractory Coating of the Pattern	43
3.3	Mould Making	46
3.4	Electromagnet Configuration	52
3.5	Scope	54
4	Magnetic Moulding Casting Process	55
4.1	Configuration and Setup	55
4.1.1	Pattern Selection	56
4.1.2	Mould Material and Electromagnet	59
4.1.3	Feeding System Design	71
4.1.4	Auxiliaries	83
4.1.5	Refractory Coating	84
4.1.6	Casting Material	87
4.2	Assembly of Components	88
4.3	Casting Procedure	94
5	Results and Evaluation	107
5.1	Evaluation of PMMA Pattern Casting Results	107
5.1.1	Sample 1: From Feeder	107
5.1.2	Sample 2: From Sprue	109

5.1.3	Sample 3: From cast metal in contact with Steel Shot	111
5.1.4	Summary	112
5.2	Evaluation of EPS Pattern Casting Results	115
5.2.1	Microstructure	115
5.2.2	Tensile-Tests	117
5.2.3	Charpy V-Notch Tests	118
5.2.4	Hardness	120
5.2.5	Summary	121
6	Summary, Conclusion and Recommendations	123
6.1	Summary	123
6.2	Conclusion	124
6.3	Recommendations	127
	Bibliography	129
	Appendices	
A	Cast Irons	134
B	Electromagnet Drawings	136
C	Steel Shot Characteristics	137
D	Safety	142

List of Figures

1.1	The contribution of various aspects to the overall expenses of foundries in South Africa as determined by <i>Davies</i> [2] in 2015	4
2.1	Sketch of a typical valve assembly	7
2.2	South African valves and actuator market by consumption in 2008 [8] . .	9
2.3	The compared cost of valve materials per kilogram	11
2.4	Demonstration: forging of hot metal billet in the hot-die forging process	19
2.5	Illustration of a sand mould assembly and the casting components . . .	26
2.6	Photo of additive manufactured sand mould half	28
2.7	Illustration of the shell moulding process	29
2.8	Illustration of the investment casting process	31
2.9	Illustration of the lost-foam casting process	34
3.1	Chemical structures of a) PMMA and b) Polystyrene (EPS)	41
3.2	Image of 3D-printed ABS stop valve halves as printed by <i>Olkhovic et al.</i> .	43
3.3	Illustration of the permeability of the coating during the gasification of the foam pattern	44
3.4	Histogram of the occurrence of the coordination number of steel shot spheres obtained from boroscope images by <i>Suganth kumara et al.</i> [26] . .	47
3.5	Histogram of the influence of sphere size on the strength of magnetic mould as studied by <i>Suganth kumara et al.</i> [26]	48

3.6	Solidification curves of different moulds as experimentally determined by Geffroy <i>et al.</i> [24]	48
3.7	The difference in microstructure of ductile iron between a sand mould and a steel shot mould as obtained by Geffroy <i>et al.</i> [24]	50
3.8	Simulation of the distribution of force between steel shot spheres in magnetic moulding and the force between sand grains in lost-foam casting, compared by Goni <i>et al.</i> Better cohesion is obtained with the magnetic steel shot mould.	51
3.9	Castings performed with steel shot as mould material with the magnetic field on and off. A decrease in shrinkage is observed in the casting with the magnetic field on [25]	52
3.10	Direction of magnetic field in U-shaped and solenoid electromagnet . . .	53
4.1	The magnetic moulding casting assembly as modelled in SolidWorks . .	56
4.2	Model of the valve assembly	57
4.3	Illustration of scaling of the valve body to 40% of the original size	58
4.4	A typical magnetisation curve for a ferromagnetic material indicating the knee of the curve	63
4.5	Pattern geometry and parameters kept constant for orientation and position simulations	65
4.6	Illustrations of pattern orientations not suitable to simulate in FEMM . .	66
4.7	Illustrations of pattern orientations suitable for FEMM simulations . . .	66
4.8	Pattern positions and flux densities in specified areas obtained by FEMM simulations	68
4.9	Low flux densities and saturation in original model of electromagnet in a FEMM simulation	69
4.10	Various geometry concepts for the effective use of material and to limit saturation in sharp inside corners as simulated in FEMM	69
4.11	Flux densities at various points of final FEMM simulation model	71
4.12	Model of concept designs of the feeding system	73
4.13	Model of the final design of the feeding system	77

4.14	Model of the feeder/pouring cup	77
4.15	MAGMASoft® casting simulation indicating the temperature distribution during casting of the molten metal	79
4.16	MAGMASoft® casting simulation indicating the flow of the tracer elements in the casting and the age of the particle in an area of the casting	79
4.17	MAGMASoft® casting simulation indicating the areas of expected porosity	80
4.18	MAGMASoft® casting simulation indicating the areas of expected hot spots	81
4.19	Model of the alumina shot cover	83
4.20	Model of the alumina electromagnet stand	84
4.21	Photos of the comparison between supplier mullite products in a) the refractory slurry and b) 2 layers of refractory coating applied to a 3D-printed sample	85
4.22	Photo of the coating suspension containing only mullite and colloidal silica indicating the high viscosity of the 3g/cm ³	86
4.23	A photo of the assembly of the magnetic moulding setup	88
4.24	Equipment used to wind the coil of the electromagnet	89
4.25	Line graph of the flux density measured as the current of the electromagnet is increased	91
4.26	The additive manufactured PMMA valve body pattern showing the feeding system mounting points and surface finish of the material	92
4.27	The magnetic moulding casting procedure as modeled in SolidWorks	95
4.28	The complete PMMA pattern with ceramic feeding system attached	96
4.29	A top view of the feeders, after molten metal was cast	97
4.30	A photo of the PMMA pattern after casting was performed	99
4.31	The PMMA pattern after casting, indicating the carbon residue due to the degradation of the PMMA.	100
4.32	The result of the casting with the PMMA pattern indicating the part of the top flange that was cast	100

4.33	The cast part after removal of the feeder and sprue, from different views, indicating the positions of the sample areas	101
4.34	The hollowed out EPS pattern halves and the combined, glued pattern	102
4.35	The wet, refractory coated EPS pattern before the final layer was applied	102
4.36	The casting of ductile iron with the EPS pattern resulting in flames during the pyrolysis of the pattern	103
4.37	The cast part obtained with magnetic moulding, with the refractory coating still in place	104
4.38	The cast part after the removal of the refractory coating	104
4.39	The cast part with the feeder and sprue removed and sectioned in two halves	105
4.40	Photo of the inner layer of the refractory coating after casting indicating carbon residue due to pyrolysis of the EPS pattern	106
4.41	The impurities observed in the casting due to entrapment	106
5.1	Microstructure of Sample 1 under different magnifications indicating the difference between no treatment and etching with 2% nital	108
5.2	Microstructure of Sample 1 indicating ferrite and graphite structures	109
5.3	Microstructure of Sample 2 under different magnifications indicating the difference between no treatment and etching with 2% nital	110
5.4	Microstructure of Sample 3 under different magnifications and treatments indicating the difference between no treatment and etching with 2% nital	111
5.5	Micrograph indicating the microstructure of Sample 3 with steel shot spheres impregnated in cast metal	112
5.6	Microstructure of a material sample obtained from casting with EPS pattern, under different magnifications indicating the difference between no treatment and etching with 2% nital	116
5.7	A line graph of the tensile strength versus the elongation of five tensile test specimens	117
5.8	Photo of the test specimens after tension tests were performed	118

5.9	Charpy V-notch impact energy absorbed by ductile iron specimens with different matrix structures.	119
5.10	The brittle fracture surface of the fracture test performed on the material sample of the casting performed with the EPS pattern	120
5.11	The fractured specimen indicating the line of fracture	120
A.1	Specifications and characteristics associated with cast irons	135
B.1	Dimensions (in mm) and materials used in the final electromagnet FEMM design	136
C.1	Position of teflon cup placed in steel shot	137

List of Tables

1.1	The decrease in South African foundries over 13 years as determined by <i>Davies</i> [2] in 2015	2
2.1	Considerations for the selection of valves based on the valve fluid	8
2.2	Typical valve materials and their applications	10
2.3	Range of compositions for common cast irons	13
2.4	Grey cast iron flake size and associated mechanical properties	15
2.5	Mechanical properties of grey cast iron and ductile iron compared	15
2.6	Maximum acceptable limits for minor elements in ductile iron	17
2.7	Summary of various forging processes and their limitations and advantages	21
2.8	Casting processes and their limitations and advantages as described by <i>Kalpakjian</i> and <i>Schmid</i> [19]	22
3.1	Percentage composition of various ceramic coatings used in the lost-foam casting process	45
3.2	Thermal properties and solidification times of various moulds obtained by <i>Geffroy et al.</i> [24]	49
3.3	Mechanical properties of ductile iron castings obtained with a steel shot mould and a sand mould as determined by <i>Geffroy et al.</i>	50
4.1	Comparison of the average pattern material properties	59
4.2	Chemical composition of the selected steel shot and AISI 1095 steel	59

4.3	Parameter values used in the FEMM simulations to obtain satisfying design results	71
4.4	Values and descriptions of parameters used in Equation 4.25 to 4.20 . . .	82
4.5	Percentage composition of refractory coating selected for the application of magnetic moulding	84
4.6	Mechanical properties of ASTM A395 60-40-18 ductile iron	87
4.7	Flux densities measured in the middle of a fully filled casting box at a depth of 90mm at increasing currents	90
4.8	The calculated weight contribution of raw materials, in the melt required to obtain ASTM A395 Grade 60-40-18 ductile iron	93
4.9	The chemical composition of ideal ASTM A395 Grade 60-40-18 ductile iron compared to the actual composition of the raw materials, as determined by the developed material analysis Excel program	94
5.1	The tensile strength of five tension test specimens obtained from the casting with the EPS pattern	117

List of Acronyms

NFTN National Foundry Technology Network

DTI Department of Trade and Industry

SOC State-owned Company

VAMCOSA Valve and Actuator Manufacturers Cluster of South Africa

CE Carbon Equivalent

AFS American Foundry Society

EPS Expanded Polystyrene

CNC Computer Numerical Control

STMMA Styrene-Methyl Methacrylate co-polymer

PMMA Poly Methyl Methacrylate

PLA Polylactic Acid

ABS Acrylonitrile Butadiene Styrene

SPG Specific Grain Number

FCC Face Centered Cubic

CFD Computational Flow Dynamics

mmf magnetomotive force

CAD Computer Aided Design

FEMM Finite Element Method Magnetics

ADI Austempered Ductile Iron

AM Additive Manufacturing

VUT Vaal University of Technology

MMC Metal-Matrix Composites

CSIR Council for Scientific and Industrial Research

PPE Personal Protective Equipment

List of Symbols & Subscripts

List of Symbols

CE	Carbon Equivalent
C	Carbon
Si	Silicon
P	Phosphorus
H	Magnetic field
n	Turns
I	Current
l	Length of coil
μ	Magnetic permeability
B	Flux Density
T	Tesla
M	Magnetisation
x	Magnetic Susceptibility
V	Liquid metal volume
W	Weight of metal to be poured
ρ	Density of metal to be poured
t	Pouring time
S	Wall thickness coefficient
F	Average filling rate
A	Choke area
g	Gravitational acceleration

d Distance

h Height

List of Subscripts

0 Vacuum

r Relative

ma Magnetic

p Pressure

s Sprue

1 One

2 Two

d Discharge

Chapter 1

Introduction

The rationale of the research topic is discussed in this introductory chapter. Background on the current status of valve manufacturing and impeding factors experienced in the foundry industry are briefly discussed. The background leads to the problem statement and the aim of the research presented in this study.

1.1 Background

South African foundries have been under remarkable pressure over the past 27 years. In 1980 local foundries totalled 450 [1]. Today, the South African foundry industry consists of 170 foundries since 100 foundries closed down as of 2003 [2] as shown in Table 1.1. The decrease in valve manufacturers in South Africa is directly related to the reduction in foundries.

Table 1.1: The decrease in South African foundries over 13 years as determined by Davies[2] in 2015

Province	Number of Foundries		
	2003	2007	2015
Gauteng	143	141	114
Kwa-Zulu Natal	26	25	20
Western Cape	33	32	14
Eastern Cape	20	20	8
Free-State	13	13	5
North-West	13	13	4
Northern Cape	7	6	3
Mpumalanga	15	15	2
TOTAL	270	265	170

There are approximately 24 valve manufacturers in South Africa. Additional supply to the local valve market is through a further 60 importers through resellers [3]. The factors contributing to the contraction of the valve manufacturing industry forms the foundation of various attempts to promote the regrowth of the industry.

Inefficient energy supply and a constant increase in electricity costs have a significant impact on the competitiveness of local manufacturing [4]. In 2012 the National Foundry Technology Network (NFTN) listed seven foundries that closed down with electricity cost hikes being the main cause [5]. Studies on the energy consumption of foundries indicate that 70 % of electrical energy is consumed in the melting division [6], which involves the melting of mainly scrap metal [4].

Scrap metal pricing is a conflicting subject between the scrap metal industry and foundries. Encouraging exchange rates and high foreign demand motivates high scrap metal prices. The conflict exists due to the fact that the government directive to offer a 20% discount to local foundries and secondary smelters is not implemented [7]. Scrap metal is sold at the same high price to local foundries as it is sold abroad. It is a matter of localisation, which is a major challenge on its own.

The factors mentioned in the preceding paragraphs, contribute to the fact that locally manufactured valves are between 10% and 30 % more expensive than imported prod-

ucts [8]. Merchantec Capital (Pty) Ltd performed industry research for the Department of Trade and Industry (DTI) and claims a difference of up to 60% between local and imported valves, where local valves are more expensive [3].

The mining industry is the largest local customer group. The rest of the valve and actuator market in South Africa consists of state-owned enterprises such as Eskom and Transnet, municipalities and water boards [4]. Existing Eskom power plants are estimated to increase the demand for valves in the next few years as more than 5500 valves need to be replaced in ongoing operations and maintenance projects [9].

In 2013 the total South African valve market revenue was around R4.15 billion, of which R2.7 billion pertained to imported products [4]. There is also a perception in the local market that imported valves are of higher quality [8], despite the fact that numerous valve manufacturing companies have been exporting locally manufactured valves for years [5].

In March 2014, the DTI required that 70% of all valves used by State-owned Company (SOC) be locally manufactured [5] [10]. As a result of the designation, the Valve and Actuator Manufacturers Cluster of South Africa (VAMCOSA) was established and local valve manufacturing companies are now competing with international producers, quality and standards.

The challenge that South African manufacturers now face is evident in the following facts. The average age of South African foundry furnaces is 25.5 years, where foundries in China and India are fairly new, with furnaces aged between 6 and 11 years. South African foundries are operational 242 days of the year, whilst China and India operate 300 days per annum. When the contribution of labour costs to the combined expenses of foundries are compared, South Africa has the highest labour costs when compared to China, India and Brazil [11].

Furthermore, Figure 1.1 indicates that our material costs and labour costs are the highest contributing factors to the typical combined cost of foundries. These factors, among various other factors, indicate why locally manufactured valves are more expensive

than imported valves.

**TYPICAL COMBINED COSTS OF SOUTH AFRICAN
FOUNDRIES**

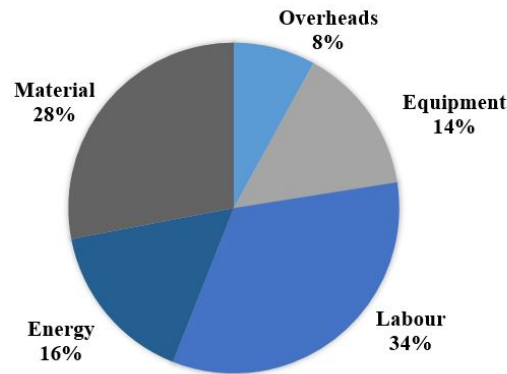


Figure 1.1: The contribution of various aspects to the overall expenses of foundries in South Africa as determined by *Davies*[2] in 2015

The affordability of locally manufactured valves is a key aspect demanding attention. Methods to lower the cost of locally manufactured valves are of great importance in order to utilise the opportunities in the valve manufacturing industry.

As a result, valve manufacturing processes are placed under scrutiny to find methods to use less material, increase the efficiency of production and improve manufacturing techniques to lower the cost of locally manufactured valves.

In 2013, 61.4% of all castings in South Africa were cast iron products. Ductile cast iron contributes to 12% of these castings [12]. The second largest end use of ductile iron is for pressurised water and wastewater systems, which includes valves [13]. Ductile iron is a favourable valve material due to its mechanical properties, castability and low cost. Therefore it is sensible to investigate processing methods of ductile iron for the application of valve production as it will contribute to the affordability of local valves.

1.2 Problem Statement

The problem is that foundries in South Africa are not functioning optimally which results in the high cost of locally manufactured valves. It is a collective problem consisting of high scrap metal prices, inefficient energy supply at increasing costs, government directives that are not implemented and manufacturing methods that are not optimised. The manufacturing method is the only factor local valve manufacturers have control over and holds the key to affordable local products.

If foundries were to implement technologies and strategies that use less material, less energy and increase production volume, the overall production cost of products will significantly decrease, resulting in a decrease in the cost of locally manufactured valves.

1.3 Aim

Firstly, to review and investigate manufacturing methods that can positively enhance both the process steps and produce higher quality valves at lower costs. Secondly, to select a manufacturing method and determine the feasibility of the selected processing method.

Chapter 2

Literature Study

Literature on aspects that are associated with the problem statement is addressed within this chapter. Essential information on valves and valve material selection leads to a discussion of cast irons. There is an evident focus on valve manufacturing and more specifically, the manufacturing of valve bodies. Finally, a manufacturing method is selected within the conclusion of the literature study performed.

2.1 Valves and Valve Material Selection

Processing plants rely on a vast selection of mechanical equipment to transport and regulate product under controlled conditions [14]. Valves are one of the basic, yet significant elements contributing to the effective transportation of products in processing plants, daily life and numerous industries.

In its most basic definition, valves are mechanical devices that regulate, control and/or direct the flow of fluids [14]. A wide variety of valve types exist, but the most common types of valves are check, ball, gate, globe and butterfly valves. Detailed literature on

the specific design of the various valve types and the components that a typical valve consists of is not within the scope of this study.

The valve body is the main element of a valve assembly and the primary boundary of a pressure valve [15]. The valve body is equipped with flanges that allow piping to be connected to the valve. Valve bodies are cast or forged in various forms and materials, depending on the specific function of the valve.

For the purpose of this study, the valve body is isolated from the rest of the valve assembly due to the importance and significant influence of the valve body on the design and manufacturing of the overall valve. A sketch of a typical valve and its basic components is shown in Figure 2.1. The valve body is indicated in the sketch.

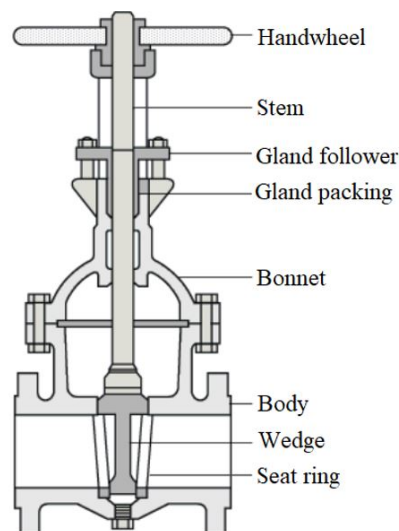


Figure 2.1: Sketch of a typical valve assembly

The variety of valve types emerges from the vast amount of applications of valves. The type of fluid that passes through the valve significantly impacts the choice of valve design as well as the valve material selection. In Table 2.1, considerations associated with the valve fluid is tabulated. It can be observed that the selection of the valve material and valve design choice may be very complex depending on the fluid [14].

Table 2.1: Considerations for the selection of valves based on the valve fluid

Fluid	Type	Considerations
Water	Demineralised	Chemically active
	Fresh	pH Value Hardness of water Carbonic acid and carbonate equilibrium
	Brackish	Suspended solids Possible industrial waste contamination Micro-organisms
	Seawater	Temperature Seawater quality Corrosion
Oils	Produced	Temperature pH Calcium/Magnesium hardness Sodium Potassium Chlorides Suspended solids Dissolved gasses etc.
	Mineral Animal Vegetable	Cloud point Pour Point Solidifying point Viscosity
Liquid-solid Mixtures	Sewage Sludge	Pure Liquid Properties Size of solid particles Density of solid particles Shape, hardness and abrasiveness of solid particles Concentration of particles in solid
	Pulp	Pulp quality Air content Solid particle content Pressure drop Tendency to thicken in reducing sections Blockage characteristics

When the fluid is known and the considerations associated with the fluid are confined, the external operational environment should also be accounted for. Additional design and manufacturing requirements arise from factors such as exposure to vibrations, external temperatures, corrosive environments, etc. It is evident that the exact application and function of the valve should be known in order to select the most appropriate material, type of valve and therefore the appropriate manufacturing method.

The South African valves and actuator market is dominated by processing sectors such as the metals and mining, chemicals and petrochemicals sector [8]. The high percentage revenues in these sectors are based on the strict safety and efficiency demands of these specific sectors. Proportionally, the chart in Figure 2.2 is still relevant today. The chart represents the percentage revenue by the end-user market in the South African valves and actuator market of 2008 [8]. It is therefore meaningful to invest in technology to increase the affordability of valves in these specific sectors.

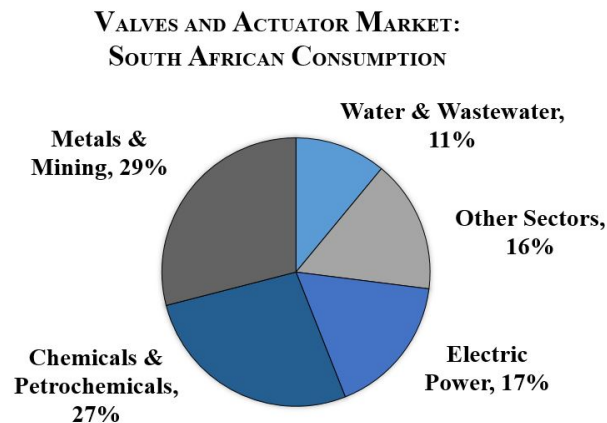


Figure 2.2: South African valves and actuator market by consumption in 2008 [8]

Finally, the cost is the determining factor that narrows down the selection of the material. Typical valve materials and their applications are shown in Table 2.2. A comparison of the average costs of these materials per kilogram is then shown in Figure 2.3. The costs were obtained using GRANTA CES EduPack, a material selection software program.

Table 2.2: Typical valve materials and their applications

Valve Material	Application
Grey cast iron	Low-pressure applications. The graphite film provides good corrosion protection as it is not damaged by high velocities, aeration, cavitation or erosion. Clean liquids and gasses.
Brass	Low-pressure clean non-corrosive gases.
High Tensile Steel	High-pressure applications with non-corrosive clean liquids and gases.
SG iron Nodular Iron Ductile Iron	Slightly higher pressure and temperatures than grey cast iron. Graphite film not as tough. Clean liquids and gasses.
11/13Cr Steel	De-aerated hot water up to 350°C. Non-oxidising gases up to 650 °C. A good replacement for carbon steel for applications over 200 °C; better thermal stability, higher pressure capabilities.
Ni-Resist iron	Hot NaOH, seawater, some acids, coke oven gas, coal tar, wet hydrogen sulphide, paper making, hydrocarbons with HCl and H ₂ S, sewage, low pressure steam.
Gunmetal, Bronze	Saltwater, seawater, brine and other moderately corrosive aqueous solutions. Aluminium bronze and nickel aluminium bronze better than tin bronze in seawater. Nickel aluminium bronze for high pressures.
Austenitic Stainless Steels	Hot water, hot gases. General corrosive applications at low to medium pressures up to high temperatures. Cyclic applications.
Higher Steel Alloys Nickel Alloys Titanium	Corrosive or oxidising applications with acids or high temperature/pressure. Chloride compounds or hot flue gases, paper making.
Non-metallic Materials	Acids, Alkalis, corrosive reagents and solvents at a low/moderate temperature and pressure. Can be resistant to erosion.

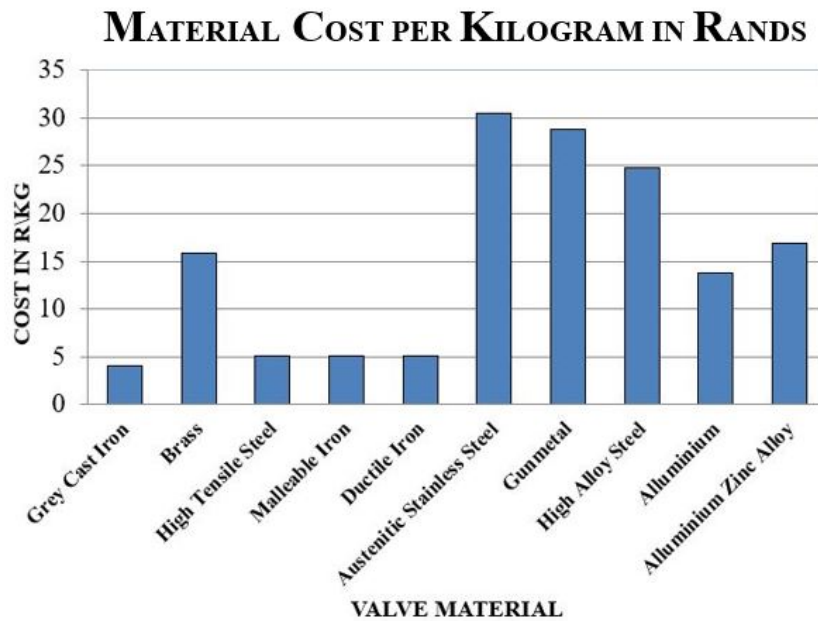


Figure 2.3: The compared cost of valve materials per kilogram

It can be observed in Figure 2.3 that cast irons, such as grey, ductile and malleable iron are significantly lower in costs when compared to other valve body materials. Based on affordability and other beneficial properties of cast irons, cast irons may be selected as the primary material to be investigated in more detail. The next section will focus on cast irons as valve body materials.

2.2 Cast Irons

Cast irons are iron alloys with a carbon content higher than 2%. Cast irons are known for their good castability as they have lower melting points, higher fluidity and are less reactive with mould materials than other casting materials such as steel [13]. There are five types of cast iron, namely white, malleable, grey, ductile and compacted graphite.

Unlike steels, cast irons are not designated based on the chemical composition because cast irons have very similar chemical compositions. The solubility of carbon in an iron-carbon alloy is limited to 2% within a single phase during solidification [13]. The type

of cast iron is defined by their unique microstructure with different graphite and/or iron carbide elements which form during solidification due to the excess carbon that was not absorbed. The chemical composition of the various cast irons may be observed in Table 2.3.

White cast iron is characterised by the formation of iron carbide which is known as cementite. The formation of iron carbide is highly dependent on the solidification cooling rate of a given composition. An increase in the cooling rate of a composition with lower carbon and/or silicon contents will result in an increase in the formation of cementite.

Rapid solidification in thin section sizes of cast irons may result in the formation of white cast iron. The formation of white cast iron may also be the result of low pouring temperatures or slow pouring rates. These properties of white cast iron may be advantageous, but may also be undesirable in cases where another type of cast iron was required. When the formation of white cast iron is undesirable, heat treatment may convert the iron carbide to iron or graphite [13].

Malleable iron was discovered during the heat treatment of white cast iron. The iron carbide in white cast iron dissociates and forms temper carbon when it is subjected to heat treatment. Temper carbon is irregularly shaped nodules of graphite and in malleable cast iron it is distributed within a matrix structure that can be varied in order to obtain different mechanical properties.

When an inadequate amount of magnesium or cerium is added to molten iron during the casting of ductile iron, a compacted graphite shape forms during solidification. The nodular shape of ductile iron is not formed, but rather a vermicular morphology is observed. In recent years, it is known that the addition of a small, but significant amount of titanium results in the reproducible production of compacted graphite cast iron [13]. This type of iron is therefore a combination of both grey and ductile iron.

Table 2.3: Range of compositions for common cast irons

Type of iron	Composition [%]				
	C	Si	Mn	P	S
Grey	2.5-4.0	1.0-3.0	0.2-1.0	0.002-1.0	0.02-0.25
Compacted Graphite	2.5-4.0	1.0-3.0	0.2-1.0	0.01-0.1	0.01-0.03
Ductile	3.0-4.0	1.8-2.8	0.1-1.0	0.01-0.1	0.01-0.03
White	1.8-3.6	0.5-1.9	0.25-0.8	0.06-0.2	0.06-0.2
Malleable	2.2-2.9	0.9-1.9	0.15-1.2	0.02-0.2	0.02-0.2

When considering valve body materials, grey and ductile iron are the most commonly used cast irons due to their favourable characteristics. These two types of cast iron have compositions that are fairly easy to obtain and control at a lower cost when compared to other cast irons. A summary of the different specifications, characteristics and applications of the five different types of cast irons may be obtained in Appendix A [16].

It is in the subsequent sections where the focus is placed on grey cast iron and ductile iron. Detailed information on these cast irons is discussed due to their applicability to the research topic.

2.2.1 Grey Iron

The transformation of austenite during the eutectoid reaction on the Fe-C phase diagram determines the matrix structure of cast irons. The graphite flakes found in grey cast iron results in low strength and ductility of the material, however, grey cast iron is the most widely used cast iron [17].

The metallurgy of grey cast irons is based on the fact that the material undergoes eutectic solidification with a solid-state eutectoid transformation. An understanding of the influence of carbon and silicon on the solidification of grey cast iron may be accomplished with the calculation of the Carbon Equivalent (CE) using Equation 2.1. In general, grey cast irons has an CE <4.3 [18].

$$CE = \%C + \frac{\%Si + \%P}{3} \quad (2.1)$$

The fluidity of grey cast iron is a critical factor as it often causes misruns, cold shuts and other defects [18]. The fluidity of grey cast iron at a specific pouring temperature decreases when the carbon content decreases as the liquidus temperature increases.

Phosphorus is an important minor element that increases the fluidity of iron. Although it is not intentionally added to the melt, the level of phosphorus should be controlled as high levels may cause shrinkage porosity. Sulfur is also a minor element in grey iron which significantly influences the nucleation of graphite. Manganese is usually added to form manganese sulphides to balance the sulphur content.

The cooling rate of grey cast irons varies from section to section as the volume to surface area changes. Grey cast iron is, therefore, section sensitive and mechanical properties may vary in different sections of the casting [19]. This implies that the selection of the composition should account for critical sections in the part where specific mechanical properties are desired.

Graphite flakes are not only responsible for the mechanical properties of grey iron, but also the physical properties. Different types of graphite flakes with different morphologies form depending on the amount of undercooling. Coarse graphite flakes produce low tensile strengths. Inoculation results in smaller eutectic cells which in turn may increase the strength of grey cast iron.

The flake size may be associated with various mechanical properties as shown in Table 2.4. Large flakes are obtained with high carbon equivalents and found in heavy sections. On the other hand, low carbon equivalents and fast cooling rates result in smaller flakes.

Table 2.4: Grey cast iron flake size and associated mechanical properties

Large Flakes	Small Flakes
Good damping capacity	Increased tensile strength
Dimensional stability	High modulus of elasticity
Resistance to thermal shock	Resistance to crazing
Ease of machining	Smooth machined surfaces

Grey cast iron is weak in tension due to the stress raised by the flakes and therefore it has very low ductility. It does however have an application in the casting of valves as a favourable property of grey cast iron, is pressure tightness. In this application of the material, uniform wall sections are required.

The various types and grades of grey cast iron make it just as versatile as ductile iron for a different set of applications. Grey cast iron does present favourable mechanical properties and is reasonably easy to obtain. The pressure tightness of grey cast iron is more often applied to pressurised parts such as engine blocks. Ultimately, the low ductility of grey cast irons limits its applicability to the casting of valves. When Figure 2.3 is observed, it can be noticed that grey cast iron is slightly cheaper than other valve casting materials, but consequently, its mechanical properties are inferior. The mechanical properties of grey cast iron and ductile iron is compared in Table 2.5 [19].

Table 2.5: Mechanical properties of grey cast iron and ductile iron compared

Cast Iron	Type	Ultimate Tensile Strength(MPa)	Yield Strength (MPa)	Elongation in 50mm (%)
Grey	Ferritic	170	140	0.4
	Pearlitic	275	240	0.4
	Martensitic	550	550	0
Ductile	Ferritic	415	275	18
	Pearlitic	550	380	6
	Martensitic	825	620	2

Ductile iron is basically a variant of grey cast iron which increases the mechanical properties of grey cast iron and extends the applications of grey cast iron.

2.2.2 Ductile Iron

Ductile iron is obtained when a small amount of magnesium or cerium is added to molten iron. The magnesium/cerium acts as a noduliser and causes the graphite to form spheroidal shapes during solidification. Ductile iron is therefore also known as nodular or spheroidal graphite(SG) iron.

In order to obtain ductile iron, it is necessary to remove sulphur and/or oxygen in the liquid metal by adding desulfurising agents. Calcium oxide is typically used in the desulfurising step. Although magnesium is the nodulising agent, the low boiling point of magnesium inhibits the addition of pure magnesium to the molten metal [17]. To prevent excessive loss of magnesium during inoculation, magnesium is added in the form of magnesium ferrosilicon (MgFeSi).

The mechanical properties of ductile iron highly depend on the level of the residual magnesium. If the level of magnesium is too low, the nodularity of the material will be insufficient which implies a deterioration of the mechanical properties. The cooling rate determines the exact amount of residual magnesium, which is in the order of 0.03 to 0.05% for ductile iron [18].

Graphite degeneration may be caused by the presence of anti-spheroidising minor elements [18]. These minor elements have acceptable maximum limits, which are specified in Table 2.6 below. The presence of these elements should not exceed the specified limits.

Table 2.6: Maximum acceptable limits for minor elements in ductile iron

Type of iron	Composition [%]
Aluminium	0.05
Arsenic	0.02
Bismuth	0.002
Cadmium	0.01
Lead	0.002
Antimony	0.001
Selenium	0.03
Tellurium	0.02
Titanium	0.03
Zirconium	0.10

The minor elements in Table 2.6 are also responsible for the shape of the graphite that forms during solidification. The shape of the graphite determines the type of cast iron and therefore the mechanical properties. The spheroidal shape of the graphite in ductile iron may also be influenced by calcium, yttrium and rare earths such as cerium.

The final step in ensuring the formation of ductile iron is inoculation. Inoculation with ferrosilicon (FeSi) prevents the formation of white cast iron by promoting the heterogeneous nucleation of graphite [17]. An increase in the nodule count results in a higher as-cast ferrite/pearlite ratio, which implies an increase in mechanical properties.

In a study performed by the American Foundry Society (AFS) in 2003, positive results were obtained with late sulphur-addition during post-inoculation and after magnesium treatment. The results included increased nodularity, increased nodule counts and a decrease in carbide occurrence [20].

A completely new set of applications for ductile iron is obtained with austempering. Austempered Ductile Iron (ADI) has a bainitic ferrite structure. The transformation in a matrix structure in various steps from ferrite to bainite results in increased hardness, strength, wear and impact resistance and also a decrease in machinability [18]. ADI is an exceptional material with strengths up to 1379MPa. The enhancement of the mechanical properties does however come at a higher cost as more processing steps are required.

There is a loss in volume during the liquid-to-solid phase change of ductile iron, but the formation of graphite counteracts this phenomenon as an increase in volume is experienced [18]. This phenomenon is advantageous as it results in a higher mould yield due to minimal use of risers. It also implies that minimal compensation is required for shrinkage, which means there is no need for much bigger patterns, which lowers the cost of patterns [18]. Generally, an allowance of 0-0.7% is used in the patternmaking of ductile iron [18].

In the production of ductile iron, metallurgic and process control is key to ensuring specifications are met. Carbon, silicon and other minor elements should be held at specific levels as these elements effect the nodulising properties of the melt, as discussed earlier. This means frequent mechanical, chemical and metallurgic testing needs to be applied. Less process control is required with the casting of other cast irons.

Although heat treatment may reduce fatigue properties, most ductile iron castings are used as-cast [18]. If heat treatment is necessary, ductile iron has the advantage that it may be cast and shipped on the same day, due to minimal dimensional changes after heat treatment [18].

An additional advantage of ductile iron is a decrease in machining costs as there is less material to remove. Ductile iron castings are also easy to machine and cutting tool wear is lower [18].

The manufacturing processes used in the casting of ductile iron require high density, rigid moulds with good heat transfer. The reason being the fact that molten ductile iron (in its liquid form) has a high surface tension which may cause mould collapse.

In summary, ductile iron is a very versatile material used in a wide range of applications due to its favourable characteristics and properties. The production of ductile iron requires evaluation and control of material elements and a rigid mould with good thermal properties is advised. It is a relatively cheap material with numerous opportunities for cost reduction in the manufacturing process.

2.3 Valve Manufacturing Methods

Valves are manufactured either by forging or casting, depending on the application of the specific valve. Both forging and casting have various extensions of the process with different parameters and steps to produce a specific set of material properties, functions and qualities.

2.3.1 Forging

Interest in near-net-shape manufacturing technologies has led to great developments in the cold and hot die forging industry [21]. Forging is known to result in high-quality products with increased material properties. Despite the numerous merits of forging, it is an expensive manufacturing technique with numerous considerations.

One of the factors contributing to improved grain alignment is the fact that the metal to be forged consists of a billet which was previously cast and then rolled. Hot forging requires the metal billet to be pre-heated to its forging temperature. The heated billet is then placed in a press where a significant force is applied to force the metal into the shape of the die. This is shown in Figure 2.4.

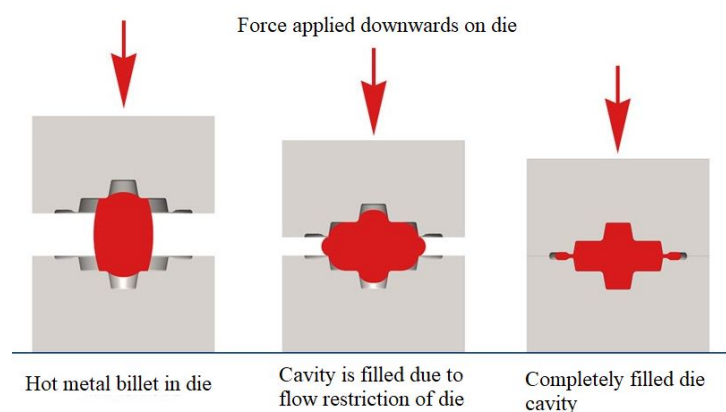


Figure 2.4: Demonstration: forging of hot metal billet in the hot-die forging process

The heating and pressing of the already rolled billet results in a part with higher integrity due to the grain structure re-alignment. The directionality of grain flow leads

to increased ductility, toughness and fatigue resistance of the forged part [19].

The increased strength-to-weight ratio provides optimised part design opportunities. A reduced section thickness is possible as well as a reduction in the overall weight of a part. It is therefore economically attractive to invest in forging.

The short lifespan of forging tools is a major drawback affecting the feasibility of the manufacturing method. High, cyclic mechanical loads and high temperatures are the main factors affecting the durability of forge tooling [21]. The quality, surface finish and dimensional accuracy of the forged part depend on the wear of the tooling. Tooling such as dies is costly as it has to accommodate these extreme working conditions and is machined from specialised materials [22]. When considering the contribution to the total production costs, the damage on tools and the time spent to replace tooling adds up to 40% [21].

Although forging is a near-net-shape manufacturing technique, finishing operation such as heat treating and machining accuracy is required [19]. It is possible to minimise finishing procedures by means of other forms of forging such as precision forging. The advantages and limitations of the various forging processes are shortly described in Table 2.7 as documented by [19].

Table 2.7: Summary of various forging processes and their limitations and advantages

Process	Advantage	Limitations
Open die	Simple and low-cost die; numerous part sizes; good strength characteristics; most appropriate for small quantities	Not appropriate for complex shapes; close tolerances not easily held; machining required; low production rate; material not optimally used; high degree of skill required
Closed die	Material well utilised; Increased properties when compared to open die; good dimensional accuracy; high production rate; good reproducibility	High die cost; not economically appropriate for small quantities; machining necessary
Blocker	Low die costs; high production rates	Machining required
Conventional	Less machining required than blocker type; high production rates; material well utilised	Higher cost than blocker type
Precision	Good dimensional tolerance; thin section sizes possible; little to no machining required; good material utilisation	High forging forces; intricate dies; provision for removing forged part from die

In summary, forged valves are considered for high-pressure and high-temperature or other specialised applications. Several factors influence the economics of forgings and therefore the size of forgings, the material to be forged, die material, die design and production method are important considerations. Forging is therefore only applied in specialised cases of valve manufacturing. As feasibility is an important factor, the casting of valves is the most feasible and therefore most popular manufacturing method in the industry.

2.3.2 Casting

The casting process involves the manufacturing of a specific product by means of pouring molten metal into a special container or cavity, called a mould. The casting of metal dates back to 4000 B.C [19]. Over time numerous casting methods were developed for different applications and requirements.

The ability to cast complex shapes has led to a vast variety of products being cast. The mechanisation and automation of casting operations have changed the traditional methods of casting. Advancements in the casting industry are driven by the need to cast high-quality products with close dimensional tolerances. Post-production processes such as heat treatment result in added flexibility and increase in mechanical properties of castings. A summary of casting processes are shown in Table 2.8 [19].

Table 2.8: Casting processes and their limitations and advantages as described by *Kalpakjian* and *Schmid* [19]

Process	Advantage	Limitations
Permanent mould	Good surface finish and dimensional accuracy; high production rate	High mould costs; limited part shape and complexity; not appropriate for high melting point metals
Die	Excellent dimensional accuracy and surface finish; high production rate	High die cost; limited part size; limited to non-ferrous metals; long lead time
Sand	Wide variety of metals can be cast; part size, shape and weight unlimited; low tooling costs	Finishing required; coarse surface finish; wide tolerances
Investment	Intricate part shapes; excellent surface finish and accuracy; wide range of metals can be cast	Limited part size; expensive patterns, moulds and labour
Evaporative pattern	Most metals can be cast; no limit to size; complex shapes can be cast	Low strength patterns; costly for small quantities

The mould plays an important role in the success and quality of the casting. Casting techniques are therefore categorised based on the type of mould and the type of pattern. A pattern is used to imprint the form of the product to be cast, into the mould. Therefore, the pattern is a replica of the part or component to be cast.

The molten metal feeding systems may be very complex and depend on the type of moulding process and materials. The process steps used in the casting of parts vary and require experience and extensive knowledge. It is, therefore, an exhausting exercise to present detail on each aspect of all the casting process.

Foundry moulds are required to have specific characteristics to ensure the success of the casting. The mould should be formable into a desired shape and be able to hold this shape while the molten metal is poured and while it solidifies [13]. After solidification, the mould should be easy to break down in order to obtain the cast product. Typically, the mould shape is a mirror image of the part or component being cast. In order to remove the cast product, the mould should typically consist of two or more parts and the pattern should be designed to increase the ease of de-moulding.

The selection of the moulding method is based on factors such as the part shape and size, the number of castings required, the tooling available and the metal being poured [13]. The feeding system which includes the runners, risers and gates forms part of the mould. The mould material should, therefore, be able to withstand the erosion action of the molten metal as it is poured. Only when these factors are considered, the mould and pattern material may be selected based on the most appropriate moulding method.

The various forms of casting may be categorised by their moulding process. The mould and the pattern are interlinked as the mould is formed by the imprint of the pattern. The casting processes will briefly be discussed in each moulding process section.

Permanent moulds are made of materials with high melting points and good resistance to erosion and thermal fatigue. The gating system and the cavity usually created with a pattern is machined into the mould. The surface of the mould cavities is often coated

with refractory materials to serve as a thermal barrier, to protect the mould and to aid in the ease of the removal of the part. Examples of these processes are vacuum casting and die casting.

Expendable mould, expendable pattern casting processes include sand moulding, no-bond sand moulding, shell moulding and slurry moulding methods. Expendable mould methods may result in lower production costs. These casting processes re-use mould materials and use patterns that are destroyed during each casting.

Expendable patterns are not reusable and are made for each individual casting. The expendable patterns are the positive shape of the part or component being cast. Castings with expendable patterns may increase the tolerance from 1.5 to 3.5 times that of permanent patterns [13]. Investment casting, replicast casting and the lost-foam casting process are all expendable pattern, expendable mould casting methods.

It is sensible to focus on the casting processes as a whole and then scrutinize and critically evaluate each process according to the feasibility of that process for valve manufacturing. The casting processes are discussed in the subsections that follow.

Vacuum Casting

Vacuum casting is often confused with vacuum moulding. The vacuum in vacuum casting is used to draw the molten metal into the mould cavities and therefore the vacuum is not used to hold the mould in place, unlike the vacuum moulding process. This is a relatively new casting method that increases the effectiveness of traditional gravity casting methods.

The mould in vacuum casting is produced by using amine vapour to cure a mixture of fine sand and urethane which is moulded over metal dies. The mould is partially immersed in molten metal in an induction furnace. The vacuum reduces the air pressure and a syringe action causes the molten metal to fill up the cavity. This process is a casting process that forces directional solidification, similar to forging. It, therefore,

produces products with enhanced mechanical properties for specialised applications.

The process is an alternative for investment casting, shell moulding and green sand casting. It is especially used to cast thin-walled, complex shapes with uniform properties, which are all favourable properties for the casting of valve bodies. It is, however, a high precision casting method used to cast parts such as gas-turbine components with wall thicknesses in the order of 0.5mm. This type of precision may be excessive when considering the requirements of most industrial valves.

Although this process may be applied to the casting of valve bodies, the execution of the process requires specialised machinery. The process costs are similar to that of green sand moulding and parts up to 70kg have been cast with this method. However, cast iron has not been cast with this method before [19].

Die Casting

Die casting is particularly used where high production volumes are required. The weight of typical die casting parts range between 90g and 25kg. With this method, full automation is possible which dramatically reduce labour costs. Equipment cost is a major concern with this method, as the costs of dies and pressurising equipment are very high [19].

The process involves molten metal forced into a cavity at high pressures. A specific volume of molten metal is forced into the cavity with a piston in the hot-chamber process and the mould is held under pressure during solidification. With high pressures and high temperatures, cooling is required to extend the equipment life.

Die casting processes allow the casting of complex shapes and thin-walled parts with good dimensional accuracy and surface details. An added advantage of this method is the increase in cooling rate due to the rapid solidification of molten metal at the die walls. This results in increased strength-to-weight ratios.

It should be considered that weight-to-part rate of die casting dies is extremely high.

A 2kg part may require a 2000kg die [19]. The high temperatures required for the casting of cast iron will require specialised dies with high-temperature materials and may result in an even higher weight-to-part ratio.

It is evident why die casting is most appropriate for high volume casting. The process does present favourable advantages, but the high equipment costs outweigh the advantages.

Sand Moulding

Sand moulding is the most commonly used method for the casting of cast irons [18]. There are two main types of sands used for the fabrication of sand moulds. Naturally bonded (bank sand) and synthetic (lake sand) where the latter is preferred by most foundries. The characteristics of the sand determine the characteristics of the mould such as surface finish, permeability and collapsibility [19]. A typical sand mould and its components are shown in Figure 2.5.

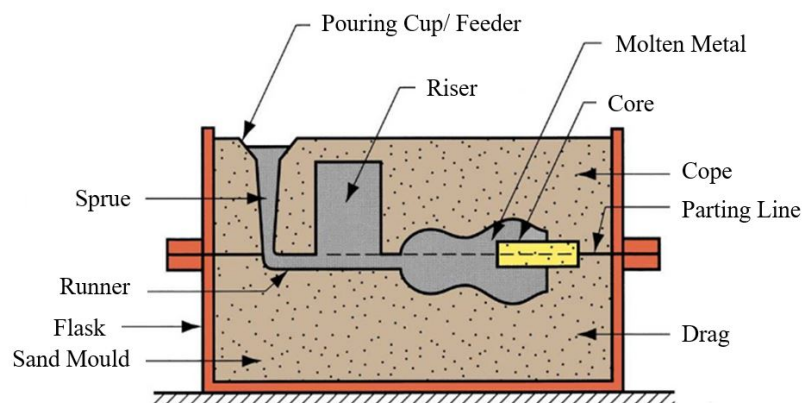


Figure 2.5: Illustration of a sand mould assembly and the casting components

The three basic types of sand moulds are green sand, cold-box and no-bake moulds. Green moulding sand refers to a moist sand mixture which consists of a sand, clay and water mixture. Green-sand moulds are the least expensive moulds and are generally used for large castings [13].

The cold-box mould is dimensionally more accurate than the green-sand moulds. The sand is chemically bonded by binders, and therefore more expensive. The sand-binder mixture hardens at room temperature and therefore it may be referred to as a cold-setting process.

No-bake moulds are also a cold-setting process. The no-bake mould consists of a synthetic liquid resin which is mixed with the sand. It is possible to oven dry sand moulds prior to casting in order to obtain stronger bonds. This may be advantageous as it will produce higher dimensional accuracy and smoother surface finishes to castings. The downside of oven baking is the fact that the production rate is lower (due to additional drying time required) and distortion of the mould is greater. Due to lower collapsibility of the mould, hot tearing may also occur.

A great advancement in the sand moulding industry is the use of Additive Manufacturing (AM) as mould manufacturing method. With additive manufacturing of sand moulds, no pattern is required which drastically reduces costs. However, additive manufacturing has major limitations. Even with the elimination of the pattern, additive manufacturing is not yet more feasible for mould making.

The cost of additive manufacturing machines are extremely high and the cost of the specialised sand used, also increases the cost. The slow speed of additive manufacturing is hampering the growth of this method as it is not suitable for large-scale production [23]. It is also not feasible to install a series of 3D-printers for large-scale production of moulds. Furthermore, there is currently a limitation on the size of moulds that can be printed with additive manufacturing. Figure 2.6 shows a 3D-printed sand mould produced at the facilities of Vaal University of Technology (VUT).

Additive manufacturing technology may also be used in the manufacturing of patterns, both as expendable and permanent patterns. Rapid advancements in the field of AM will soon result in dimensionally more accurate patterns. As with the printing of moulds, the cost and time constraints of AM does not allow its application for high production rates. Additive manufacturing is therefore preferred for a limited amount

of castings.



Figure 2.6: Photo of additive manufactured sand mould half

No-bond Sand Moulding

No-bond moulds consist of free-flowing particles which do not require binders, additives or mulling equipment. The sand or mould particles are held together by compaction in the casting box or flask (as with the lost-foam process) or by an applied force.

Magnetic moulding is an extension of the lost-foam process where the sand is replaced by mould material of magnetic iron. A coated Expanded Polystyrene (EPS) pattern is positioned in a flask and the flask is filled with magnetic shot particles. A magnetic field is then applied to provide rigidity to the mould prior to casting the molten metal.

Vacuum moulding also referred to as the V-process, is a process where sand is held in place by means of a vacuum on a flask. The V-process is popular for castings with high surface-area-to-volume ratios.

Shell Moulding

Shell moulding is a sand casting process where a box filled with fine sand that is mixed with a thermosetting resin, is clamped to a mounted pattern. The pattern is mounted, heated and coated with a parting agent before it is clamped to the sand box. The box

is then turned upside down or the sand mixture is blown over the pattern. The resin is cured when the box and pattern are placed in an oven for a short period. The process is shown in Figure 2.7

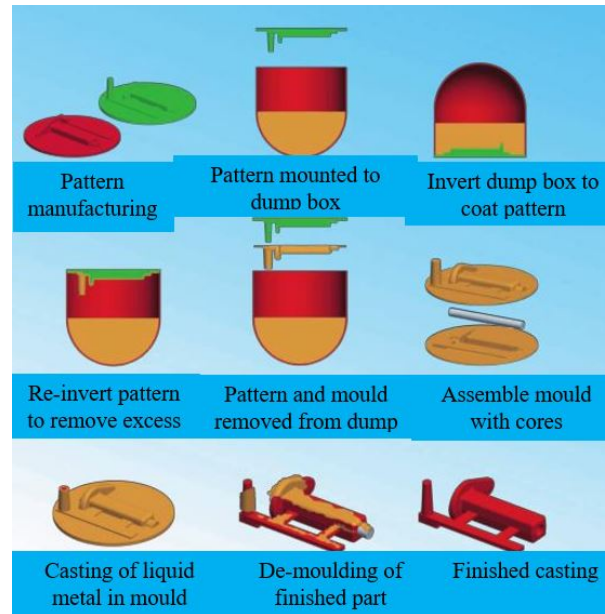


Figure 2.7: Illustration of the shell moulding process

Shell moulds are light-weight and thin, which provides different thermal characteristics when compared to other moulds. High quality and complex shapes are cast with shell moulding which requires minimum finishing operations.

The grain size of the sand is much smaller when compared to green-sand moulding and the resin produces high volumes of gas when it decomposes. Defects may result due to the lower permeability of the mould if the moulds are not well vented.

This process uses less sand and it provides more design flexibility when compared to green sand moulding. A disadvantage is the high cost of patterns that are machined from metal. The resin binder is also very expensive [13].

Shell mould thicknesses range from 5 to 10mm and can be controlled with the time the pattern is in contact with the mould. The rigidity and strength of the mould may then be sufficiently controlled to hold the weight of the molten metal. The thin thickness of the mould may pose advantages as the cooling rate may be faster than other traditional

sand moulds which may increase the mechanical properties.

Slurry Moulding

Plaster moulding and ceramic moulding are the two types of slurry moulding methods known as precision casting [13]. These methods are used for applications requiring high dimensional accuracy, smooth surface finish and fine detail.

Plaster mould casting is a casting process used to cast lightweight castings in the range of 125-250g [19]. The mould is made of a mixture of plaster of paris (gypsum or calcium sulphate), talc powder, silica powder and water. The slurry is then poured over the pattern. The mould is removed from the pattern once set and dried at 120-260°C.

The low permeability of the mould requires molten metal to be cast in a vacuum or under pressure. Methods to increase the permeability of the mould involves the use of foam plaster (containing trapped air bubbles) or by means of the Antioch process. The mould is dehydrated in an autoclave for 6-12 hours and re-hydrated in air for 14 hours during the Antioch process.

The materials cast by means of plaster moulding all have melting temperatures below that of the plaster mixture. This implies that aluminium, magnesium, zinc and copper base alloys are cast with plaster moulds. The low thermal conductivity of the plaster allows for slower cooling rates and thus more uniform grain structures.

Ceramic moulds consist of refractory materials for high-temperature applications. The ceramic moulds differ from those of investment casting as it consists of a cope and a drag and in some cases a drag only.

The application of ceramic moulding includes the manufacturing of castings that requires patterns too large for investment casting. It is also ideal for castings in limited quantities.

The cost of slurry moulding is very high as it is a lengthy process. The mould materials

are also not reusable. It is a process requiring more equipment than other moulding processes. The permeability of slurry moulds are very low which results in slow cooling rates and pressure or vacuum is required during pouring of molten metal.

Investment Casting

Investment casting is also referred to as the lost-wax process. The process involves the melting of a wax or plastic pattern. Prior to melting the pattern, the wax or plastic pattern is dipped into refractory coatings, dried and dipped again to increase the layer thickness. The mould material is, therefore, the refractory coating. The wax is then melted out in an inverted position. Once the wax is melted out, the mould is heated at high temperatures to drive off the water and fire the refractory material. The investment casting process is illustrated in Figure 2.8.

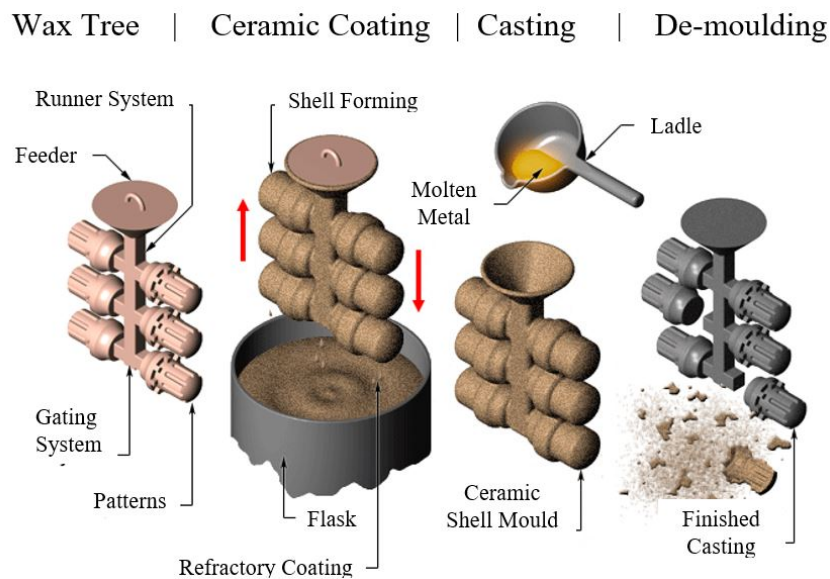


Figure 2.8: Illustration of the investment casting process

The mould materials and labour involved in this process are rather costly. The use of wax has the advantage that it may be reused, but it is more fragile than plastic patterns and may easily be damaged during the mould making process [19]. Wax-blends are often preferred as the addition of resins, plastics and fillers increase the properties of the wax pattern [13].

Urea-based patterns are also developed and used in the investment casting process. Urea-based patterns are strong and are dissolved out in water. This pattern material is advantageous as it decreases the cost of the casting, by decreasing the production time by eliminating the step where wax is melted out at an elevated temperature [13].

EPS has been used in the investment casting process, but the dimensional accuracy is lower than when wax patterns are used. EPS is therefore mostly used in the gating systems of investment castings.

Investment casting is, therefore, the preferred casting method when high dimensional accuracy is required. It is also used when the complexity of the part exceeds the capabilities of other casting methods and where parting lines are not normal. Another advantage of this process is the freedom of alloy selection. High-temperature alloys may be cast with this method as well as alloys that are too difficult to machine [13].

Replicast Casting

The Replicast process is a modification of both investment casting and the lost-foam process. A refractory covered polystyrene pattern is burned out prior to casting the molten metal. The Replicast moulding process is patented by a UK company Casting Technology International [13].

The lost-foam casting process is prone to carbon defects due to the carbon residue produced by the decomposition of the polystyrene mould. The Replicast process was therefore developed to overcome this problem by burning out the pattern prior to casting, as with investment casting. The Replicast process can, therefore, be used for a wider range of alloys, such as low carbon stainless steels [13].

The advantages of both the lost-foam casting process and investment casting are therefore combined and result in the decrease of casting costs. The ceramic mould is thinner than the shells used in investment casting. Sand-mould related problems as experienced with the lost-foam process are eliminated and carbon residues are no longer a

problem. The Replicast process is however not suitable for thin sections and is more expensive than the lost-foam process [13].

Lost-foam Casting

The lost-foam casting process is also referred to as evaporative-pattern casting. Typically, a polystyrene pattern is used and the molten metal is directly cast on to the pattern. Unlike investment casting and the Replicast process, the pattern is not melted out prior to casting. The molten metal takes on the shape of the pattern as the pattern is evaporated. By means of thermal degradation, the pattern is replaced with the molten metal.

The process starts with the manufacturing of the pattern. Polystyrene beads are placed in a pre-heated die. The beads expand and take the shape of the cavity. The beads are bonded together by additional heat. Once the die has cooled, the pattern is released. The pattern is then coated with a refractory slurry and dried.

The pattern is placed in a flask which is filled with fine, loose sand. In some occasions, additional strength of the mould is obtained with bonding agents. After the sand is compacted, the molten metal is poured. The vapours and degradation of the pattern are vented into the sand. The process is illustrated in Figure 2.9.

Directional solidification and microstructure improvements are obtained by the lost-foam process due to the large thermal gradient at the metal-polymer interface [19]. This process is simple and no parting lines or cores are required. The affordability of the pattern material also contributes to the economics of this process. It should, however, be considered that the cost of the die used in pattern manufacturing is high and results in the need for additional tooling [19].

An impressive advancement in the lost-foam process is the production of Metal-Matrix Composites (MMC). The pattern is embedded with fibers or particles that become part of the casting. Fibres such as graphite, boron, silicon carbide and alumina have been

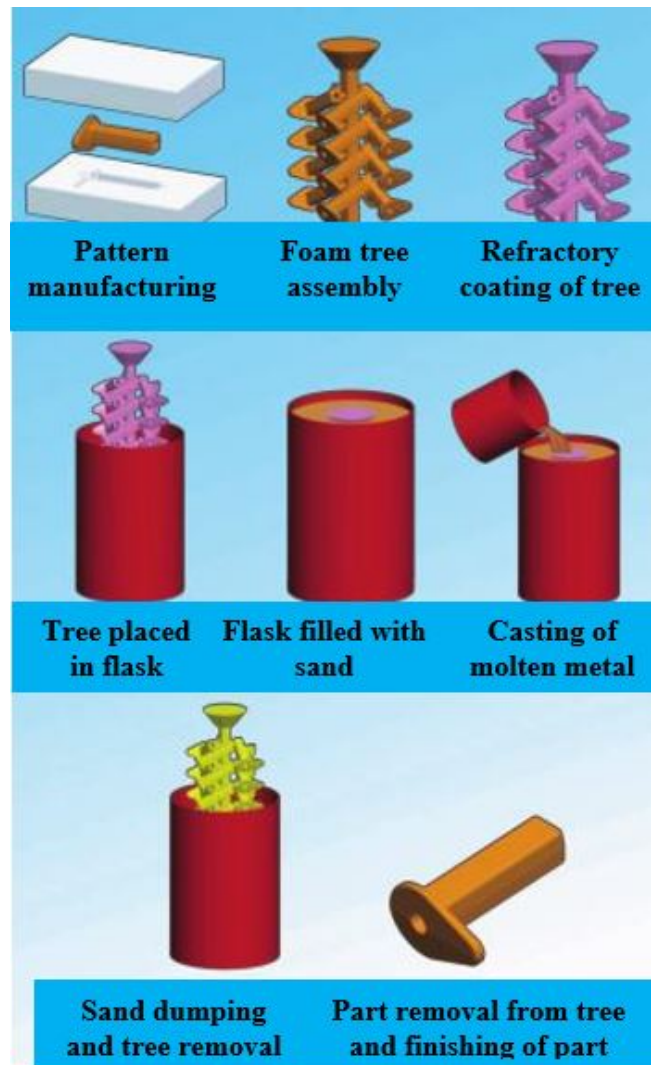


Figure 2.9: Illustration of the lost-foam casting process

used in this process. Typical matrix materials are aluminium, magnesium, copper and superalloys [19]. MMC increases the properties of these materials. If applied to valve casting, less material may be used to obtain the same mechanical properties. In effect, the cost of valve manufacturing may decrease.

An extension of the lost-foam casting method was developed by Wittmoser in the 1960's [13]. The process is referred to as magnetic moulding and instead of loose unbonded sand, iron or steel shot is used as the mould material. This process allows the casting of complex shapes at significantly lower costs [24]. Machining steps are minimised and the operating costs are reduced by this method.

Although the process has been investigated since the 1960's, the process has not made it to the industrialisation phase. Reasons may involve the lack of understanding the electromagnetic concepts [24]. In 2004 a co-operative research project was launched where the magnetic moulding process was investigated by various European foundries [25]. The project acronym was MAGNET.

The MAGNET research team concluded that the magnetic moulding process is indeed an economical extension of the lost-foam casting process. A reduction in grain size was observed which resulted in an increase in the mechanical properties of ferrous and non-ferrous metals. Furthermore, it was found that the magnetic field has a positive effect on the dimensional tolerances of grey cast iron castings. Various metal flow orientations are also possible with this method [25].

In 2006 the MAGNET project was completed and Suganth kumar *et al.* continued research in 2007 on the magnetic moulding process by investigating the mould strength of magnetic moulding. Insight into the mould properties, packing arrangement of steel shot and pattern position was obtained in this study [26].

Geffroy *et al.* continued with an investigation of the thermal and mechanical behaviour of ductile iron and grey cast iron castings using magnetic moulding in 2008. Geffroy *et al.* concluded that steel shot moulds lead to higher cooling rates which result in finer grain structures, which supports the findings of the MAGNET project [24].

The advantages of magnetic moulding build on the advantages of the lost-foam process. The decrease in cooling rate is significant and the flexibility of the process at decreased production costs makes this process a viable variant of the lost-foam process. The question is then raised why this process has not been applied in more recent years. There is still very little information available on this process. A wide range of investigations are yet to be performed before foundries will be comfortable to implement the process.

The lost-foam casting process has numerous extensions and is a very versatile casting process. It may be concluded that this process has low production costs without com-

promising the quality and dimensional accuracy of the casting. The absence of binders in the sand makes it environmentally more friendly and no mixers and moulding machines are required [27]. The effect of carbon residue, should however, be considered when selecting a casting material.

2.4 Summary

A review of manufacturing methods resulted in significant insight into methods to lower production costs. It is evident that the application of the valve and the material selection of the valve will greatly influence the manufacturing method.

Ductile iron is a versatile material with an extensive list of applications. It is particularly suitable for the casting of industrial valves. Close control of minor elements and magnesium will aid in the successful casting of ductile iron. The increased mechanical properties at a similar cost as grey cast iron, makes ductile iron the preferred material for the casting of an affordable valve body.

Forging is a costly valve manufacturing method, often applied when a special set of mechanical properties are required, such as directional strength. Casting is the most commonly used valve manufacturing method with a wide range of possibilities.

Permanent mould castings present favourable advantages such as high casting temperatures, complex and thin-walled parts may be cast and the process is ideal for high production volumes. The cost of the dies and equipment for permanent mould casting is very high and due to the high melting temperature of cast irons, cast irons are not usually cast with permanent mould casting methods.

The lost-foam process is a viable manufacturing method. The process has gained popularity as complex, high-quality castings may be cast at a relatively low cost. It is a simple process with exceptional variants. The use of an alternative mould material, other than sand, may result in significant advancements in the casting industry.

Due to the traditional mould materials used for the casting of cast irons, variation and control of the microstructure, determined by cooling rate, is limited. If the thermal conductivity of the mould material can be varied or controlled, substantial microstructural variation becomes possible that can also substantially improve the properties of the cast product and contribute to technology intellectual property development and lower the overall cost of local valve manufacturing. The magnetic moulding process was therefore selected as valve body manufacturing method.

Casting methods have unique processing parameters and vary in complexity. The selection of the magnetic moulding process necessitates a thorough understanding of each step involved in the process. Only then can the feasibility of the process be revealed in the application.

Chapter 3

Magnetic Moulding

An in-depth investigation of the magnetic moulding process as an extension of the lost-foam process is revealed within this chapter. This chapter builds on the literature study and serves as the foundation of the process design with the aim of investigating the feasibility of this manufacturing method.

Magnetic moulding shares common processing steps with the lost-foam process in pattern design and selection as well as refractory coating selection. The most influential difference in this method is the mould material. Limited information on magnetic moulding required deeper insight into the principles of the lost-foam process. Ultimately, the extent of knowledge on the process steps and components will reflect in the feasibility of this method.

3.1 Pattern Making

The pattern material and manufacturing method is critical in the lost-foam casting process, and therefore also in the magnetic moulding process. The pattern is an exact copy

of the part to be cast. The dimensional accuracy of the pattern and the quality of the pattern material contribute to the final quality of the cast product.

The pattern manufacturing method greatly impacts the surface finish and contributes to the overall quality of the pattern and therefore the cast part. Depending on the material, the manufacturing method differs. It is only in recent years that additive manufacturing has been recognised as an alternative to pattern making.

Additive manufacturing is well known for rapid prototyping and has cumulatively been used in the casting industry. Additive manufacturing has successfully been applied to investment casting where 3D printed materials are melted out of the mould prior to casting [28]. The application of additive manufacturing in lost-foam casting is an initiative with potential to change lost-foam casting drastically and therefore change the casting industry for years to come.

In 2016 research was presented on Polylactic Acid (PLA) and Acrylonitrile Butadiene Styrene (ABS) 3D printing material as pattern material for the use of thermal destructive casting, as applied in the lost-foam casting process [29]. The properties of these materials include low melting temperature, biodegradability and stability during production. Complex shapes are easily obtained at a lower cost. The possibilities of additive manufacturing in the foundry industry are endless.

Typically patterns are machined from blocks of expanded polystyrene EPS with Computer Numerical Control (CNC) machines or by wire-cutting simple patterns. A process similar to injection moulding is also used to create a pattern by injecting pre-expanded polystyrene beads into a pre-heated die [19]. The cost of complex pattern manufacturing for the lost-foam casting process may be decreased when additive manufacturing is applied. Ultimately, the choice of material will impact the choice of the manufacturing method.

EPS is the most commonly used pattern material for lost-foam casting [13]. It is also the only material that has been used in research on the magnetic moulding process. Styrene-Methyl Methacrylate co-polymer (STMMA) is a popular pattern material used

especially in China and Japan. In recent years Poly Methyl Methacrylate (PMMA) was specifically developed for the lost-foam casting process for the casting of ferrous materials. These materials are discussed in more detail in the subsections.

3.1.1 EPS

EPS is a relatively inexpensive material and readily available, hence its popularity in the industry. High-quality castings are obtained with high-quality foam patterns. The quality of the foam pattern depends on the polystyrene beads.

There are several grades of EPS depending on the bead size. The raw bulk density of EPS (640kg/m^3) needs to be reduced to a value between 16 and 27 kg/m^3 . After expansion, EPS with a bulk density of 24kg/m^3 and bead sizes of 0.75 - 1.5mm and 0.61 - 1mm are generally accepted as the preferred grades for lost-foam casting applications [13].

Pattern moulding proceeds with filling of the mould with the pre-expanded beads at the desired density. The beads are then fused together by adding heat in the form of steam to the filled mould. The material in the mould softens and expands again in order to fill the air gaps between the beads to form a solid mass of EPS. The cavity walls are then cooled to stop the expansion process of the beads. The pattern is then ejected.

Typical casting defects experienced in lost-foam casting include fold defects, misruns, inclusions, flow marks and pores. Fold defects are associated with bead fusion and are common among aluminium alloy castings [30]. The other defects are caused or influenced by the pyrolysis of the EPS.

In recent years methods to increase the speed of degradation has been implemented to increase the casting quality of the lost-foam process. One of these methods is the addition of organic brominated additives to the EPS pattern. Brominated additives release hydrogen bromide gas during the casting process which reduces the number

of byproducts entrapped in castings [31].

Although the speed of degradation may be increased, the pyrolysis of EPS remains disorderly and carbon residue is still formed. The chemical formula of EPS is $(C_6H_5C_2H_3)_n$ which contain a carbon content of up to 92% [32]. Due to the problem experienced with the high carbon content of EPS, various other materials have been investigated to reduce the number of defects experienced with the lost-foam casting process.

3.1.2 PMMA

PMMA decomposes with minimal carbon residue. The resin was specifically developed for the application of lost-foam ferrous castings. The chemical composition of PMMA has three carbon atoms less than EPS, as observed in the chemical structures in Figure 3.1 [18].

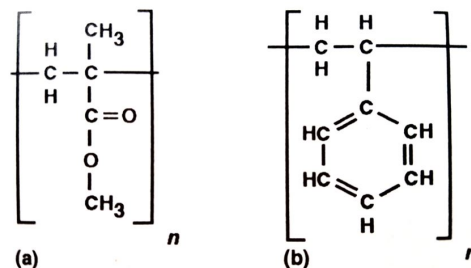


Figure 3.1: Chemical structures of a) PMMA and b) Polystyrene (EPS)

The oxygen atoms in PMMA also aid in decreasing the carbon residue. At high casting temperatures, excess carbon may escape in the form of carbon monoxide. The most significant difference between PMMA and polystyrene is the absence of a carbon-rich benzene ring in the PMMA structure. The thermal decomposition of EPS is made more difficult due to the stability of the benzene ring [18].

A study on the fraction liquid viscous residue formed by the decomposition of EPS and PMMA, supported the reduction in carbon residue expected when observing the chemical structures of these polymers. At a temperature of 750°C, PMMA produced

30% residue whilst EPS formed 60% liquid viscous residue in aluminum alloy castings [31].

The fact that PMMA produces lower carbon residue is also linked to the observation that 60% of the PMMA pattern decomposes as gaseous product at the metal front [31]. The gas layer at the metal front of PMMA degradation was also observed to be thicker than with EPS [31]. The gaseous product results in a new limitation. The formation of the gas layer during degradation of PMMA results in a decrease in the velocity of the molten metal during casting as observed by Shivkumar *et al.*, which in turn may result in casting defects.

The casting process and the study of defects are constantly under scrutiny to improve casting quality and to lower production costs. A material with similar advantages as PMMA was developed by Caschem (Hangzhou, China) in 2001. This material contains 30% styrene and 70% methyl-methacrylate with a carbon content of 69.6% [32]. China and Japan particularly use STMMA for ductile iron castings. Both PMMA and STMMA are manufactured similarly to EPS.

3.1.3 PLA and ABS

PLA is an organic polymer manufactured from corn starch or sugar cane. The advantage of this material is the fact that it is biodegradable and does not produce toxic gasses. ABS, on the other hand, does emit low-level toxic agents.

Although PLA is environmentally more friendly, it is prone to distortion. The uneven cooling of layers in the printing of PLA is more prominent than with ABS [29]. A problem encountered with the printing of a stop valve is the fact that the holes are often not circular and out of the plane. Dimensional control of 3D printed parts is a field not extensively investigated yet. An image of the 3D printed ABS valve halves is shown in Figure 3.2

The thermal destruction of both PLA and ABS was investigated by Olkhovik *et al.* and



Figure 3.2: Image of 3D-printed ABS stop valve halves as printed by *Olkhovik et al.*

by burning of a PLA and ABS filament wire, the speed of burning PLA was 2.25mm/s whilst ABS was much higher at 3.33mm/s. An increase in the filling temperature may overcome the problem experienced by low thermal destruction of plastics [29].

In the study performed by *Olkhovik et al.*, it was concluded that additive manufacturing can be used as pattern material in applications such as the lost-foam process. It should, however, be noted that in their investigation, the casting of metal was not performed. A refractory coating was applied to the patterns, and patterns were burned out with an induction oven. It was observed that the 3D printed material transforms to a liquid and is not fully burned out. In the casting of metal, this may be problematic and may result in casting defects.

3.2 Refractory Coating of the Pattern

It is possible to successfully cast products without coating the pattern prior to casting. These castings do however have a rougher surface finish than castings with a refractory coating.

The role of the refractory coating is evident in the quality of the casting. Not only is it a barrier between the steel shot and the pattern, but it performs a vital role in the escape of gaseous products produced by the degradation of the pattern as illustrated in Figure 3.3. If the refractory coating permeability is too low, gaseous products cannot escape, which may lead to defects in the casting. In magnetic moulding, it prevents the diffusion of molten metal into the mould material.

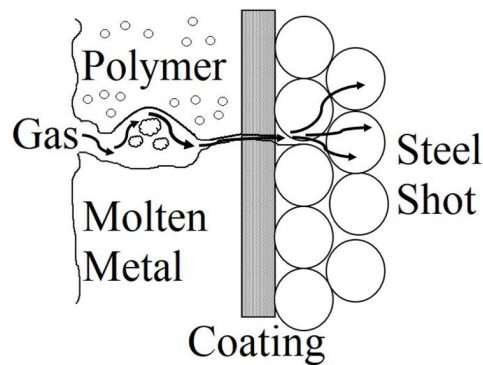


Figure 3.3: Illustration of the permeability of the coating during the gasification of the foam pattern

The properties of the refractory coating depend on the metal being cast, the volume of the pattern, the pattern material and density and also the wall thickness of the pattern.

In the case where ductile iron is the casting material, it is important to note that the higher casting temperature will result in increased volumes of gas released during the degradation of the pattern. It is required that the coating material have good thermal resistance to avoid mould collapse and good permeability to allow the escape of gaseous product. Coating thickness is, therefore, an important factor to consider.

The coatings typically applied in the lost-foam casting process are ceramic coatings such as Talc, Mullite, Zirconium and Cordierite. The composition of these coatings are foundry specific and recipes may vary. Typical compositions of these coatings are tabulated in Table 3.1 [33].

Table 3.1: Percentage composition of various ceramic coatings used in the lost-foam casting process

Refractory [%]	Binder [%]	Agent keeping suspension stable [%]
Zirconium: 90 Granulation 35-40 μm	Bentonite: 3-4 Bindal H: 5-6	Dextrin: 0.5-1 Lucel: 0.5-1
Talc: 88 Granulation: 30-35 μm	Bentonite: 5-6 Bindal H: 6-8	Dextrin: 0.5-1 Lucel: 0.5-1
Mullite: 90 Granulation: 40-45 μm	Bentonite: 3-4 Bindal H: 5-6	Dextrin: 0.5-1 Lucel: 0.5-1
Cordierite: 92 Granulation: 35-40 μm	Bentonite: 1-2 $\text{Na}_5\text{P}_3\text{O}_{10}$: 6-10	Carboxymethyl cellulose: 0.5-1

A water base suspension with densities ranging between 2-3g/cm³ are used in the lost-foam casting process [33] [34]. Solvents containing hydrocarbons and chloride will break down an EPS pattern, and therefore water is the most popular solvent.

Research performed on the coating of EPS patterns with these coating materials, indicated that a coating layer thickness higher than 0.5mm and lower than 1.5mm is most effective for casting aluminium alloys [34]. The layer thickness will differ for ductile iron castings, but these values may be used as guidelines.

The application of the refractory coating may be performed by dipping the part in the refractory coating, by brushing, spraying or flow coating. The method of applying the coating depends on the size of the pattern. Dipping is usually performed on small to medium patterns.

Mullite is widely used as a coating material in the lost-foam casting process. It is an aluminosilicate refractory with an ideal composition of 62.92 wt% alumina and 37.08 wt% silica [35]. Mullite is rarely found in nature, but the base minerals are readily available in big quantities. Mullite has a high thermal stability, low thermal expansion and thermal conductivity and the highest fracture toughness when compared to the other coating materials [36]. Mullite is manufactured using refractory clays, bauxite

and alumina silicates such as sillimanite, andalusite and kyanite [35].

3.3 Mould Making

The principal of magnetic moulding is based on replacing the conventional sand of the lost-foam process with magnetic iron or steel shot. In addition to the lost-foam casting advantages the process inherits, it adds profound value to the application of the process on complex shapes, such as valve bodies.

This process allows for the production of parts without joint-lines, which is especially applicable to the production of valve bodies. The absence of a joint-line implicates an increased pressure resistance of the valve. Defects associated with joint-lines are eliminated and the accuracy of castings are increased. A higher quality valve may thus be cast at a lower cost.

Furthermore, the increased thermal conductivity of steel shot or iron has numerous microstructural advantages, such as grain refinement of the cast metal [13]. According to Geffroy *et al.*, the increase in thermal conductivity results in an increase in the cooling rate [24]. An increase in the cooling rate results in grain refinement, which increases the nodule count and may lead to the improvement of the mechanical properties of the cast material [24].

The shape of the iron or steel shot is important as the homogeneous and good compaction of the mould material increases the mechanical properties of the magnetic mould [26]. According to Geffroy *et al.* and Suganth kumara *et al.*, a spherical particle with a diameter between 0.4mm and 1mm and a bulk density of 4.5g/cm³ has shown to result in successful castings.

Suganth kumara *et al.* has studied the nature of the packing of the spheres during magnetisation. In their numerical prediction, the Specific Grain Number (SPG) was determined based on the assumption that the spheres arrange themselves in a Face

Centered Cubic (FCC) structure when closely packed [26]. In an FCC arrangement, 4 atoms exist in a unit cube and under observation, the majority of spheres are surrounded by 4 spheres in one plane, hence the assumption of an FCC packing structure.

The packing factor was verified by the analysis of images produced by a boroscope inserted at various points in a mould. The results are shown in Figure 3.4. The experiment was conducted with 0.4, 0.6 and 0.8mm diameter spheres. From the histogram, the numerical prediction of a coordination number of 4, is justified.

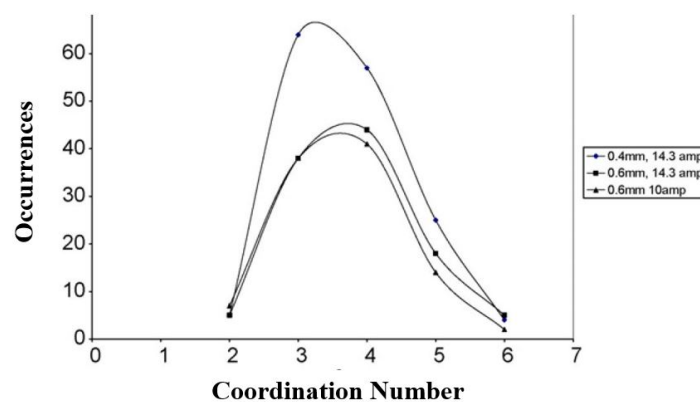


Figure 3.4: Histogram of the occurrence of the coordination number of steel shot spheres obtained from boroscope images by *Suganth kumara et al.* [26]

In the same study, the effect of shot size on the strength of the magnetic mould was studied [26]. It was concluded that the strength of the magnetic mould is highest with a sphere diameter of 0.4mm. This is seen in Figure 3.5. Although smaller spheres have increased strength characteristics, it should be noted that a smaller sphere diameter also implicates lower permeability, which is associated with defects such as porosity and blow holes [26].

The cooling curves and thermal conductivity of grey cast iron were measured by *Geffroy et al.* The solidification curves for a sand mould, steel shot mould and steel mould were documented in the histogram shown in Figure 3.6. It can be observed that the solidification time decrease with an increase in the thermal conductivity.

With the use of Chvorinov's rule, the solidification times of the casting in sand, steel and steel shot moulds were calculated by *Geffroy et al.* It was then compared with

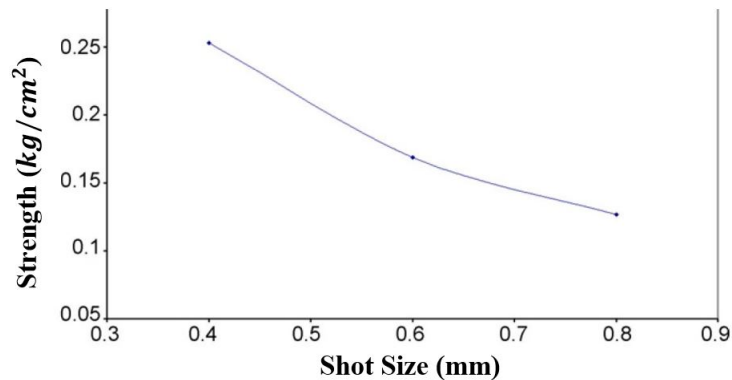


Figure 3.5: Histogram of the influence of sphere size on the strength of magnetic mould as studied by *Suganth kumara et al.* [26]

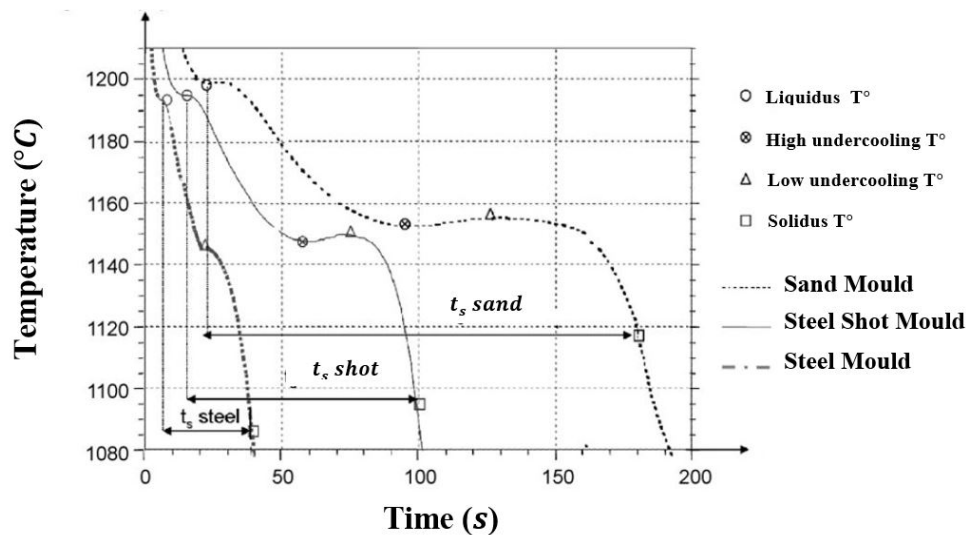


Figure 3.6: Solidification curves of different moulds as experimentally determined by *Geffroy et al.* [24]

experimentally measured values and it was found that the values do not coincide with the theoretical values for the steel mould. *Geffroy et al.* concluded that Chvorinov's rule cannot be applied to steel due to the fact that the thermal resistance of the metal/mould contact has a very similar value to that of a steel mould [24]. Table 3.2 indicates the correlation between the calculated solidification times and the measured solidification times.

Table 3.2: Thermal properties and solidification times of various moulds obtained by Geffroy *et al.* [24]

Properties (at room temperature)	Sand Mould	Steel Shot Mould	Steel Mould
X: Thermal conductivity(W/mK)	1	1.2	17
C: Specific heat(J/kgK)	730	475	475
ρ : Specific heat(Kg/m ³)	1770	4710	7800
Calculated solidification time/ solidification time in sand mould	160	80	3
Measured solidification time	160	85	30

The number of steel shot spheres surrounding the pattern should be sufficient to ensure effective heat transfer. The conduction from one steel sphere to the next steel sphere most definitely impacts the rate of cooling. It can be assumed that the cooling rate of the molten metal is faster when more spheres are available to transfer the heat. In the case where too little shot is used as mould material, the steel shot may reach the magnetic transition temperature (Curie temperature) at 770°C and the mould may collapse. Ideally, a 3-dimensional heat distribution analysis of the part being cast in the steel shot would give significant insight into the determination of the optimal amount of steel shot for a specific part being cast.

The thermal properties obtained by Geffroy *et al.* may be used as starting point to minimise the number of unknown parameters in a Computational Flow Dynamics (CFD) analysis. A thermal analysis may also shed light on the possibility of casting functionally graded materials. An investigation of various steel shot sizes at strategically positioned areas such as the use of larger diameter shot at thin sections may slow the cooling rate and prevent cold shuts. Revolutionary insight may be gained into the alteration and enhancement of mechanical properties of castings by the thermal study of magnetic moulding.

When the microstructure of ductile iron obtained with magnetic moulding was compared with the microstructure obtained with a standard sand mould, an increase in the nodule count was observed as shown in Figure 3.7 [24]. The increase in nodules correlates with the increase in mechanical properties obtained with the magnetic mould.

This is shown in Table 3.3.

Table 3.3: Mechanical properties of ductile iron castings obtained with a steel shot mould and a sand mould as determined by *Geffroy et al.*

Process	Lost-Foam	Magnetic Moulding	SSM/SM
Young's Modulus	152GPa	166GPa	1.09
Yield Strength	292MPa	318MPa	1.09
Ultimate Strength	450MPa	453MPa	0.99
Elongation	15.5%	14.8%	0.95

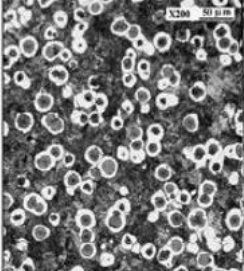
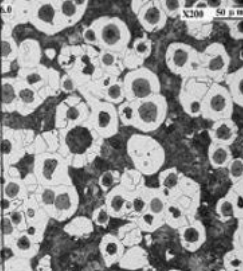
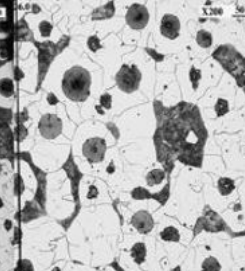
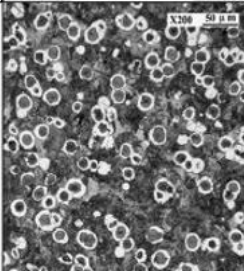
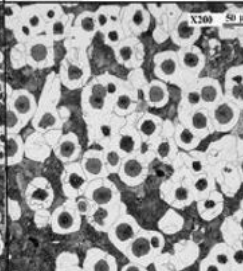
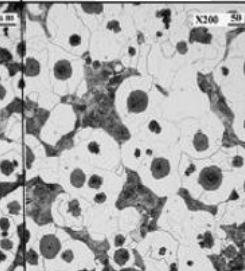
Thermal Modulus	0.2 cm	0.4 cm	0.8 cm
Sand Mould			
Ferritic Matrix Nodule Size:	10% 18-20 μm	55-60% 22-25 μm	90% 32-42 μm
Steel Shot Mould			
Ferritic Matrix Nodule Size:	5-10% 16-18 μm	45-50% 20-22 μm	70-80% 28-40 μm

Figure 3.7: The difference in microstructure of ductile iron between a sand mould and a steel shot mould as obtained by *Geffroy et al.* [24]

The function of applying a magnetic field to the steel shot mould, is primarily to increase the cohesion of the mould. In Figure 3.8 the cohesion of a sand mould and steel shot mould were modelled. It is evident that the magnetic field results in increased cohesion of the mould.

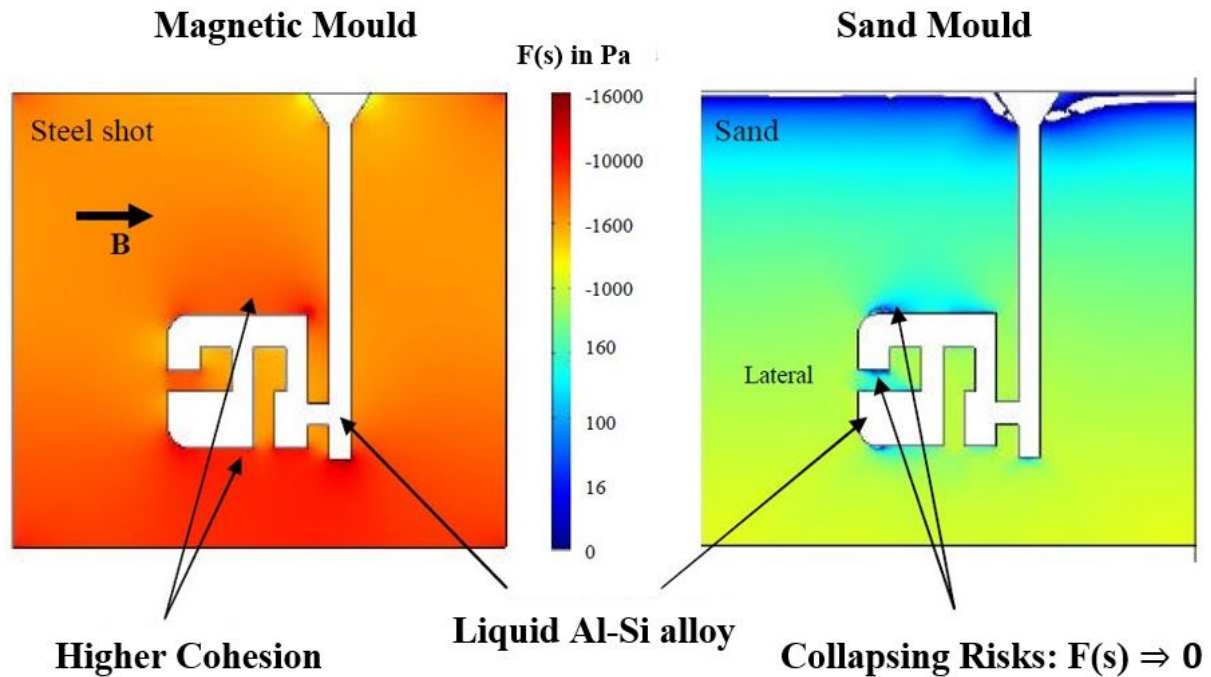


Figure 3.8: Simulation of the distribution of force between steel shot spheres in magnetic moulding and the force between sand grains in lost-foam casting, compared by Goni *et al.* Better cohesion is obtained with the magnetic steel shot mould.

The increase in cohesion leads to an increase in the dimensional accuracy of the castings when compared to the conventional lost-foam process [25]. The increased cohesion of the mould also results in a decrease in casting defects, such as shrinkage. This is shown in Figure 3.9 where two grey cast iron casting were cast with the magnetic moulding process where no magnetic field was applied and in the case where the magnetic field was applied [25]. The electromagnet thus plays an important role in the quality of castings.

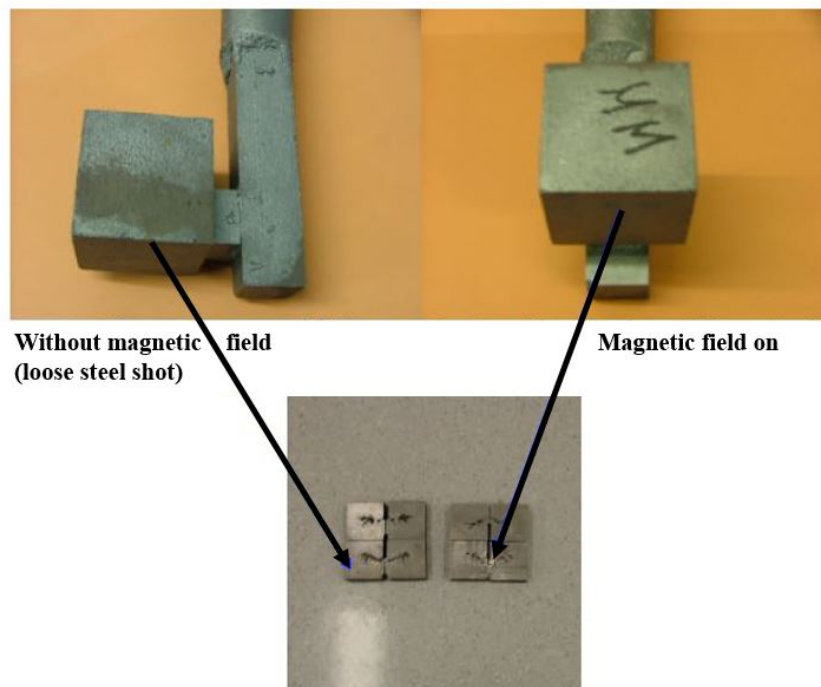


Figure 3.9: Castings performed with steel shot as mould material with the magnetic field on and off. A decrease in shrinkage is observed in the casting with the magnetic field on [25]

3.4 Electromagnet Configuration

An "u"-shaped magnet or solenoid coil magnet has been used in the magnetic moulding process. The main difference between the two types of equipment lies within the orientation of the magnetic field. The right-hand rule applies and the direction of magnetic field in a u-shaped magnet is horizontal, whilst the direction of the magnetic field for a solenoid is vertical. The flow of the magnetic field in both cases are illustrated in Figure 3.10.

The influence of the magnetic field on the microstructure of aluminium alloys and grey cast iron castings was studied by a co-operative research project group in 2004. The group concluded that no influence on the orientation of the microstructure of any phase due to the magnetic field alone, was observed [25]. The influence on the direction of the magnetic field was also studied.

In an experiment where a part was cast with the magnetic field direction parallel and

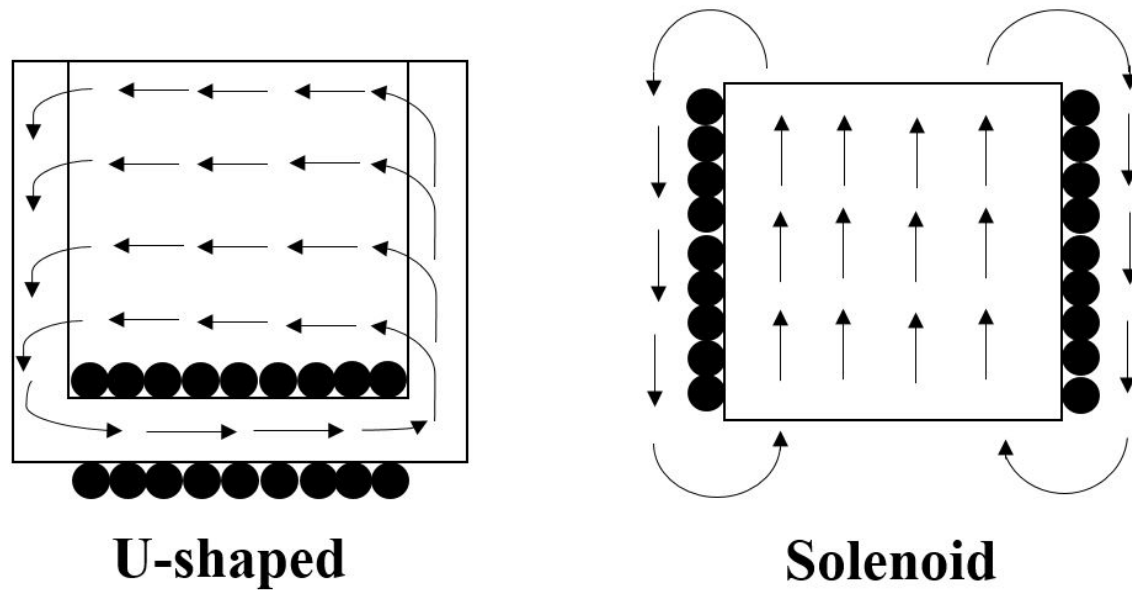


Figure 3.10: Direction of magnetic field in U-shaped and solenoid electromagnet

perpendicular to the part being cast, it was found that no appreciable difference between the two castings could be observed [25]. In an additional experiment, the same pattern was cast, but different pattern orientations in the mould were used.

In the lost-foam casting process where sand is used, different orientations of patterns in moulds are not always possible due to low rigidity of the sand mould [25]. Both orientations produced sound casting and it was concluded that the cohesion of the magnetic field allows for different orientation castings, without any loss in integrity of the cast part [25]. The selection of the type of electromagnet, therefore, depends on the available materials and manufacturing capabilities, and not on the orientation of the magnetic field.

The literature review on magnetic moulding may now be applied in the design of the casting process. The appropriate selection of process components will reflect in the success or failure of the cast part.

3.5 Scope

The extensive literature review on valve manufacturing and magnetic moulding in particular, contributed to the establishment of the scope. The scope is listed below:

1. Configure all components of the magnetic moulding process based on knowledge obtained in literature.
2. Use software packages to simulate and investigate the electromagnetic field and the feeding system design with casting simulation software.
3. Manufacture the components of the designed magnetic moulding process.
4. Assemble all components of the magnetic moulding process and verify design parameters.
5. Define a casting procedure with specifications associated with the implementation of the process during casting.
6. Complete a safety study with precautions to prevent damage to equipment or injury of personnel during operation of magnetic moulding process.
7. Perform a set of castings with the magnetic moulding process.
8. Evaluate the casting process and the results obtained with the magnetic moulding casting process.
9. Summarise the observations and evaluation to establish the feasibility of the process.
10. Conclude on the feasibility of the magnetic moulding process and recommend improvements for future studies.

Chapter 4

Magnetic Moulding Casting Process

The implementation of the magnetic moulding casting process is established with the selection and design of various components in the process steps. The rationale behind the design of the process components is discussed and finally a casting procedure is developed with detailed steps and instructions.

4.1 Configuration and Setup

The application of magnetic moulding in the casting of a ductile iron valve started with the drawing of the part to be manufactured, which is the pattern of a valve body. The pattern dimensions and geometry determined the size of the electromagnet. The exact dimensions and geometry of the electromagnet were determined by iterations of various simulations performed in Finite Element Method Magnetics (FEMM), a software package that simulates the electromagnetic field.

The complete SolidWorks model of the magnetic moulding process components is shown in Figure 4.1. The components are discussed in the subsequent sections.

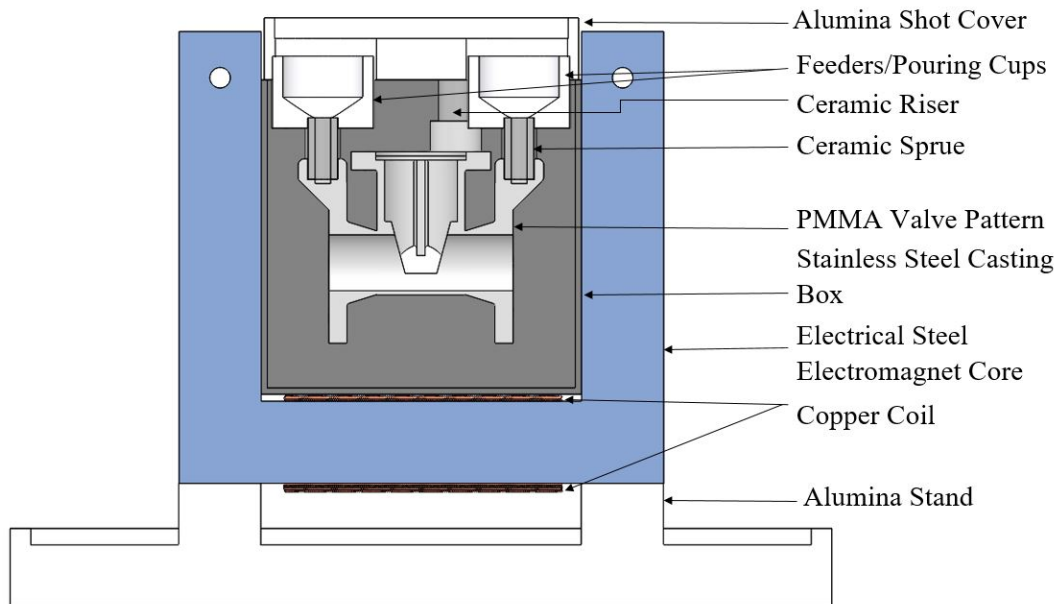


Figure 4.1: The magnetic moulding casting assembly as modelled in SolidWorks

4.1.1 Pattern Selection

In the lost-foam process, the pattern is a replica of the final part to be cast. It was, therefore, necessary to select a valve and design the pattern based on the selected valve design.

Sketches with dimensions of industrial valves are not easily obtained and generally have to be purchased. A valve was available for measuring to create a Computer Aided Design (CAD) drawing. The use of a 3D-scanner was considered, but it was not financially feasible to apply this method to this project.

Manual measurements were made with the use of a vernier and measuring tape and a 1:1 scale model was created in the software program, SolidWorks. The software model of the complete valve assembly is shown in Figure 4.2 below. As discussed earlier, the valve body was considered the primary focus and therefore the part to be cast. The valve body was scaled to 40% of the original part size. The scaling comparison is shown in Figure 4.3.

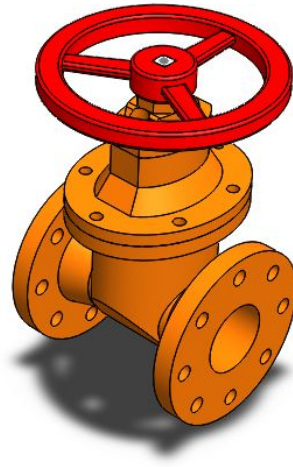


Figure 4.2: Model of the valve assembly

Scaling was necessary due to the following considerations:

- A decrease in the size of the pattern results in a decrease in pattern material (Lower pattern material costs)
- The manufacturing cost of the pattern is lowered by a decrease in size of the pattern (Fewer machine hours)
- The pattern manufacturing facility's capabilities limit the size of the pattern
- A smaller part requires less casting material
- The required capabilities of the casting facility depends on the scale of the part to be cast
- The size of the electromagnet depends on the size of the pattern
- The overall cost of the project is decreased by a decrease in the scale of the pattern
- It is easier to handle and control a smaller pattern, and therefore a smaller electromagnet

The pattern material requirements were:

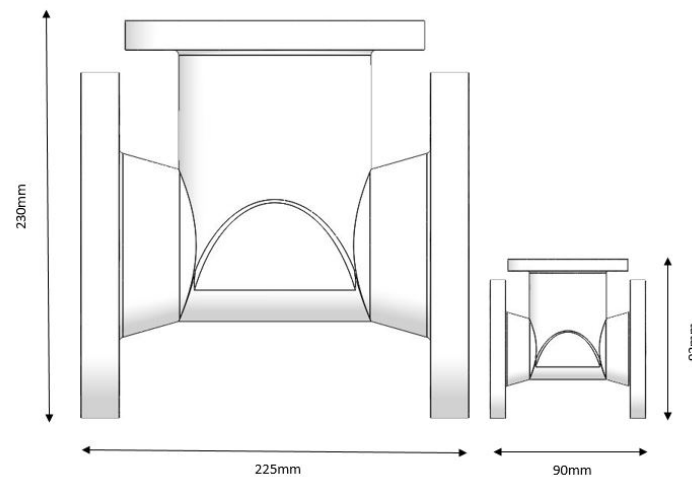


Figure 4.3: Illustration of scaling of the valve body to 40% of the original size

- Low thermal conductivity for fast thermal degradation
- Ease of manufacturing
- Cost of manufacturing
- Material cost

The properties of EPS, PMMA, ABS and PLA were compared as shown in Table 4.1. It is interesting to observe that EPS has the lowest thermal conductivity and the lowest cost. The carbon content of the cast part was not a high priority as the feasibility of the method of casting was the main focus. With the aim of a very low quantity of castings, the low volume of patterns required and the complexity of the part, machining of an EPS valve was ruled uneconomical.

The best alternative to EPS was PMMA. As with EPS, the material could not be machined. With additive manufacturing, the cost of low quantity patterns would be significantly lower. Due to the fact that PMMA may be 3D-printed, PMMA was selected as pattern material and the manufacturing method was additive manufacturing.

Table 4.1: Comparison of the average pattern material properties

Property	EPS	PMMA	ABS	PLA
Density [kg/m ³]	1045	1185	1050	1320
Glass Temperature [°C]	89.5	95	104	163.5
Thermal Conductivity [W/mK]	0.126	0.209	0.230	0.280

4.1.2 Mould Material and Electromagnet

The shot material plays an important role in the cohesion of the mould. The selection of the shot material required a spherical shape with a diameter between 0.4 and 1mm and a ferritic chemical composition. Shot in an austenitic state would be of no use as the magnetic field would have no influence on this non-magnetic material.

Spherical steel shot used for blasting abrasives were selected as mould material based on the available chemical composition. The selected steel shot material correlates best with the composition of an AISI 1095 steel. The steel shot and AISI 1095 composition are shown in Table 4.2. The composition of the mould material is important as the calculations of the magnetic field produced by the electromagnet is influenced by it.

Table 4.2: Chemical composition of the selected steel shot and AISI 1095 steel

Element	Steel Shot	AISI 1095
Iron (Fe)	>96%	98%
Carbon (C)	0.8 - 1.2%	0.9 - 1.03%
Silicon (Si)	0.3 - 1.2%	0.15 - 0.3%
Manganese (Mn)	0.5 - 1.3%	0.3 - 0.5%
Sulphur (S)	<0.04%	≤ 0.05%
Phosphorus (P)	<0.04%	≤ 0.04%

The design of the electromagnet is based on the principles of electromagnetism as described mathematically. In most cases, the aim is to increase the magnetic field intensity. A magnetic field(H) is produced when electric current (I) is passed through a coil with n amount of turns and a length of l meters. The relationship is shown in Equation

4.1.

$$H = \frac{nI}{l} \quad (4.1)$$

From the equation, it can be derived that the magnetic field is increased by an increase in the number of turns of the coil or by an increase in the current. The number of turns is often limited due to the increase in length with more turns. An increase in the length of the coil will decrease the magnetic field. It is also most often more practical to vary the current, rather than changing the number of turns of the coil.

The magnetic field intensity in ampere-turn/m produces insufficient information to describe the effect of the induced magnetic field or the effect of the materials involved. This is where the magnetic flux density comes in. The flux density of inductance(B) is the number of lines of flux that are induced when a magnetic field is applied in a vacuum and is given by Equation 4.2. The magnetic permeability of vacuum, μ_0 , is a constant with a value of $4\pi \times 10^{-7}$.

$$B = \mu_0 H \quad (4.2)$$

In the case where a material is placed in the magnetic field, the magnetic flux density change according to how the magnetic dipoles of the material interact with the field. According to Wittmoser, a flux density between 0.1 and 0.5T is sufficient to increase the mechanical properties of the steel shot mould [24]. The permeability of the material(μ) is incorporated in Equation 4.3 below:

$$B = \mu H \quad (4.3)$$

The relative permeability μ_r is a relationship between the permeability of the material and the permeability of vacuum given by Equation 4.4. If the permeability of the magnetic material is very high compared with the material surrounding it, such as free space, most of the flux is confined to the highly permeable material [37]. A material with a large permeability carry magnetic flux easily and increases the magnetic field.

$$\mu_r = \frac{\mu}{\mu_0} \quad (4.4)$$

The effect of the magnetic material may be included in Equation 4.2. This is known as the magnetisation(M) which is responsible for the increase in inductance. Equation 4.2

can then be written as:

$$B = \mu_0 H + \mu_0 M \quad (4.5)$$

Equation 4.5 may be simplified to Equation 4.6 in the case of ferromagnetic and ferrimagnetic materials because $\mu_0 M > \mu_0 H$. In order to produce a high inductance or magnetisation, materials with high relative permeabilities should be selected.

$$B \approx \mu_0 M \quad (4.6)$$

Another indicator of the degree to which the material enhances the magnetic field is the magnetic susceptibility x_{ma} , which is the ratio between magnetisation and the magnetic field. Steel shot is a ferromagnetic material with a susceptibility of $x_{ma} \gg 1$ for low magnetic fields where $B < 0.4\text{T}$ [24].

$$x_{ma} = \frac{M}{H} \quad (4.7)$$

Ferromagnetic and ferrimagnetic materials have permeabilities that depend on the applied magnetic field, and therefore their permeabilities are not constant [17]. Each magnetic material has a magnetisation characteristic curve, referred to as a B-H curve. The saturation region of each magnetic material is of importance, as it is the point where all magnetic dipoles are aligned with the applied magnetic field. The flux density is then at a maximum. At this point, a saturated magnetic material has a permeability very close to that of free space. It may be assumed that all non-magnetic materials have the same permeability as free space, which is 1.00 [37].

A magnetic circuit can be analysed by using an equivalent reluctance circuit, which is similar to resistance in an electric circuit [37]. This rule may only be applied in a linear magnetic circuit. This implies that the permeability of each section of the magnetic circuit should be linear, which is not the case in magnetic moulding.

It is, however, possible to determine the required magnetomotive force (mmf) to maintain a certain flux density. In a magnetic circuit, the total current enclosed is referred to as the mmf which is measured in ampere-turn (A.t). The flux density in each magnetic section may be calculated and the magnetic field, H , may then be obtained from the B-H curve. The mmf drop over each magnetic section may then be determined and

summed to obtain the total mmf required. This method also has its limitations, due to the fact that it is an iterative process.

A guess value is required in one of the sections of the magnetic circuit. The applied mmf and the calculated mmf is compared and the guess value is adjusted for the next iteration. The application of this technique to the magnetic moulding process is unproductive as it is time-consuming and inaccurate. Today there are numerous software packages that may be used to simulate and design magnetic circuits. Examples are Ansys, COMSOL Multiphysics and FEMM.

FEMM is a user-friendly computer software program with a platform that enables the user to create or import drawings and solve magnetic problems by simulation. The program was used to obtain valuable information associated with the magnetic field and the design of the electromagnet. FEMM was used to:

- obtain the best position and orientation of the pattern in the mould,
- investigate the geometry and dimensions for the best electromagnet design and to
- select the magnetic field design parameters to obtain a flux density between 0.1 and 0.5T.

Before a simulation could be executed a basic design had to be selected and the materials of which the electromagnet will consist had to be chosen.

The dimensions of the cast box, which is the container in which the pattern is placed and then surrounded by the mould material were selected first. It was important that the container consists of a non-magnetic material. Based on the size of the pattern, roughly 20mm was added to the sides of the pattern in all directions. A cubic container was selected as the shape of the casting box.

The wall thickness of the casting box was an important factor to consider because if it is too thick, the magnetic field is weakened as the gap between the mould material

and the electromagnet core is increased. Yet, the casting box wall had to be rigid to withstand the force caused by the weight of the contents. The casting box also had to be able to withstand thermal conduction and radiation. Aluminum or austenitic stainless steel was, therefore, the preferred materials for the manufacturing of the casting box. Both these materials are readily available and affordable whilst adhering to the specified requirements.

The flux density region in which the electromagnet should effectively operate is between 0.1 and 0.5T, therefore the B-H curve of the electromagnetic core should have a knee higher than 0.5T before the saturation region starts. The knee of the magnetisation curve is the region where magnetic saturation starts to set in. Although various materials may be appropriate to be used as an electromagnetic core, electrical steel is widely used in the electro-mechanical industry. A typical magnetisation curve or B-H curve is shown in Figure 4.4.

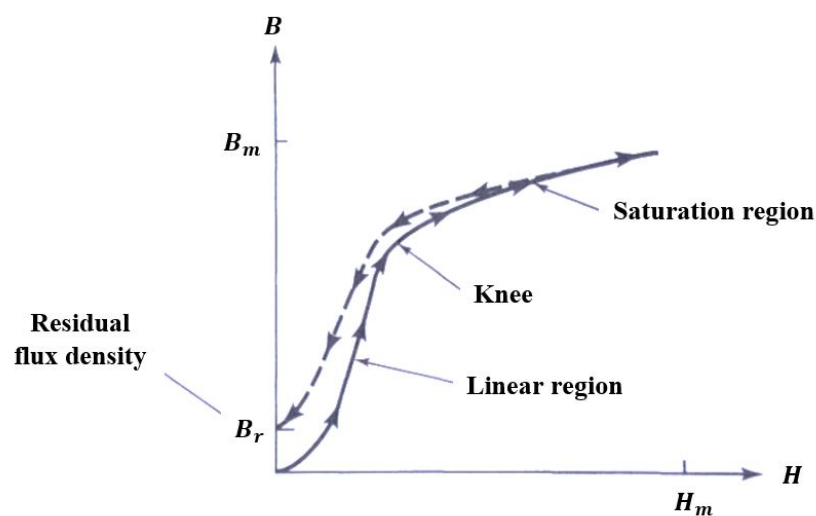


Figure 4.4: A typical magnetisation curve for a ferromagnetic material indicating the knee of the curve

Electrical steel is also referred to as silicon steel. It may be grain orientated or non-grain orientated. Non-grain orientated electrical steel was used. Non-grain orientated magnetic properties are equal in all directions and are used in applications where low cost is favoured. Electrical steel has exceptional electrical conductivity and has a lower density, which makes it a lighter material as opposed to other standard steels and iron.

The relative permeability of the steel shot is not linear and unknown. The packing factor of the steel shot spheres is assumed to be 0.74 for an FCC structure [26]. This implies that if all spheres in the casting box follow this packing arrangement, 74% of the mould material is steel shot and 26% is air. There is no B-H curve available for this "material".

In order to accurately simulate the shot material, each individual sphere should be drawn in a FCC packing arrangement in the casting box. This would be an extremely labour intensive and time-consuming task, especially in FEMM, with no guarantee of success. Furthermore, it is not acceptable to simulate the mould by dividing the mould material in a 26% air and 74% shot composition. The exact position of each sphere and air gap directly influence the magnetic flux density and field. With no other alternative, the mould material was simulated as if the casting box was filled with AISI 1095 steel, without any air gaps.

The first set of simulations were performed on a fixed geometry with fixed dimensions. The aim of the simulations was to investigate the effect of the orientation of the valve on the magnetic flux density. The current, number of turns and materials were kept consistent in each simulation, as shown in Figure 4.5.

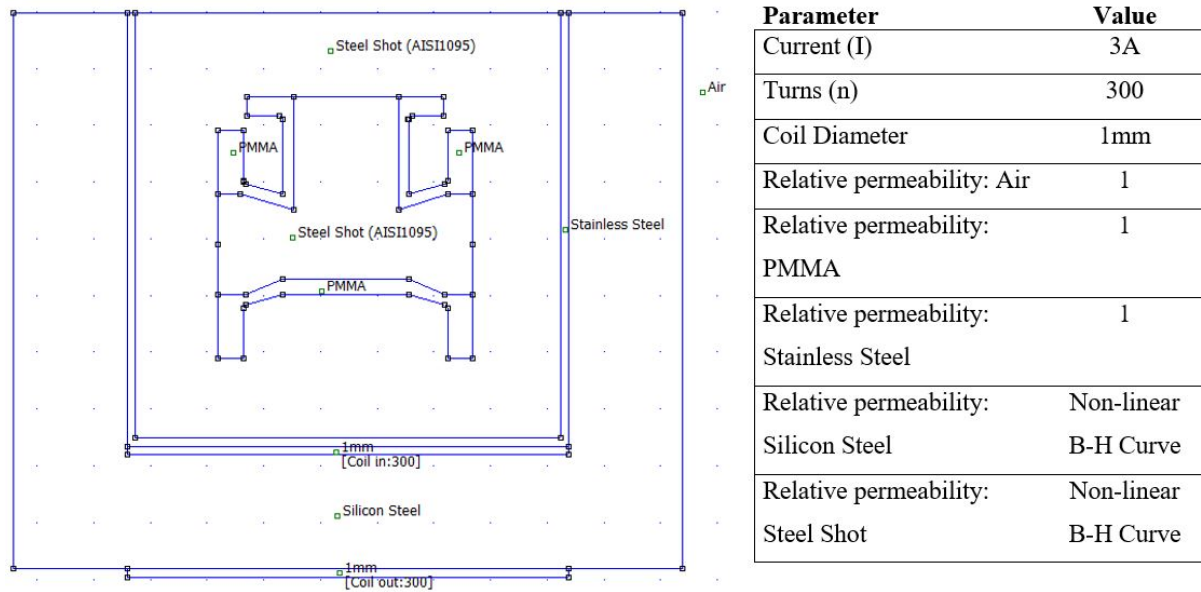


Figure 4.5: Pattern geometry and parameters kept constant for orientation and position simulations

The number of possible orientations was limited as FEMM is not equipped to simulate complex three-dimensional parts. A depth can be specified as an approximation as it assumes the geometry is consistent through the z-plane, but in the case where the valve is to be positioned as shown in Figure 4.6, the flux density is even more difficult to simulate.

When the valve pattern is positioned in the casting box and the box is filled with steel shot, the steel shot should effectively fill up all cavities because no cores are used in this method. The cohesion of the steel shot in these cavities should be very high to ensure dimensional accuracy. The orientation of the pattern should thus allow maximum cohesion.

If the positions shown in Figure 4.6 are discarded, four other orientations are possible. If the valve is positioned as shown in A of Figure 4.7 and it is flipped or the direction of the magnetic field is changed to flow in the opposite direction, similar results are obtained. The magnetic field always follows the path with the highest permeability, and due to the low permeability of the PMMA, a very low flux density is observed in

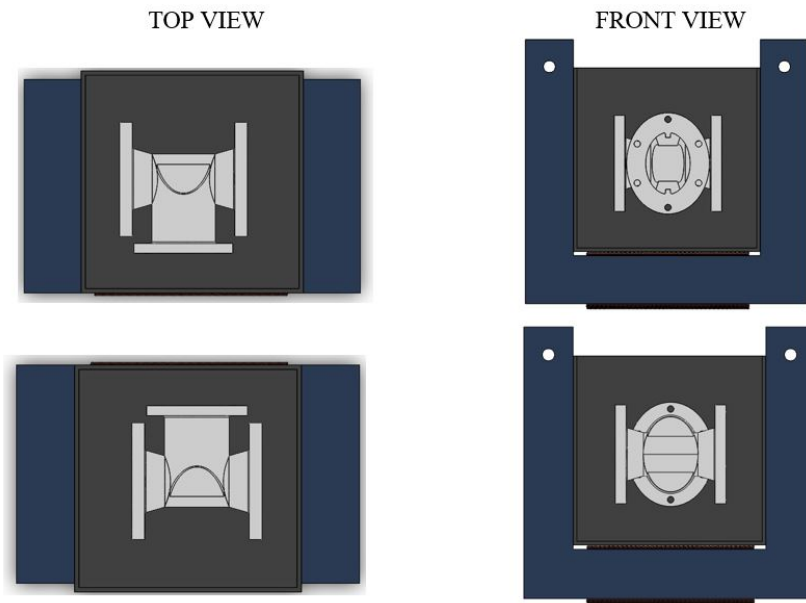


Figure 4.6: Illustrations of pattern orientations not suitable to simulate in FEMM

area 1. In orientation position A, maximum cohesion cannot be assured in the fluid pathway of the valve pattern. The three main orientations are A, B and C as shown in Figure 4.7.

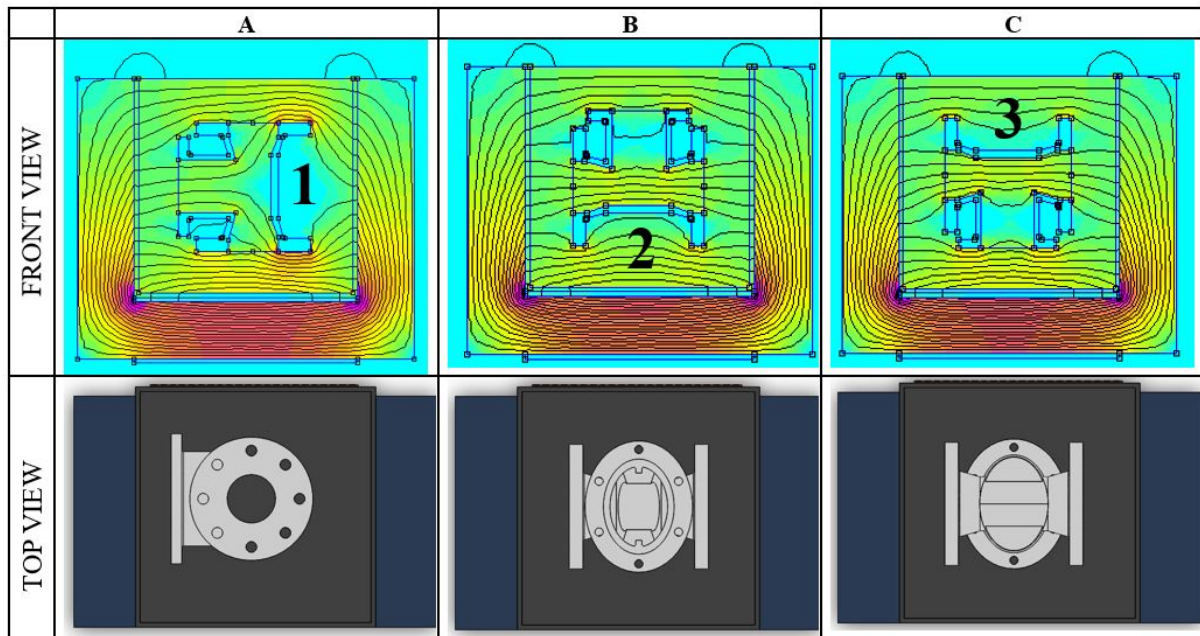


Figure 4.7: Illustrations of pattern orientations suitable for FEMM simulations

The orientation shown in C permits similar magnetic fields and flux densities as shown in orientation B. The difference in orientations are the flux densities observed at area 2 and 3. Area 3 in orientation C has a lower cohesion than area 2 in orientation B. Areas 1, 2 and 3 are areas where the wall thickness of the valve pattern is low. Good cohesion and rigidity of the mould in these areas will ensure a dimensionally accurate casting. Orientation B was therefore selected as the preferred orientation for the valve pattern, based on the following considerations.

When the flux densities and magnetic field lines are observed, better cohesion of the mould is obtained when the valve is in orientation position B, with top flange facing up. In this position, the magnetisation of steel shot through the pattern openings are most advantageous. The upward facing flanges in orientation B provides room for a feeding and riser system. If the feeding system is to be mounted on the top flanges, the flanges are likely to be machined after casting to remove the feeders. The slightly lower flux densities experienced at the top flange in orientation B is therefore not a problem. In the unlikely case where dimensional accuracy is insufficient due to lower cohesion of the mould at the top flange, the holes may be bored and the flanges machined as part of the finishing process. In orientation C, the bottom part of the valve may not be machined as easily as the top flange.

Once the orientation was determined, the optimum position could be evaluated. Five positions and the flux densities in the surrounding areas were simulated and compared as shown in Figure 4.8. It was concluded that a position closer to the coil core resulted in higher flux densities in most of the surrounding areas (area 1,3,4). It should be noted that the maximum flux density of the core was higher when the valve pattern was placed close to the core of the coil. This implies that although a higher flux density is achieved in this position, saturation may result in the coil core quicker than other orientations. All flux densities in area 6 are equal as the same electromagnetic parameters were used in all the position simulations. The colour differences in the schematic indicate the density plot. A deep pink indicates maximum flux density.

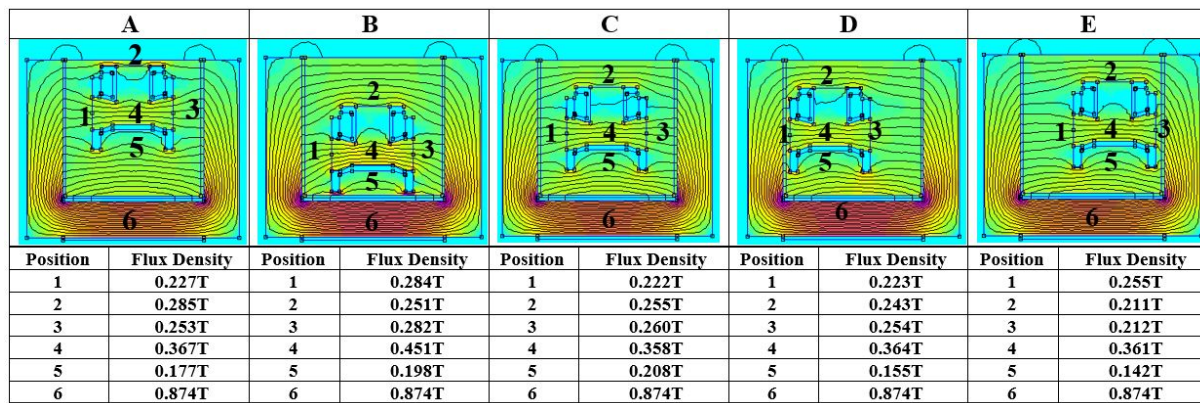


Figure 4.8: Pattern positions and flux densities in specified areas obtained by FEMM simulations

The flux densities of position C, D and E correlates with the findings of Suganth kumar *et al* [26]. They concluded that the best position to place a valve is in the centre of the casting box. Due to the magnetic field flowing in one direction, a slightly increased magnetic flux density is experienced at the side where the magnetic field originates and flows from. On the other side of the pattern, the magnetic flux density is lower. Position C allows for uniform magnetisation as there is no advantage in placing the pattern on either side of the electromagnet.

When Figure 4.9 is observed, low flux densities are seen in the top and bottom corners of the electromagnet. Furthermore, saturation may occur at the inside corners of the electromagnet core due to high flux densities, as indicated by the arrows. The possibility to increase the efficiency of the electromagnet by preventing saturation and utilising the complete geometry of the electromagnet was investigated. The possibility to exclude the corners indicating low flux density was also simulated.

The effect of various geometries and electromagnet dimensions were investigated. Geometry has a significant effect on the distribution and value of the flux densities. The maximum flux density should be lower than the knee of the core material's B-H curve. The selected electrical steel used in the simulations has a knee of 1.49T at 2500H.

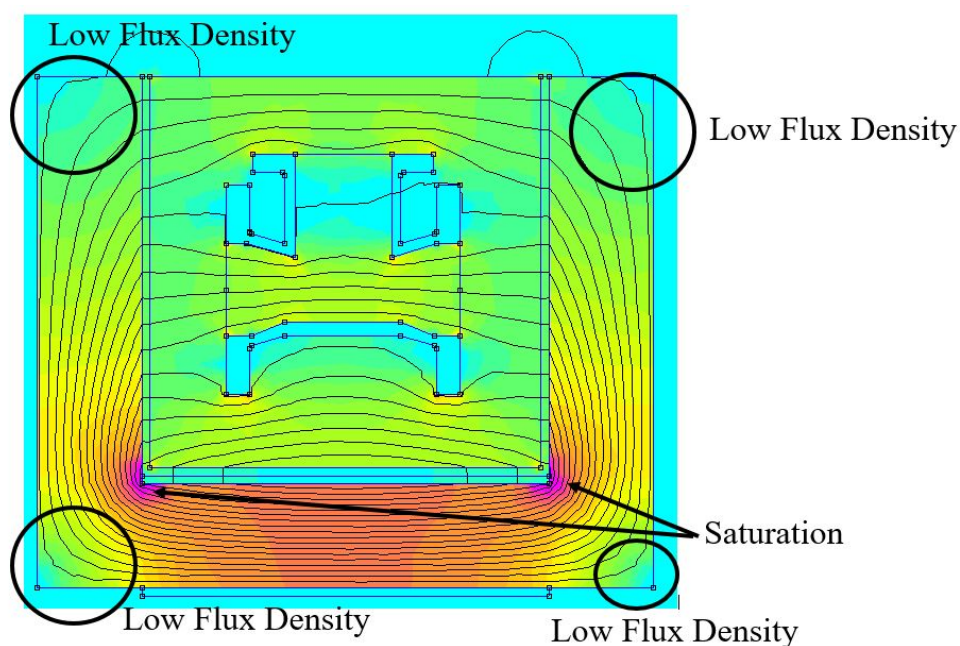


Figure 4.9: Low flux densities and saturation in original model of electromagnet in a FEMM simulation

In an effort to eliminate unutilised material and reduce the magnetic flux concentrations caused by sharp corners, the geometries seen in Figure 4.10 were some of the concepts investigated. The concentration of high flux densities at the coil core is expected. If the high concentration of the flux density at the coil core is better distributed, the heat generated by the coil will be lower and therefore the electromagnet will function more effectively.

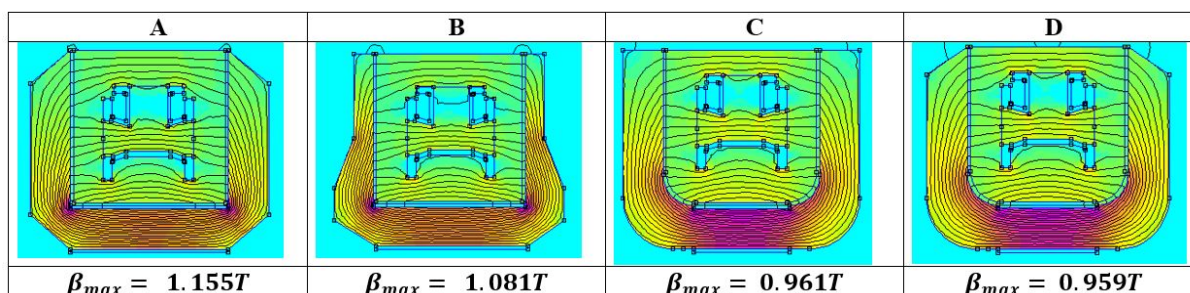


Figure 4.10: Various geometry concepts for the effective use of material and to limit saturation in sharp inside corners as simulated in FEMM

The geometries with the possibility to increase the efficiency of the electromagnet by reducing the areas of low flux density such as geometry A, B and D have the added

advantage of decreasing the weight of the electromagnet. The use of electrical steel has the advantage of lower weight than other core materials, but depending on the selected depth and number of electrical steel plates used, the weight of the complete electromagnet was a factor to consider.

Ultimately the ease and cost of manufacturing were considered and it was established that geometries C and D do present a better distribution of flux densities when the sharp corners are eliminated, but it results in a higher concentration of flux in the coil core. The U-shape will also lead to the insufficient use of electrical steel plates, which in turn will increase the cost. This is also true for geometry A and B.

Furthermore, the possibility of saturation in the sharp corners of the electromagnet may result in the saturation of the steel shot in the corners. This, however, will not result in dimensional defects in the casting due to the position of the pattern in the casting box. For this project, it was not worth the additional costs to implement the geometries as shown in Figure 4.10.

A simple rectangular shaped electromagnet was selected as the geometry to be used for further simulations. Various dimensions of the electromagnet and the effect of changing the parameters of the electromagnet were investigated to obtain the best combination for the electromagnet design. The result is shown in Figure 4.11. A drawing with dimensional and material information may be found in Appendix B.

The results in Figure 4.11 were obtained with the following parameter values in Table 4.3. In the positions indicated on the figure, it can be seen that all values were below the knee flux density of the material. The requirement to maintain a magnetic flux density between 0.1T and 0.5T was also satisfied in all areas surrounding the valve.

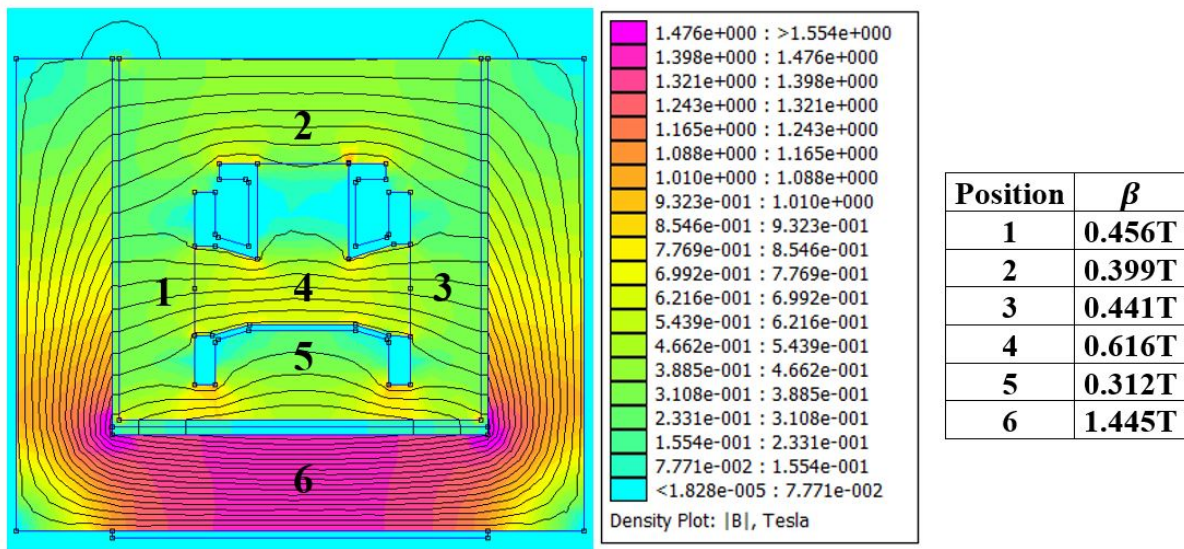


Figure 4.11: Flux densities at various points of final FEMM simulation model

Table 4.3: Parameter values used in the FEMM simulations to obtain satisfying design results

Parameter	Value
Current (I)	5A
Turns (n)	300
Coil Diameter	1mm
Relative permeability: Air	1
Relative permeability: PMMA	1
Relative permeability: Stainless Steel	1
Relative permeability: Silicon Steel	Non-linear B-H Curve
Relative permeability: Steel Shot	Non-linear B-H Curve

4.1.3 Feeding System Design

The molten metal is poured into an opening referred to as the pouring cup or feeder. In complex pattern geometries, it may be necessary to include runners, which are pathways that direct molten metal to areas, especially where there is a risk of casting de-

fects. The production of gaseous products during the degradation of the pattern often requires the need for risers that allow the escape of gasses and force impurities to the surface in the risers, rather than in the part itself. Risers may also be used as an indication of a fully filled mould and as the part cools, risers may provide additional molten metal as required by the solidifying casting.

The design of a feeding system may be very complex as it is influenced by the geometry of the pattern, the casting material, the casting process and various other limiting factors. In the past, the implementation of feeding systems greatly relied on the experience and workmanship of individuals in the foundry industry. A process of trial and error significantly increases expenses.

In recent years advanced computer software programs have been developed to simulate the flow of molten metal in a part that is cast. It is now also possible to predict the position and severity of casting defects of most casting techniques. Other tools such as video x-ray radiography have significantly contributed to the understanding of the behaviour of metal liquids in real life casting applications [13].

An initial design is, however, necessary before a casting simulation can be performed. The designer is required to make an informed decision on the position of the feedings system and the initial dimensions and geometry. The simulation results are often used to alter the design to obtain satisfactory casting results.

The orientation of casting the valve was determined in the previous subsection. The flanges of the valve are the heaviest sections and require immediate filling and therefore the top of the side flanges was considered the most viable position for the pouring cup. On the scale of this casting, it is advisable that molten metal is poured into one pouring cup. A conical pouring cup is used for small castings. The highest point of a casting is used to position a riser, and therefore the top flange was selected as a possible place to mount the risers. The concept design is shown in Figure 4.12.

The first step in the calculations of the feeding system is determining the liquid metal volume that will be poured. The weight of total metal to be poured should be incor-

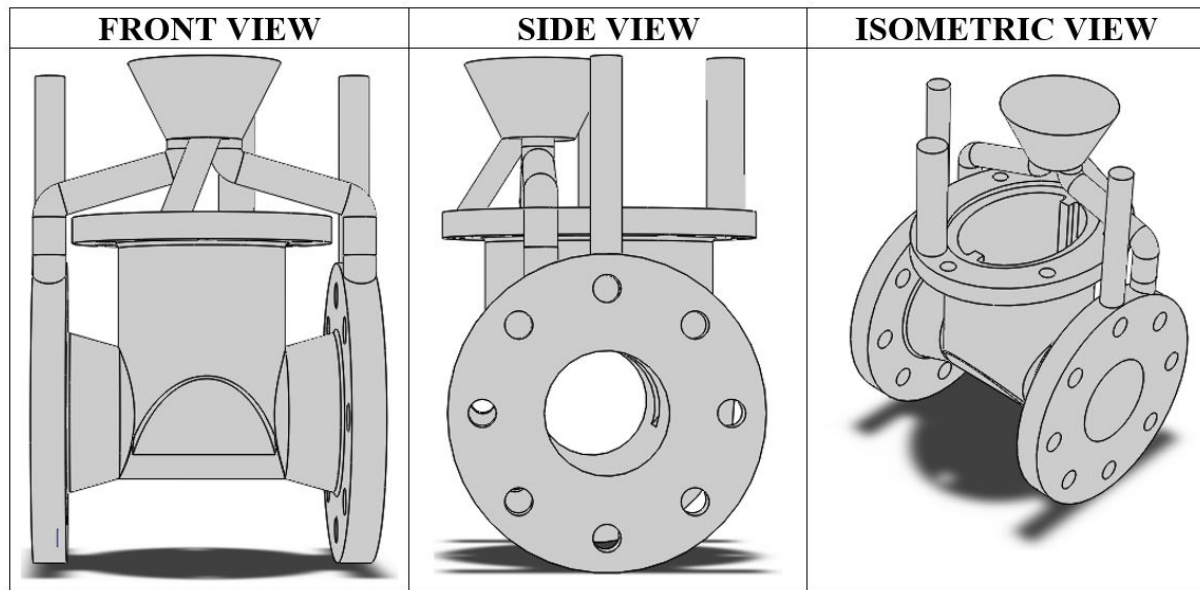


Figure 4.12: Model of concept designs of the feeding system

porated and therefore the design in Figure 4.12 was used to estimate the weight of the metal to be poured. Ductile iron with a density of 7100kg/m^3 was assigned to the valve assembly and an estimated weight of 1172.65g was obtained from SolidWorks.

$$V = \frac{W}{\rho} \therefore V = 0.165\ell \quad (4.8)$$

The pouring rate was determined with experimentally determined equations for grey iron castings. Equation 4.9 that applies to thin-walled castings with thicknesses between 2.5 and 15mm and a weight below 450kg was used:

$$t = S\sqrt{W} \quad (4.9)$$

where $S = 1.85$ is the coefficient for wall thicknesses between 3.5 and 8mm. Therefore:

$$t = 1.85\sqrt{1.173} \therefore t = 2s \quad (4.10)$$

The average filling rate is therefore:

$$F = \frac{W}{t} \therefore F = 0.587\text{kg/s} \quad (4.11)$$

The choke area can be determined and used as the sprue exit area. The choke area is the smallest area that may regulate the flow of liquid metal. The exit area of the pouring

cup may then be determined. In order to determine the choke area, the effective metal head of the casting should be known. This is determined as follow:

$$h_p = H_s - 0.5\left(\frac{h_1^2}{h_2}\right) \quad (4.12)$$

The value of the height of the sprue (H_s) may be varied as this value depends on the position of the pattern in the mould. The casting box has a height of 150mm, and the height of the casting (h_2) is 92mm. The maximum height of the pouring cup and sprue was limited to 58mm, as the feeding system should also be submerged in the steel shot, which is effectively the mould. It was also considered that the pattern cannot be placed directly on the floor of the casting box. A 5mm shot layer below the pattern was incorporated in the calculation of the height of the sprue and pouring cup. An allowance of 30mm was allocated to the pouring cup, and therefore the maximum height of the sprue was limited to 23mm. A program may be written to enable the possibility of various iterations to obtain a satisfactory choke area if the height of the sprue is varied.

As discussed the point of metal entry was selected as the side flanges. The height of the casting above the points of metal entry h_1 is 9mm. This value too may be varied if the point of metal entry is moved. The effective head was therefore calculated as follow:

$$h_p = 0.023 - 0.5\left(\frac{0.009}{0.092}\right) \therefore h_p = 0.023m \quad (4.13)$$

The choke area was then calculated with the equation below. The discharge coefficient (C_d) is 0.8, g is 9.8 m/s^2 , which is gravitational acceleration. With all values known, the choke area was calculated.

$$A = \frac{W}{\rho t C_d \sqrt{2gH}} = \frac{1.173}{7100 \times 2 \times 0.8 \sqrt{2 \times 9.8 \times 0.023}} \therefore A = 155 \times 10^{-6} m^2 \quad (4.14)$$

Another method to calculate the choke area is when the velocity of flow is accounted for. The velocity of flow of the metal should be lower or equal to the critical velocity of the liquid. For copper based alloys and iron alloys, the critical velocity (V) is 0.5m/s. Therefore:

$$A = \frac{W}{\rho t V} = \frac{1.173}{7100 \times 2 \times 0.5} \therefore A = 165 \times 10^{-6} m^2 \quad (4.15)$$

The use of the metal head in Equation 4.14 may be inaccurate because the metal head is very low since metal at the metal entry point is not much lower than the entrance of the sprue. The pressure head is thus very low. On the other hand, the velocity of flow of the liquid metal is very difficult to control by hand. The most conservative value for the choke area will thus be used to determine the area of the top of the sprue.

When Bernoulli's Theorem, $v^2 = 2gh$ is rewritten and substituted in the Law of Continuity $Q = A_1v_1 = A_2v_2$, the equation to calculate the area of the top of the sprue is formulated:

$$A_1 = A_2 \sqrt{\frac{d_1}{d_2}} \quad (4.16)$$

The distance between the ladle and the sprue top d_1 is the height of the pouring cup, which was limited to 0.03m and the distance from the ladle to the bottom of the sprue is the distance from the top of the pouring cup/feeder to the bottom of the sprue, which is 0.058m. The area is then calculated:

$$A_1 = 155 \times 10^{-6} \sqrt{\frac{0.058}{0.03}} \therefore A_1 = 216 \times 10^{-6} m^2 \quad (4.17)$$

The radius of the top of the sprue should, therefore, be in the range of 8mm, therefore 16mm diameter. The top area of the sprue is also the bottom area of the pouring cup/feeder. A conical feeder may be used for small castings. The dimensions of the feeder should be compatible with the ladle that will be used. The feeder should also allow a slight pressure head to form prior to entering the sprue.

It is possible to additive manufacture the pattern and the feeding system as one unit, but due to the reasons that follow, it was not considered an option. The high thermal gradient formed at the metal-PMMA interface results in faster cooling of the molten metal. By the time the molten metal reaches the pattern, a significant amount of energy will be lost and this may result in the inadequate filling of the pattern and possible defects.

Although the pattern and feeder may be coated with a refractory coating, the erosion caused by the flow of the molten metal may be too high and may lead to the collapse of the feeding system, resulting in poor to no feeding of the pattern.

Other materials were considered when a refractory coating alone could not be used for the feeding system. High-temperature materials with high thermal shock resistance were required for this application. Furthermore, the molten metal should not wet the feeding system.

Limited funding and the appropriateness of the use of a ceramic, such as alumina for a feeding system resulted in the selection of alumina as feeding system material. The feeder was designed based on available alumina fibre board. These boards are often used as insulation materials due to its high heat capacity, ease of machining and light weight. This material was selected for the feeder.

The selection of an alumina pipe significantly influenced the design of the feeding system. The limitation involved with the selection of alumina pipe as sprue material is the fact that bends are not possible. The implication of this is that both side flanges can no longer be fed from the same feeder. The concept design in Figure 4.12 then becomes impractical and irrelevant.

The final design of the feeding system is shown in Figure 4.13. An alumina pipe with an outer diameter of 17mm and an inner diameter of 15mm was used as sprue material. The sprue size was well within the range of the theoretically calculated estimate of 16mm. The feeder design is shown in Figure 4.14. Risers to allow for the escape of gas during the pyrolysis of the PMMA was added to the design of the feeding system.

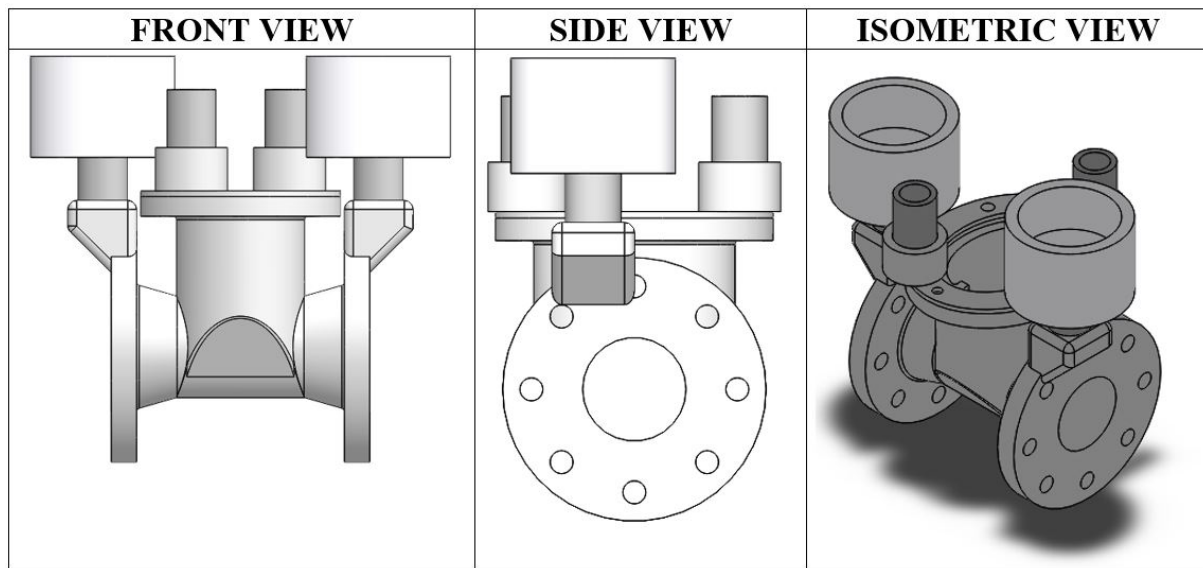


Figure 4.13: Model of the final design of the feeding system

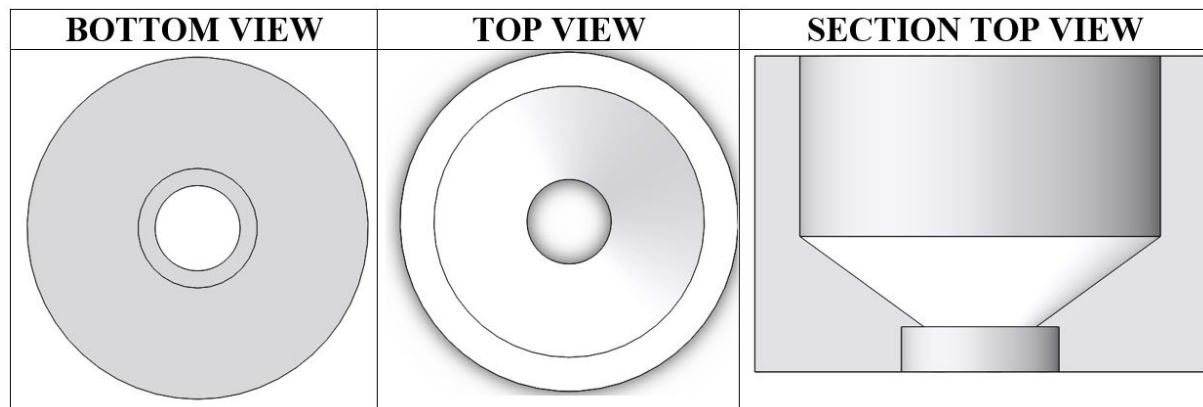


Figure 4.14: Model of the feeder/pouring cup

The feeder design was then simulated with MAGMASoft® to investigate the effectiveness of the feeding system. The use of steel shot as mould material has never been defined for MAGMASoft® simulation and does not fall within the scope of this study. Lost-foam casting with a sand mould was therefore used to simulate the filling of the pattern. PMMA in additive manufactured form has also never been simulated as pat-

tern material. Therefore there are two factors that influence the accuracy of the simulation.

Although the results of filling time and temperature could not be accurately simulated due to the difference in mainly the mould material and the printed PMMA pattern, the results were still useful. The results were used to obtain valuable information on the solidification and cooling characteristics of the pattern and feeding system.

The temperature distribution during casting was visually represented and areas with slower cooling rates could be identified as shown in Figure 4.15. The simulation of the flow tracer material indicated the flow of molten metal and the time an element of the molten metal stays in the casting before solidification. The flow tracer distribution and age is shown in Figure 4.16. The areas where porosity could be expected were identified and hot spots in the casting were identified. The hot spots are areas that cool slower than other areas of the casting which then result in casting defects. Figure 4.17 and Figure 4.18 shows the results of the casting simulations performed in MAGMASoft® for the porosity and hot spot investigation.

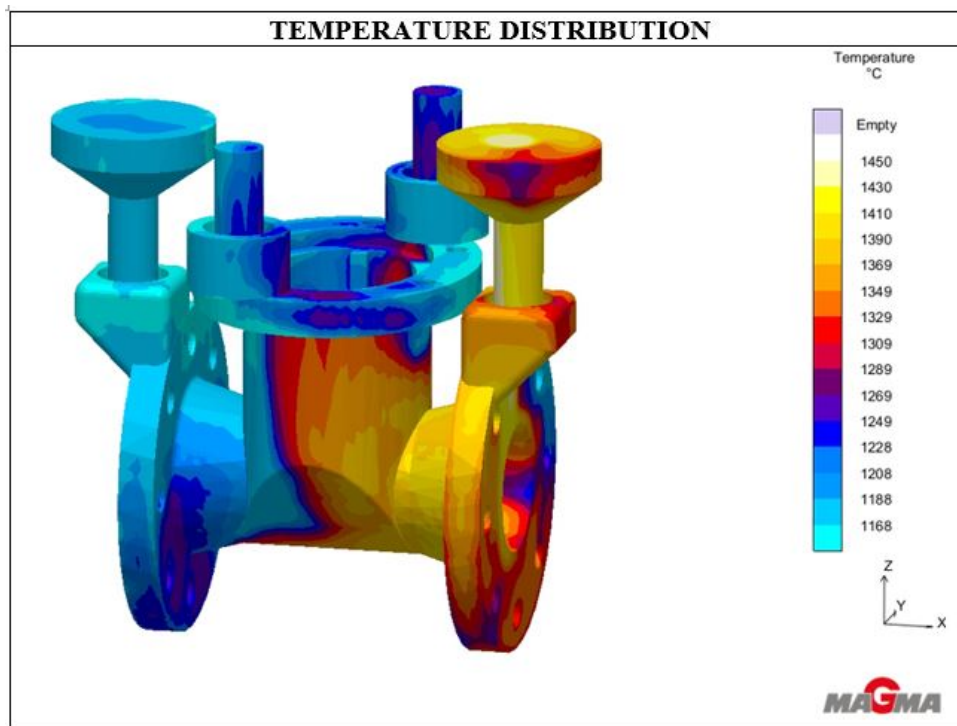


Figure 4.15: MAGMASoft® casting simulation indicating the temperature distribution during casting of the molten metal

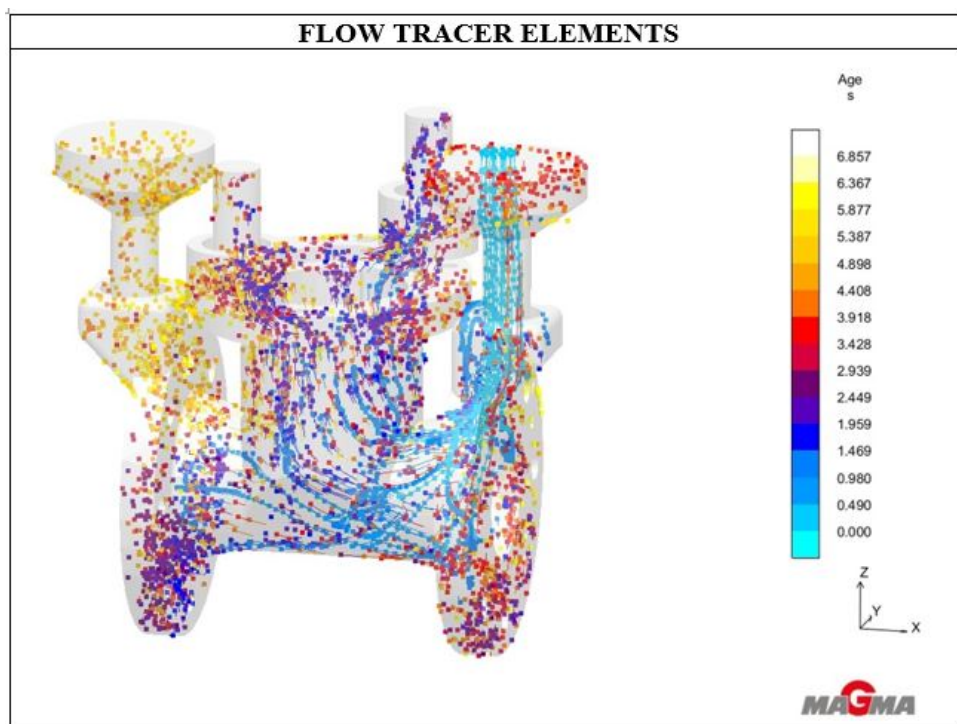


Figure 4.16: MAGMASoft® casting simulation indicating the flow of the tracer elements in the casting and the age of the particle in an area of the casting

When Figure 4.17 is observed, it can be deduced that the expected porosity areas correlate with the hot spot areas. When casting quality is considered, the high level of expected porosity in the central valve body area is undesirable and evidence of a poor casting. However, the effort to lower the porosity level was not essential in this study since the focus of this study was the effective casting of a valve with this method. Future studies may be performed to increase the quality of the cast valve with this method.

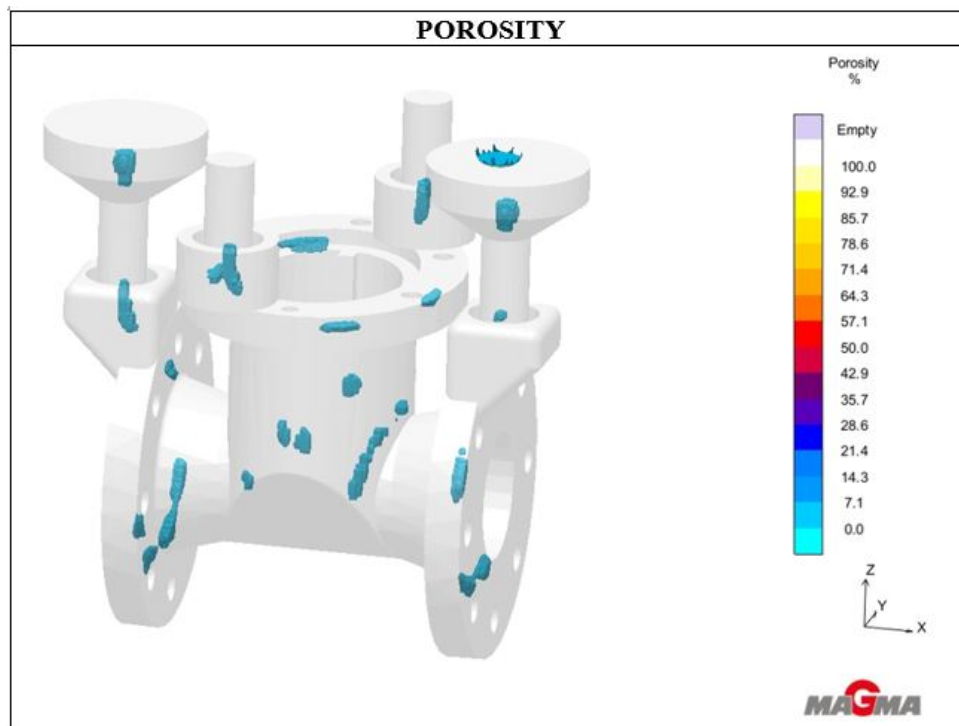


Figure 4.17: MAGMASoft® casting simulation indicating the areas of expected porosity

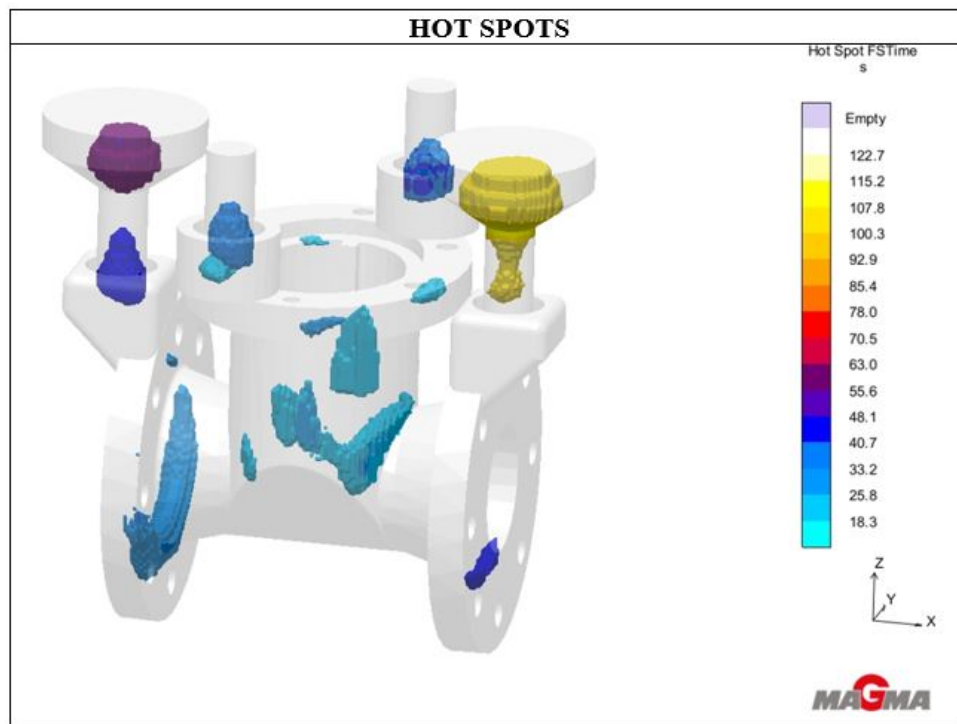


Figure 4.18: MAGMASoft® casting simulation indicating the areas of expected hot spots

The design of the feeding system required mounting areas on the pattern that were 3D-printed. The alumina feeder and sprue as well as the mounting of the sprue to the PMMA may be accomplished with the use of high alumina cement.

The solidification time (t_s) of a casting may be determined theoretically with Chvorinov's Rule as shown below. V_c is the volume of the casting and A_s is the surface area of the casting, B_m is a constant taking the casting material into account and B_M is a constant that depends on the mould. In this case, the volume of the casting is without the feeding system. The weight of the casting is therefore 956.92g as obtained from a SolidWorks model estimation.

$$t_s = \frac{\pi}{4} \times B_m B_M \left(\frac{V_c}{A_s} \right)^2 \quad (4.18)$$

Where

$$B_m = \rho_m \left(\frac{C_m(T_p - T_m) + \Delta H_m}{T_m - T_0} \right)^2 \quad (4.19)$$

and:

$$B_M = \frac{1}{K_M \rho_M C_M} \quad (4.20)$$

The values of the parameters used in Equations 4.20 to 4.25 are tabulated below.

Table 4.4: Values and descriptions of parameters used in Equation 4.25 to 4.20

Description	Parameter	Value
Volume of the casting	V_c	$134.77 \times 10^{-6} \text{ m}^3$
Surface area of the casting	A_s	0.058 m^2
Density of ductile iron	ρ_m	7100 kg/m^3
Pouring temperature of ductile iron	T_p	1673 K
Melting temperature of ductile iron	T_m	1393 K
Specific heat of ductile iron	C_m	603 J/kgK
Latent heat of solidification of metal	ΔH_{melt}	280 K
Initial temperature of mould	T_0	298 K
Thermal conductivity of mould	K_M	Eq.4.21
Density of mould	ρ_M	Eq. 4.22
Specific heat of mould	C_m	610.68 J/kgK

The density of the mould and the thermal conductivity of the mould should account for a combination of air and steel shot. The packing factor of 0.74 is used to estimate the ratio of steel shot to air. The calculations are shown below.

$$K_M = 0.74(k_s) + 0.26(k_a) = 0.74(49.8) + 0.26(0.0515) \therefore K_M = 36.87 \text{ W/mK} \quad (4.21)$$

$$\rho_M = 0.74(\rho_s) + 0.26(\rho_a) = 0.74(7850) + 0.26(0.524) \therefore \rho_M = 5809.14 \text{ kg/m}^3 \quad (4.22)$$

The constants can then be calculated to calculate the solidification time:

$$B_m = 169.36 \times 10^6 \quad (4.23)$$

$$B_M = 7.65 \times 10^9 \quad (4.24)$$

The solidification time is therefore

$$t_s \approx 5.49 \times 10^{-6} s \quad (4.25)$$

The value obtained for t_s indicates an instantaneous solidification time that strives to zero seconds. It is not an accurate estimation. The calculation of the solidification time is therefore incorrect and proves Geffroy *et al.*'s [24] observation that Chvorinov's Rule cannot be applied to magnetic moulding applications due to the similarity in parameter values between the casting material and the mould material. Furthermore, the complexity of the design of the pattern results in a high surface area-to-volume ratio which interferes with the accuracy of the solidification time calculations.

4.1.4 Auxiliaries

An alumina cover was designed to prevent liquid metal spillage entering the steel shot. The Curie temperature of the steel shot is in the range of iron, which is 750°C. This implies that the temperature of the liquid metal during pouring (1400°C) is so high that if it is spilled on the steel shot, the steel shot will no longer be magnetic. Spillage of the molten metal on the steel shot will also complicate the release of the cast part. The alumina shot cover design is shown in Figure 4.19.

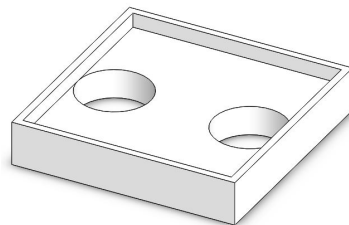


Figure 4.19: Model of the alumina shot cover

An alumina stand was designed to protect the coil isolation material, allow airflow over the coil and to prevent spillage of the molten metal on laboratory equipment.

Damage to the coil isolation material may cause an electrical short circuit. If the coil was to be placed directly on a flat surface, the coil would heat up faster and the efficiency of the coil would decrease. As multiple benefits arise from a stand to place the electromagnet on, the stand was designed as shown in Figure 4.20

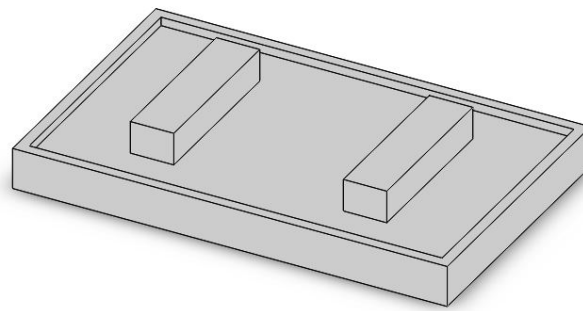


Figure 4.20: Model of the alumina electromagnet stand

Due to the high-temperature resistance, ease of machining and availability of alumina, alumina was used for both the shot cover and the stand.

4.1.5 Refractory Coating

A typical slurry mixture recipe used in the lost-foam casting process was selected from literature and investigated to be applied to a PMMA pattern. The selected coating was a waterbased suspension with mullite powder as refractory and composition shown in Table 4.5.

Table 4.5: Percentage composition of refractory coating selected for the application of magnetic moulding

Refractory [%]	Binder [%]	Agent keeping suspension stable [%]
Mullite: 90 Granulation: 40-45 μ m	Bentonite: 3-4 Colloidal Silica: 5-6	Not applicable for the scale of this application

The wettability of the selected coating on the PMMA pattern had to be investigated as part of the design. In a mini-experiment, the products of two different suppliers

were tested in the ratios specified in the selected recipe. In Figure 4.21 it may be observed that Coating 2 shows more favourable characteristics than Coating 1. Coating 2 resulted in a higher density, higher viscosity suspension, therefore fewer layers are required to obtain the desired coating thickness. Both coatings showed good wettability to machined 3D-printed PMMA samples.

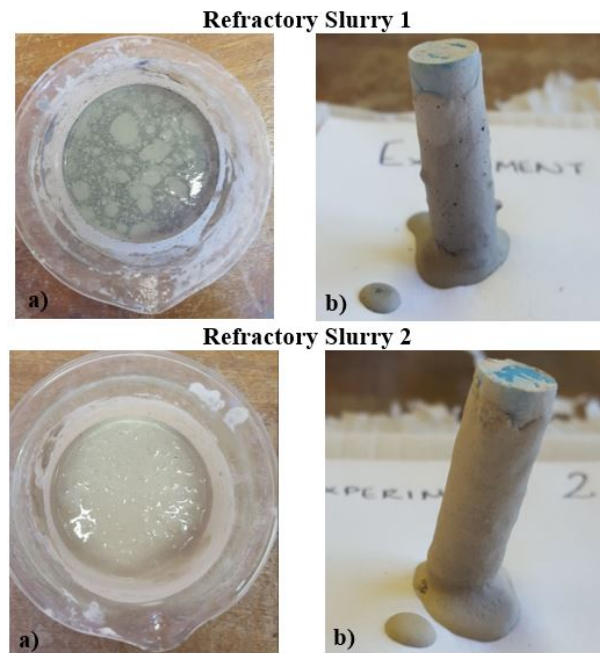


Figure 4.21: Photos of the comparison between supplier mullite products in a) the refractory slurry and b) 2 layers of refractory coating applied to a 3D-printed sample

The coated samples were left to dry for 12 hours. Both coatings were very brittle once dried and showed very low toughness. Bentonite is a swelling clay that undergoes a reduction in volume when the coating dries. This may cause micro-cracks in the coating and results in the brittleness experienced in the samples. The weak spots caused by the micro cracks in the layers of the coating may cause the coating to crack, especially due to thermal shock of the molten metal during casting, which may have disastrous effects.

After consulting experienced foundrymen, it was advised that a suspension consist solely of mullite and colloidal silica with a density of 3g/cm^3 should be used. The recommended suspension was tested and the viscosity was very high as shown in Figure 4.22. The coating was difficult to apply and the layer thickness of the coating

was difficult to control. The fluidity was increased by adding more colloidal silica and reducing the density to $2\text{g}/\text{cm}^3$. It was then established that this recipe could be used as refractory coating in the casting process of magnetic moulding.

Due to the fact that refractory coatings are primarily used to improve the surface finish of the product, parts are often cast without a refractory coating in the lost-foam process. If the coating step is skipped, the production time may be increased and costs could be saved on coating materials. It was therefore decided to perform two castings. One casting with a refractory coating and one casting without a refractory coating. For investigative purposes, the behaviour of the casting process and the surface finish were then evaluated.

Casting without a refractory coating was expected to result in a deformed casting. The high temperature of the molten metal may cause the steel shot to reach its Curie temperature and lose its magnetic properties. The high fluidity of the liquid metal may result in liquid metal seeping through the steel shot as less energy is required to move through the air gaps than through the pattern material. It was therefore expected to be interesting to observe the behaviour of the liquid metal, the effect on the electromagnetic field and the casting to obtain information not yet documented.



Figure 4.22: Photo of the coating suspension containing only mullite and colloidal silica indicating the high viscosity of the $3\text{g}/\text{cm}^3$

4.1.6 Casting Material

The biggest problems experienced in the casting of ductile iron with the lost-foam process is related to the carbon content of the casting [32]. Methods to limit the carbon content include removing most of the carbon residue during casting by vacuuming or by increasing the pouring temperature to promote complete classification of the pattern. There is, however, a limit on the pouring temperature as an increase in pouring temperature leads to the degradation of the spheroidising process.

The simplest way to limit the carbon residue is to select a casting material with a carbon content lower than 3.6 % [32]. A lower carbon content leaves room for the absorption of carbon during casting and therefore decreasing the carbon residue.

Specification ASTM A395 Grade 60-40-18 is typically used for applications requiring high ductility and impact resistance, such as valve bodies [18]. The grade is an indication of the tensile strength, yield strength and elongation, as shown in Table 4.6.

Table 4.6: Mechanical properties of ASTM A395 60-40-18 ductile iron

Hardness	Tensile Strength	Yield Strength	Elongation in 50mm
143-187HB	414MPa(60ksi)	276MPa(40ksi)	18

This grade of ductile iron has a carbon content between 3.2% and 3.6%. Although it falls within the range where room is left for carbon absorption, the absorption of carbon may be very limited if a 3.6% carbon ductile iron is cast. It may, therefore, be expected that carbon residue may be present in the cast part.

It should be noted that due to the high casting temperature of ductile iron, the liquid ductile iron is nonmagnetic as casting takes place above the Curie temperature of ductile iron. Therefore, during casting, the magnetic field has no effect on the liquid metal being cast.

4.2 Assembly of Components

During the configuration of the magnetic moulding process, the interdependence of the components was observed. It became clear that each component contributes to the success of the casting. When each step in the magnetic moulding process is considered in isolation, appreciation is gained for the extensive development of that specific step over the years. The interdependence of the components does, however, complicate the design. It is not always possible to configure the optimal combination of components of each casting step of the complete process. In engineering design, trade-offs are unavoidable and greatly depends on the specific part to be cast.

Financial limitations often dictated design choices, but not at the cost of the integrity of the process. Ultimately, the availability of materials, the cost of materials and manufacturing were three factors contributing to a more affordable configuration.

Once the final configuration was manufactured, the components were assembled to be tested. The experimental setup is shown in Figure 4.23.

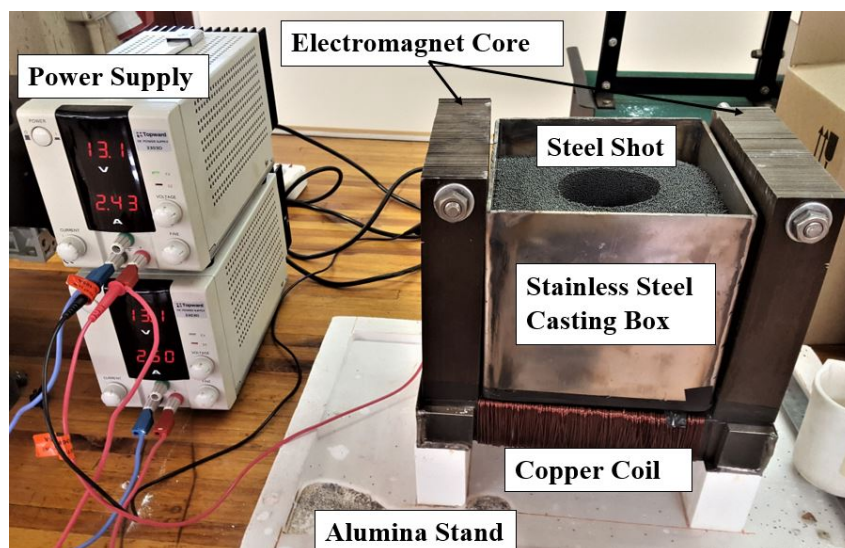


Figure 4.23: A photo of the assembly of the magnetic moulding setup

The power supply consisted of two 3A converters connected in series to obtain a maximum current of 6A at 32V. The power supply was connected to the ends of the coil

with crocodile clamps. Prior to winding the coil, the coil area was isolated with isolation tape to prevent damage to the isolation material of the coil. The bottom area of the casting box that would be in contact with the coil, was also isolated to prevent damage to the coil. Damage to the isolation material presents a risk of an electrical short circuit.

The coil consisted of 1mm copper wire and 300 turns were wound to form the electromagnet. Due to the sheer weight of the electromagnet core (27kg) and the shape and dimensions of the core, it was not possible to wind the coil on a lathe. The electromagnet core was placed on one of the vertical sides on a platform that was mounted on a shaft and placed in a bearing to enable a 360° rotation to wind the coil by hand. The electromagnet on the platform of the equipment used to wind the coil, is shown in Figure 4.24.



Figure 4.24: Equipment used to wind the coil of the electromagnet

Non-grain orientated V470 silicon steel plates were punched at AMC in Germiston. To lower the material cost, the u-shape was punched in 3 separate segments of 300×0.5 mm thickness plates each. As a continuous u-shape was expected, provision was only made for fastening with a threaded rod and nuts at the top. When the silicon steel plates arrived, clamps had to be designed to fasten the lower parts of the u-shape.

The steel shot was supplied by Blastrite. A 25kg S280 bag of spherical steel shot used

as blasting abrasive was obtained with shot diameters ranging between 0.6 and 1mm. The bulk weight of the steel shot is 4.164kg/ ℓ . The specifications of the steel shot is very similar to the shot used by Geffroy *et al* [24].

The casting box was manufactured from 3mm thick 304 stainless steel (austenitic) sheets. Five 150x150mm squares were purchased and welded together in the faculty workshop. The welded areas were tested for magnetic properties. It was established that the casting box was completely non-magnetic, as required. If a ferritic material was used, the magnetic field in the steel shot would decrease as the ferritic material would have a higher permeability causing the magnetic field to follow the path of highest permeability rather than the steel shot mould which contains air gaps.

After assembly of the magnetic moulding setup, the flux density produced by the electromagnet was measured with a Gaussmeter. The casting box was filled with steel shot and a measurement was taken in the middle of the casting box, 90mm deep. It was important to orientate the probe perpendicular to the direction of the magnetic field to ensure an accurate measurement. The average results are shown in Table 4.7 and graphically represented in Figure 4.25.

Table 4.7: Flux densities measured in the middle of a fully filled casting box at a depth of 90mm at increasing currents

Current (A)	Voltage (V)	Flux Density (T)
1	5	0.006
2	10	0.013
3	16	0.016
4	20	0.022
5	26	0.027
6	32	0.035

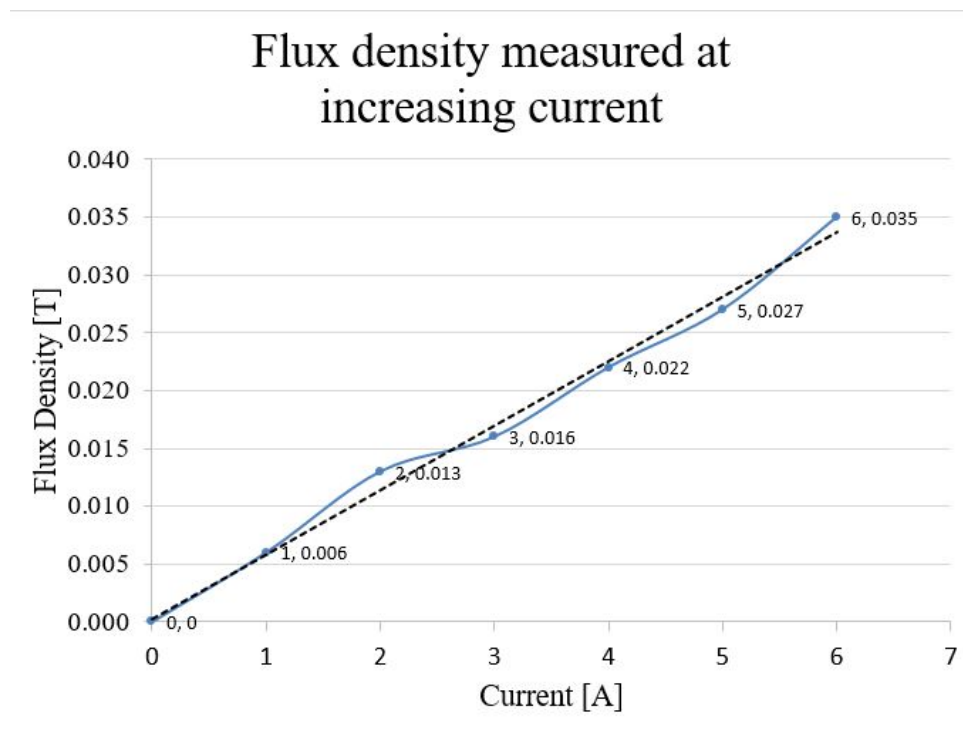


Figure 4.25: Line graph of the flux density measured as the current of the electromagnet is increased

The maximum flux density of the designed electromagnet in this area, area 4, as determined through FEMM, was 0.616T. There was therefore an immense difference between the designed value and the actual value. The main reason for a 94% difference between the designed value and the actual value is the fact that not all losses of magnetic flux were compensated for in the FEMM analysis. Furthermore, the complex geometry of the part and the limited capabilities of FEMM inhibits the accurate design of the magnetic flux density.

Although the values of the electromagnet was not in the range of 0.1 to 0.5T, the cohesion of the steel shot during application of the magnetic field, was more than sufficient. In photos shown in Appendix C, the characteristics of the steel shot during magnetisation is shown. An object was placed in the steel shot whilst the magnetic field was switched off. The magnetic field was then switched on and adjusted to various currents. The shape of the object remained in the magnetised steel shot.

The pattern was additive manufactured at the Vaal University of Technology with a

Voxeljet VX500 jetting 3D-printer. The pattern model was converted to an STL file and by means of jetting technology, the PMMA pattern material was selectively deposited onto a bed to form a 3D-part. The complete pattern is shown in Figure 4.26. The assembly of the feeding system and coating of the pattern was performed a day before casting to prevent damage to the assembly and limit damage and cracks of the alumina cement and refractory coating.

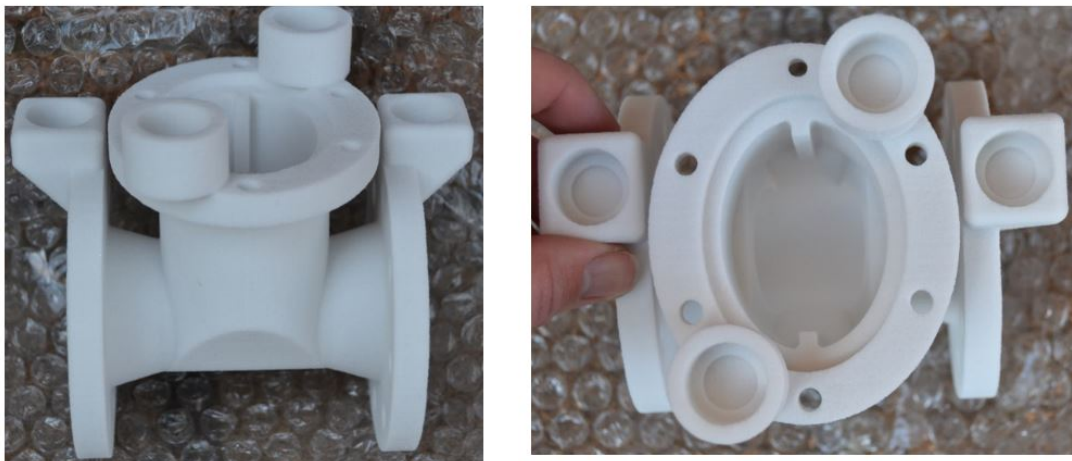


Figure 4.26: The additive manufactured PMMA valve body pattern showing the feeding system mounting points and surface finish of the material

The configuration and implementation of the magnetic moulding process were based on the assumption that the part would be cast at the mechanical engineering faculty of the NWU. Although the 20kW induction furnace is specified to reach temperatures above 1200 °C, the furnace took more than 8 hours to reach 700 °C. In order for the ferro silicon (FeSi) to melt, 1600°C was required. Therefore, due to financial and time constraints, the melting of the casting material had to be performed at a facility where ductile iron can be cast at 1400°C.

The experimental setup and therefore the casting process had to be performed at a facility with a laboratory-scale furnace capacity. The casting facility at the Council for Scientific and Industrial Research (CSIR) has the capacity to perform small castings up to 15kg. Foundries did not comply with the requirements of the experiment as much larger volume melts are performed.

It was estimated that 1172.65g ductile iron would be sufficient to cast the valve body, however, more material was required due to the larger scale induction furnace that was used. In order to sufficiently melt the material, the 15kg cupola requires more than 1.172kg melt as communicated by Mr. Pierre Rossouw from CSIR. Furthermore, pig iron is supplied in bricks that weigh between 4 and 7kg. The pig iron was very difficult to separate into smaller pieces without proper equipment. It was therefore concluded that one pig iron brick would be used to determine the composition of the ductile iron melt.

The chemical composition of an ASTM A395 Grade 60-40-18 ductile iron was known and the weight of the pig iron brick was 4.486kg. By means of iteration, the composition of the melt could be determined in an excel program with the goal seek function, which was developed by a colleague [38]. The materials used to obtain ASTM A395 Grade 60-40-18 ductile iron and their respective weight contribution is shown in Table 4.8. The ideal composition and the calculated composition based on the weight of the raw materials are shown in Table 4.9.

Table 4.8: The calculated weight contribution of raw materials, in the melt required to obtain ASTM A395 Grade 60-40-18 ductile iron

Material Component	Description	Kg	%
Base Materials:	Pig Iron (F ₂)	4.32	95.4
	FeSi (Low Al)	0.15	3.30
Noduliser:	Elkem Elmag 7311	0.02	0.40
Inoculant:	Elkem Zircinoc	0.04	0.90
Total:		4.53	100

Table 4.9: The chemical composition of ideal ASTM A395 Grade 60-40-18 ductile iron compared to the actual composition of the raw materials, as determined by the developed material analysis Excel program

Element	Ideal	Actual
C%	3.70	3.60
Si%	2.59	2.60
P%	0.04	0.04
Mn%	0.03	0.15
Cu%	0.00	0.00
Mg%	0.01	0.04
Cr%	0.00	0.00
S%	0.02	0.02
Ca%	0.01	0.00
Al%	0.02	0.00
Ba%	0.000	0.00
Sr%	0.000	0.00
Zr%	0.000	0.00
Fe%	92.36	93.55

4.3 Casting Procedure

The casting procedure and detail on each step was finalised prior to the stage where the casting of the part was performed. Once the setup was complete, the general procedure shown in Figure 4.27, was performed.

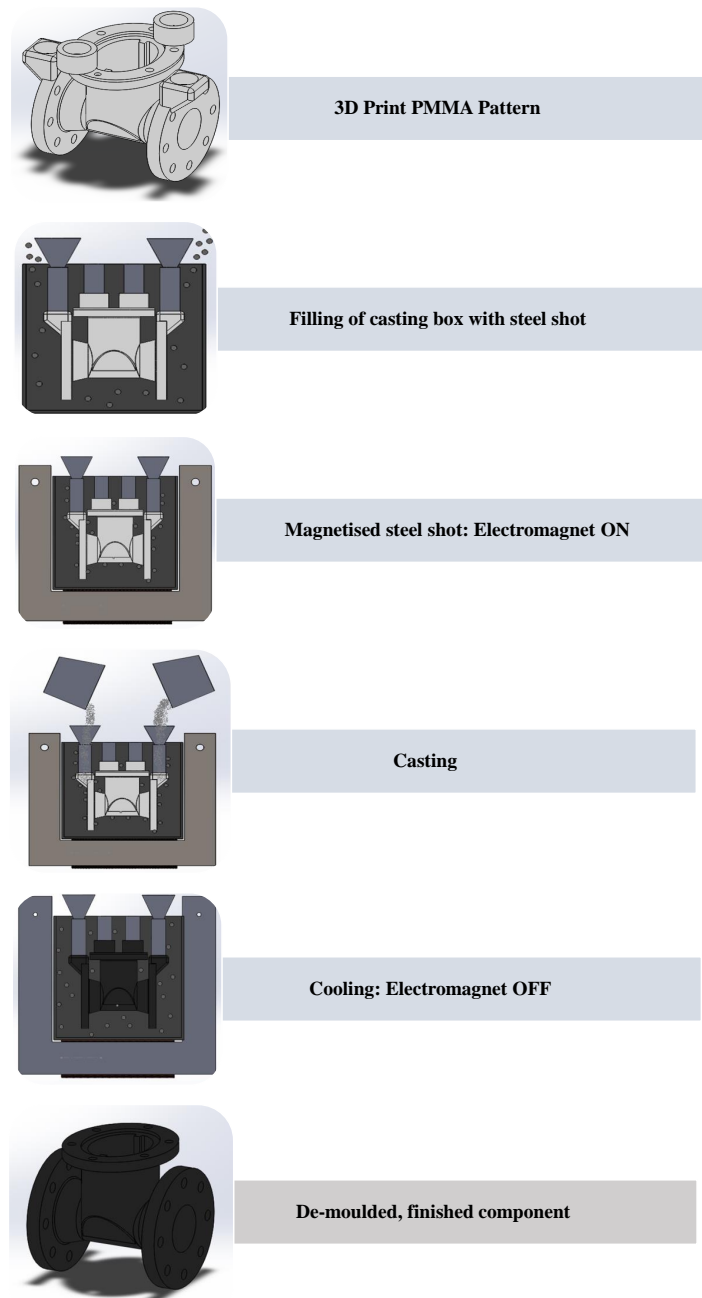


Figure 4.27: The magnetic moulding casting procedure as modeled in SolidWorks

The procedure was executed once the safety hazards were identified and precautions were implemented and followed. A list of safety hazards involved in the casting procedure may be found in Appendix D. The correct safety equipment and Personal Protective Equipment (PPE) wear, was in place prior to the execution of the procedure. The

minimum PPE required, included safety shoes, overalls, leather apron, leather gloves, safety mask and goggles.

The pig iron brick was melted as is, as it could not be broken down into smaller parts with the equipment available. The FeSi, noduliser and inoculant were hammered to smaller fragments to increase the absorption of the materials in the melt. The raw casting materials were then weighed and packaged in labelled containers before the casting procedure was initiated.

The pattern and feeding system were prepared and complete before the casting procedure was initiated. Two PMMA patterns were 3D-printed. The feeding system of one of the patterns was attached with alumina cement and no refractory coating was applied as shown in Figure 4.28. The other pattern was coated with the refractory coating prior to attaching the feeding system. During the coating of the pattern, no refractory coating came in contact with the areas where the feeding of metal occurred.



Figure 4.28: The complete PMMA pattern with ceramic feeding system attached

The size of the casting facility did not allow for direct casting from the cupola of the induction furnace. A ladle was therefore used to cast more accurately. The experimental setup was much smaller in scale than what the facility is intended to accommodate.

The melting procedure form part of the casting procedure and was initiated before the casting procedure. The melting procedure was performed as follow:

1. A solid pig iron brick and FeSi fragments were placed in the cupola of the induction furnace to initiate the melting process. The materials were heated up to 1600°C to ensure that the FeSi melts completely
2. The noduliser (Elmag) fragments were placed in the ladle.
3. Once the pig iron was completely melted and the temperature reached 1300°C, the molten metal was cast into the ladle to absorb the noduliser and then it was immediately cast back into the furnace cupola to reheat the mixed content.
4. When the molten metal was probed and a temperature of 1400°C was reached, the molten metal from the cupola was cast into the ladle and immediately continuously cast without any hesitation into one of the feeders of the pattern, whilst simultaneously adding inoculant and the rest of the noduliser to the stream.
5. Casting stopped when molten metal was observed in the other feeder, which was an indication of a possible full casting. This is shown in Figure 4.29.

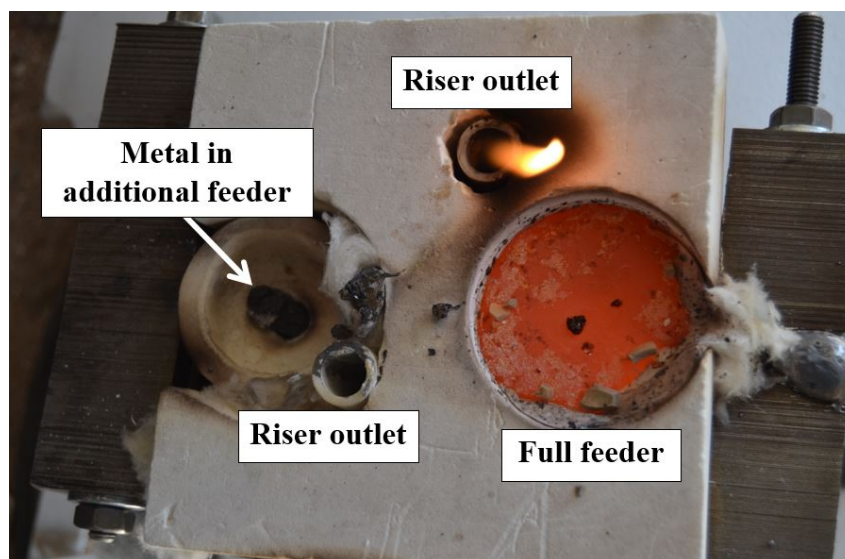


Figure 4.29: A top view of the feeders, after molten metal was cast

Steps from the melting procedure were performed during the casting procedure as both procedures form part of the complete magnetic moulding casting process. The casting procedure was executed in the following order and is illustrated in Figure 4.27.

1. After step 1 and 2 of the melting procedure was performed, the magnetic moulding equipment was set up as shown in Figure 4.23.
2. A 1cm thick layer of steel shot was inserted into the casting box. The casting box was shaken to level the contents.
3. The pattern was then positioned in the middle of the casting box, on top of the levelled steel shot. The feeders and risers faced upwards.
4. Towel paper was carefully inserted into the openings of the feeding system to prevent steel shot from entering the feeding system.
5. The casting box containing the pattern was then completely filled up with steel shot. During the filling of the casting box, it was ensured that steel shot surrounds all surfaces of the pattern, especially the fluid passageway of the valve pattern. The pattern and feeding system was very fragile and therefore, the casting box was not shaken after the casting box was full.
6. The power supply was switched on and the current adjusted to 5A. The magnetic field was then tested with the Gaussmeter to ensure that the shot was magnetised.
7. It was determined that the shot was magnetised and the shot cover was placed in position.
8. Step 3 to 5 of the melting procedure was then performed.
9. After 5 minutes, the magnetic field was switched off by adjusting the current to 0A and switching off the power supply.
10. The shot cover was removed and solidified metal was observed in the top layer of the steel shot. Once the shot cover was removed, it was clear that the liquid

metal observed in the other feeder was not due to a full casting, but rather liquid metal leakage from the main feeder.

11. Once the metal in the feeders turned grey/blackish in colour, the casting box was removed from the electromagnet. The casting box was tilted at a 45 degree angle in order to release the part from the loose steel shot. The casting box and steel shot was still very hot.
12. The part was air cooled at room temperature.

The experiment failed to cast a complete valve body. Only a small amount of the liquid metal reached the pattern. The remaining part of the pattern is shown in Figure 4.30.



Figure 4.30: A photo of the PMMA pattern after casting was performed

When the pattern was inspected after removal from the casting box, it was observed that the PMMA was still very soft and viscous in the area near the feeder. The steel shot attached to the hot pattern was in a tight packing arrangement, possibly indicating that the magnetic field ensured sufficient cohesion of the mould. On the remaining part of the pattern, the section of the top flange was no longer there and the part of the flange where the feeder was situated, was no longer part of the pattern. These areas were the areas that were cast.

In Figure 4.31 the part of the flange situated below the feeder can be observed. In the encircled area, black steel shot spheres are noticed, indicating the carbon residue,

possibly due to the degradation of the PMMA. The tight packing arrangement of the steel shot can also be observed in Figure 4.31.



Figure 4.31: The PMMA pattern after casting, indicating the carbon residue due to the degradation of the PMMA.

The small part of the metal that reached the pattern is shown in Figure 4.32. In the photo on the right of Figure 4.32, a semi-circular path where the liquid metal degraded the pattern to form part of the top flange, was noticed. The analysis of the cast part is documented in the next section.



Figure 4.32: The result of the casting with the PMMA pattern indicating the part of the top flange that was cast

In order to evaluate the result of the casting, it was necessary to remove the alumina feeder and ceramic sprue. The small part was then sectioned through the middle to inspect the integrity of the part. Three sample areas were selected for microstructure inspection. The areas are marked 1, 2 and 3 on the part shown in Figure 4.33.



Figure 4.33: The cast part after removal of the feeder and sprue, from different views, indicating the positions of the sample areas

The samples from the sectioned cast part were mounted, polished and etched. Each sample was then analysed under a microscope to investigate the microstructure. Etching was performed to reveal the ferrite in the microstructure. Although Nital indicates the grain boundaries, nital is orientation sensitive and therefore, not all grain edges are indicated. Picral was used to observe carbides and makes it easier to identify cementite. However, no significant difference between the observations of the microstructure obtained from nital and picral were observed. Therefore, only the nital micrographs were used in the analysis of the material. The evaluation of the microstructure of the samples and the results are discussed in Chapter 5.

Due to unsatisfactory results obtained in the casting with the PMMA pattern, a simple casting was performed with an EPS pattern. A 100×100mm low density EPS pattern with a 40mm thickness was wire-cut from an EPS block to serve as a pattern in the experiment. High-density EPS will result in a better surface finish of a casting, but for this experiment the focus was on the successful casting of a fully filled casting by

means of the magnetic moulding process. The lower the density of the pattern, the higher the chances of a completely filled casting.

In order to increase the chances of a fully filled casting, the EPS pattern was made in two halves of which the material was slightly hollowed out. During casting there was therefore less material to degrade, resulting in less carbon residue and increasing the chances of a fully filled casting. The pattern prior to coating is shown in Figure 4.34. The wet, unfinished coated pattern is shown in Figure 4.35. Three layers of the refractory coating was applied by means of dipping the pattern in the refractory slurry.



Figure 4.34: The hollowed out EPS pattern halves and the combined, glued pattern



Figure 4.35: The wet, refractory coated EPS pattern before the final layer was applied

Casting of ductile iron at 1400°C was performed with the EPS pattern. The same melting and casting procedure was followed as with the casting with the PMMA pattern. During casting of the liquid metal, the degradation of the EPS pattern caused flames that continued to burn for a period after casting. In Figure 4.36 the casting of molten metal and the flames may be observed. The result of the casting process is shown in Figure 4.37.



Figure 4.36: The casting of ductile iron with the EPS pattern resulting in flames during the pyrolysis of the pattern



Figure 4.37: The cast part obtained with magnetic moulding, with the refractory coating still in place

In Figure 4.37, the coating is still intact. When the part was removed after casting, the coating was undamaged. Small cracks were visible in the refractory coating. The refractory coating was then removed to observe the cast part. The cast part without the coating is shown in Figure 4.38.



Figure 4.38: The cast part after the removal of the refractory coating

The casting process where EPS was used as pattern material, was successful. A completely filled casting was obtained. The pyrolysis of the EPS was very fast as gasification of the EPS resulted due to the high casting temperature.

By visual inspection, the surface finish was very rough and the shape of the EPS beads was clear. However, the visibility of the bead shapes indicates the dimensional accuracy of the casting with the refractory coating. If a high-quality pattern was used, the dimensional quality of the surface finish would be immaculate.

The cast part was cut into two halves to investigate the integrity of the part. No defects were observed on the plane of the section, as shown in Figure 4.39. No graphite flotation was observed. The section where the part was cut in half, had a dull grey colour, which was a possible indication of grey cast iron. The part was easy to machine.



Figure 4.39: The cast part with the feeder and sprue removed and sectioned in two halves

The coating was easy to remove from the cast part. The inner layer of the coating which was in contact with the molten metal, was covered in black powder, which is the carbon residue formed by the pyrolysis of the EPS. The layer thickness of the coating was measured to be 2.8mm on average. The layer thickness was not very consistent. The thickness of the coating contributed to the high level of carbon residue observed. The coating layer was 1.3mm thicker than the suggested coating layer thickness of 1.5mm. The correct coating thickness would be more permeable, allowing the gaseous product to escape during casting. A photo of the coating and the carbon residue on the inner layer is shown in Figure 4.40.

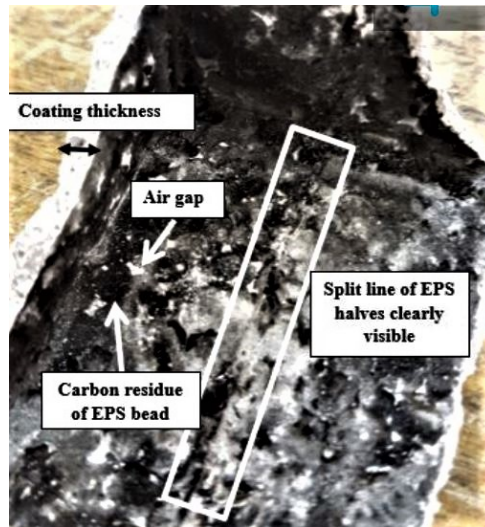


Figure 4.40: Photo of the inner layer of the refractory coating after casting indicating carbon residue due to pyrolysis of the EPS pattern

The absence of risers also contributed to the level of carbon residue. Impurities were observed near the top surface of the cast part. As metal was poured into the feeder, the impurities were entrapped and forced to the top of the casting. The impurities are shown in Figure 4.41.

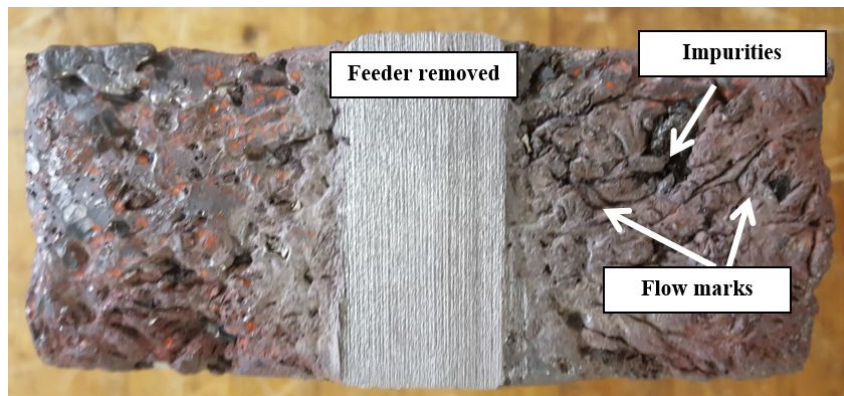


Figure 4.41: The impurities observed in the casting due to entrapment

Tension-test specimens and Charpy-test specimens were machined from the square cast part. A material sample of the cast part was obtained just below the sprue, in the middle of the casting. The material sample was used to investigate the microstructure and identify the material type as discussed in the next chapter.

Chapter 5

Results and Evaluation

The evaluation of the casting results is documented in this chapter. Evaluation of micrographs obtained from material samples was used to determine the success of the material casting. Visual inspection and evaluation of tests performed on the mechanical properties of the castings performed with the EPS pattern, contributes to determining the overall feasibility of the magnetic moulding casting process.

5.1 Evaluation of PMMA Pattern Casting Results

5.1.1 Sample 1: From Feeder

Sample 1 is a section from the metal that solidified in the feeder of the casting with the PMMA pattern. Cast iron with impurities was expected in this sample. The aim of the microstructural analysis was purely to determine the type of cast iron that was cast. The microstructure of sample 1, under magnification, is shown in Figure 5.1.

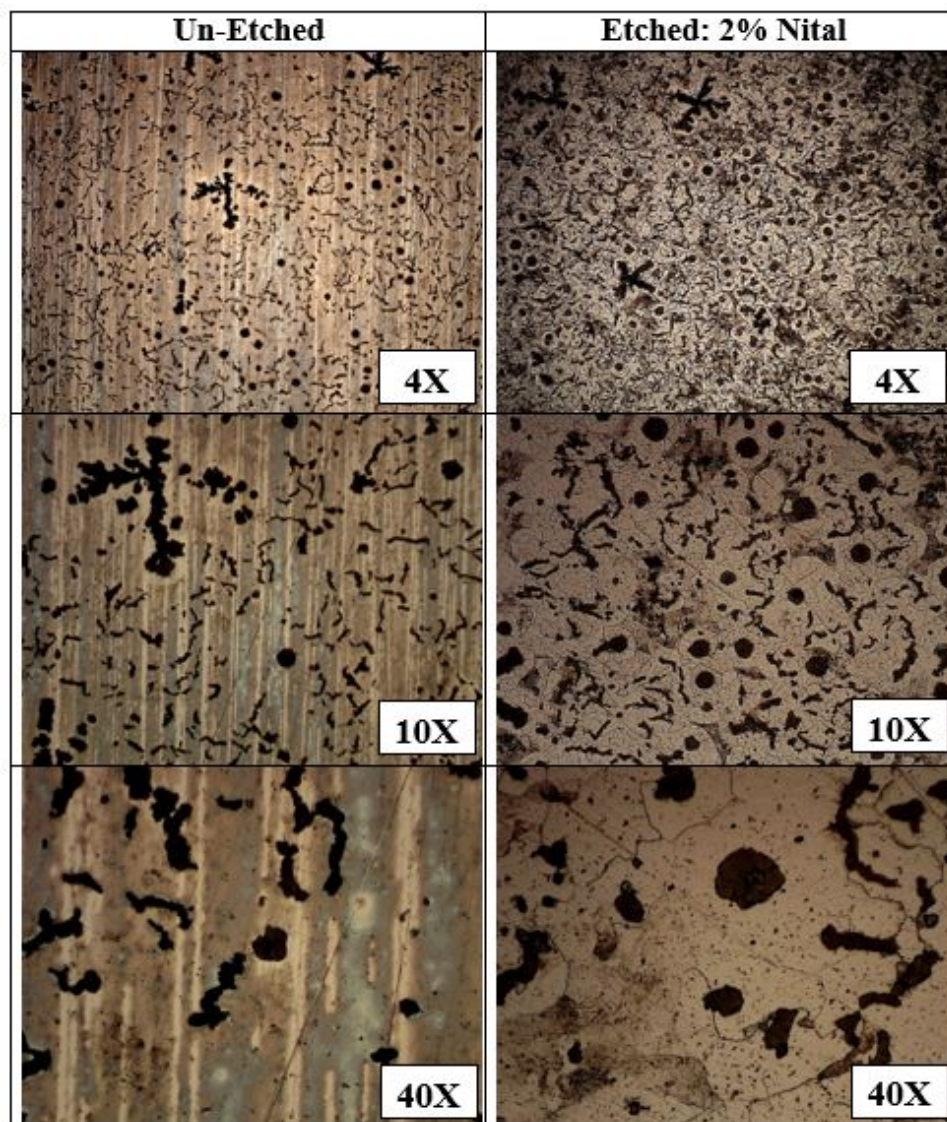


Figure 5.1: Microstructure of Sample 1 under different magnifications indicating the difference between no treatment and etching with 2% nital

When the sample was untreated, it was observed that the majority of the microstructure formed vermicular shaped, compacted graphite and only a few degenerate graphite nodules. The formation of vermicular shaped graphite is an indication of insufficient magnesium, leading to the formation of grey cast iron instead of ductile iron.

After etching with 2% nital, ferrite became visible and the spheroids were more prominent. Star-like dark structures with dendrites were observed and were identified as integrated graphite nodules surrounded by ferrite. The grain boundaries were very

clear after etching. The ferrite and graphite nodules are indicated in the micrograph shown in Figure 5.2.

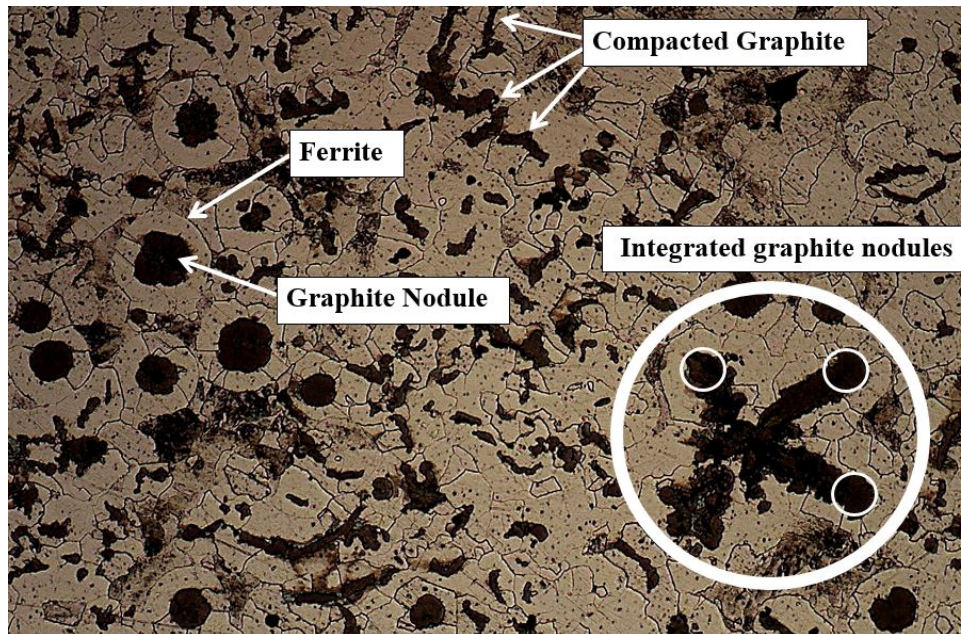


Figure 5.2: Microstructure of Sample 1 indicating ferrite and graphite structures

The formation of grey cast iron may be expected as it is the part of the casting that remains at a high temperature for the duration of the casting process. It should, however, be considered that the metal in the sprue and feeder will be removed from the final casting, and therefore a compacted graphite microstructure is not problematic given the position of the sample.

5.1.2 Sample 2: From Sprue

This sample is a section from the material that solidified just below the sprue. This area is the first contact area where molten metal reaches the PMMA pattern. The microstructure is shown under different magnifications and treatments in Figure 5.3.

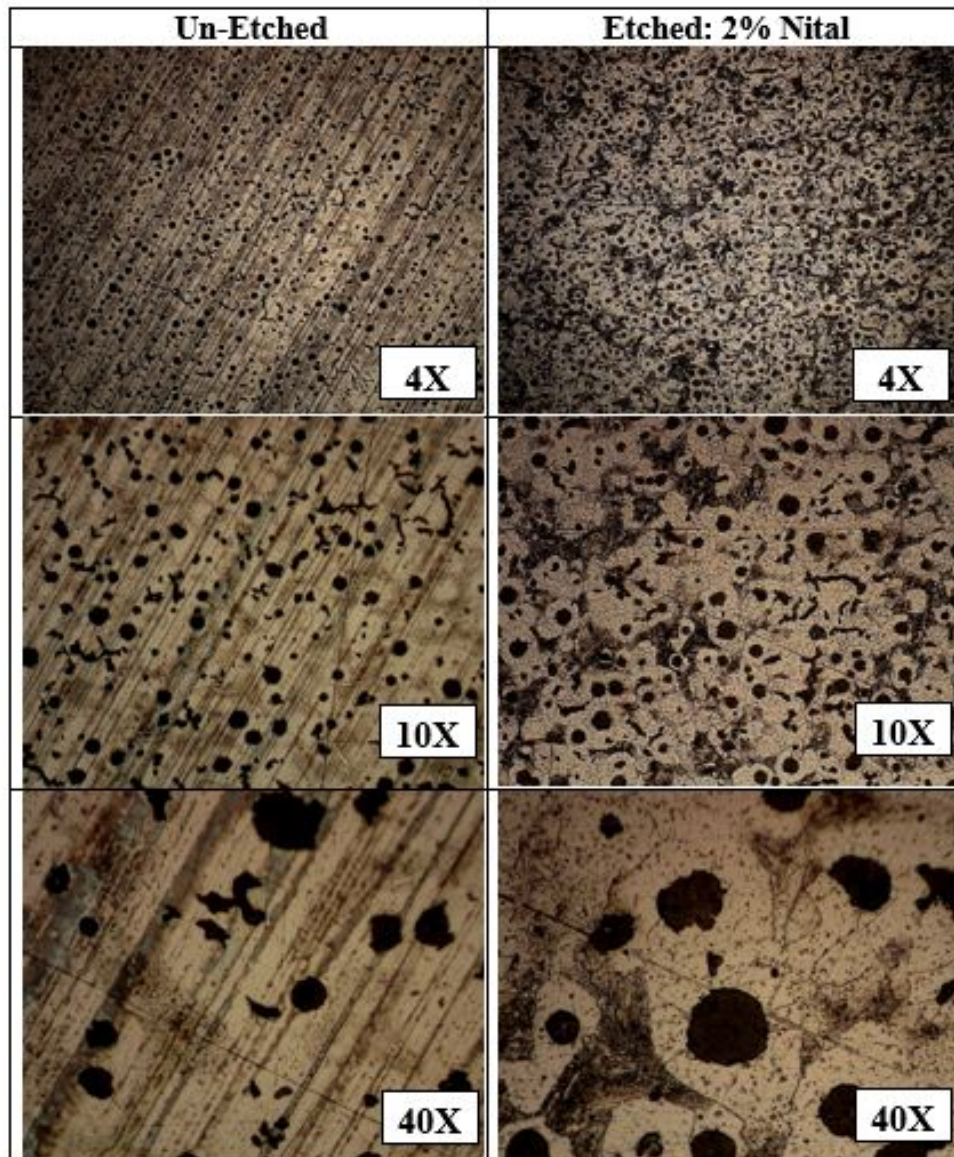


Figure 5.3: Microstructure of Sample 2 under different magnifications indicating the difference between no treatment and etching with 2% nital

The amount of compacted graphite observed is considerably lower in this sample. A significant increase in the number of nodules was observed in Sample 2, which allows this to be classified as ductile cast iron.

5.1.3 Sample 3: From cast metal in contact with Steel Shot

Sample 3 is a section of the cast material that was in contact with the steel shot. It is the section of the casting that included the side flange. The microstructure in the middle of the sample is shown under different magnifications and treatments in Figure 5.4.

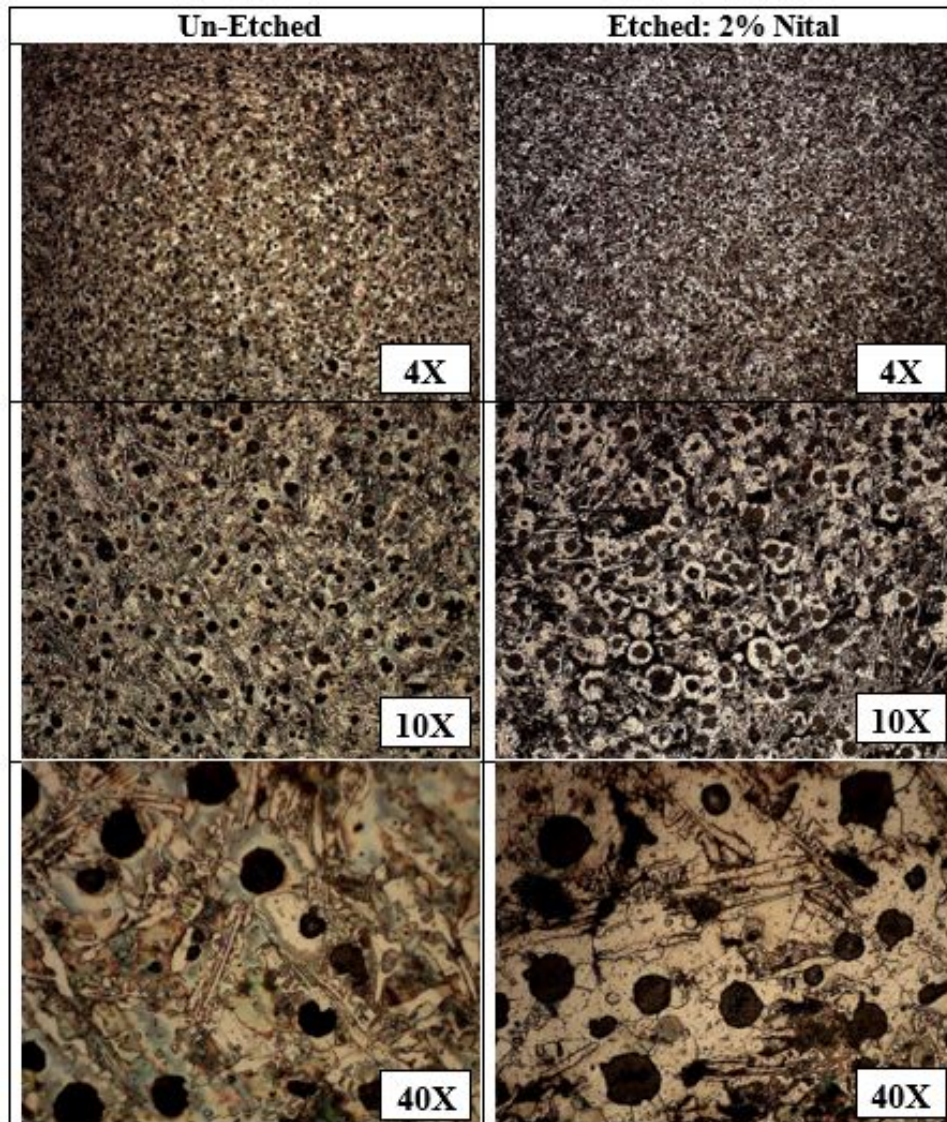


Figure 5.4: Microstructure of Sample 3 under different magnifications and treatments indicating the difference between no treatment and etching with 2% nital

A high number of nodules was visible in sample 3, indicating ductile iron. It was interesting to observe ferrite in the eutectic state. In Figure 5.5 parts of the steel shot

impregnated in the cast metal is shown. From observation, the steel shot was surrounded by a black powder. The black areas between the cast metal and the steel shot were therefore, identified as carbon residue due to the pyrolysis of the PMMA.

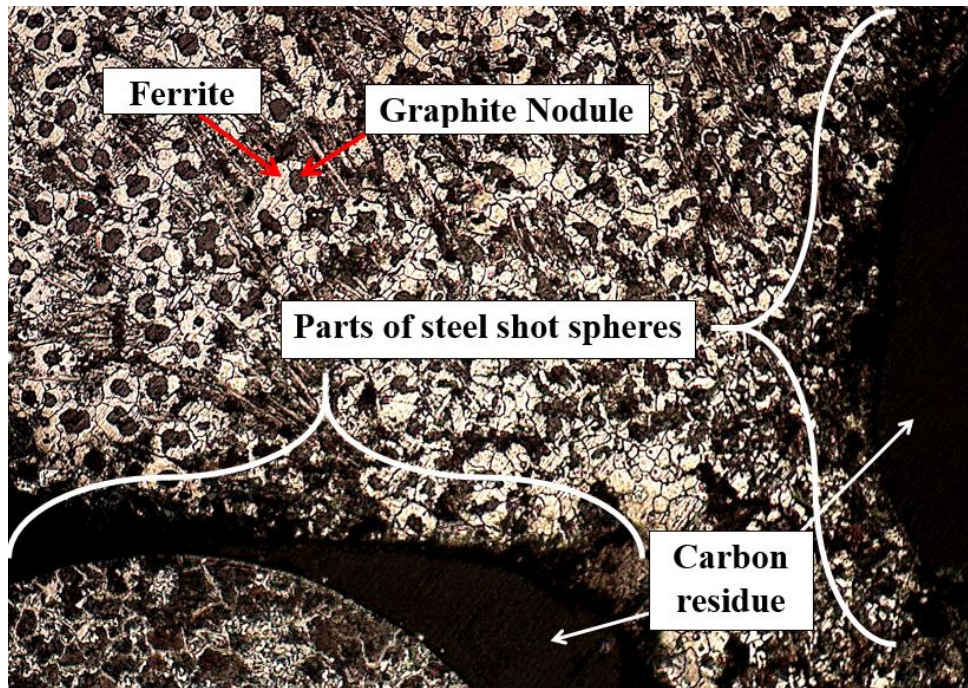


Figure 5.5: Micrograph indicating the microstructure of Sample 3 with steel shot spheres impregnated in cast metal

5.1.4 Summary

The use of a PMMA pattern in the casting of a valve body with the magnetic moulding process was unsuccessful. The casting result was not sufficient to evaluate the feasibility of the process. The following factors were identified as possible causes of an unsuccessful casting:

- Poor feeding of casting material: Feeding system not functioning properly.
- Insufficient cohesion of mould material: The Curie temperature of the steel shot was reached which causes the steel shot to lose its magnetic properties.
- Too high pouring rate: Pattern not able to degrade fast enough.

- Too low casting temperature: Temperature not high enough to degrade pattern material efficiently.
- Low thermal conductivity of 3D-printed PMMA: The low rate of thermal destruction of 3D-printed PMMA in combination with the high pouring rate and fluidity of the liquid metal causes the liquid metal to seep through the steel shot mould rather than degrading the pattern.

The feeding system did allow sufficient flow in order for the metal to penetrate the pattern. However, the liquid metal did not follow the path of the pattern, but seeped into the steel shot and formed a layer of metal on the steel shot surface.

The temperature of the mould during casting was not measured and therefore, there was no way to determine whether the Curie temperature of the steel shot was reached. It may be assumed that due to the high pouring temperature of 1400°C, it was possible that the Curie temperature was reached. However, inspection of the part of the pattern that was penetrated by the liquid metal during casting, showed that the packing of the steel shot was dense, indicating no lack in cohesion of the mould.

If a refractory coating was applied, it might have increased the possibility of a fuller casting by aiding in directing the liquid metal in the pattern and preventing leakage. However, it was suspected that a refractory coating would not have ensured a successful casting since the problem experienced with the PMMA pattern would have caused back-flow of the molten metal and prevented further pouring of metal because the pattern could not degrade fast enough at the pouring rate.

When casting molten metal manually, it is difficult to control the pouring rate. The factor of a too high pouring rate should not be a problem. It is necessary to cast the metal at a high pouring rate to prevent defects such as cold shuts. A slower pouring rate may cause the liquid metal to cool faster, resulting in lower fluidity and decreasing the effectiveness of casting. If fluidity is too low due to the low temperature of the liquid metal, the metal may solidify in the feeding system or in areas with small section thicknesses.

An even higher casting temperature may result in the faster degradation of the PMMA pattern, perhaps even gassification of the pattern. It is, however, not a viable solution to the problem experienced with the slow rate of degradation of the pattern. A casting temperature above 1400°C will result in the loss of magnesium and therefore the loss of graphite nodules, which will imply that ductile iron will not be cast. Furthermore, the advantage of cast irons is the fact that casting may be performed at much lower temperatures than steels. If the casting temperature increases, the cost of the casting increases and the advantage of lower casting temperatures is lost.

Additive manufactured PMMA has not been used in the lost-foam casting process or the magnetic moulding casting process before. All possible causes of an unsuccessful casting may be connected to the slow rate of degradation of the PMMA pattern in 3D-printed form. Even though the thermal conductivity of PMMA is slightly higher than that of EPS, the problem lies with the high bulk density of the printed PMMA. If the bulk density can be lowered to the range of EPS, which is 24kg/m³, the casting issues experienced in this procedure may be eliminated.

The increase in the number of nodules observed in Sample 2 and 3 when compared to sample 1, may be due to the fact that the part of the casting where sample 2 and 3 were obtained were in contact with the steel shot. The increased cooling rate may have lead to grain refinement, resulting in the increase in the number of nodules in the casting. However, the vermicular graphite structure observed in sample 1 may also be contributed to the slower cooling rate in the feeder because the feeder was a hotspot throughout the casting process.

The direct influence of steel shot due to its close proximity to the cast material did not result in a change in microstructure. The microstructure did not change from the edge where the material was in contact with steel shot to the middle of sample 3.

The casting material obtained from the casting with the PMMA pattern presented non-homogeneous microstructures. Due to the high concentration of nodular graphite observed, the material may be classified as low-quality ductile iron. The casting process

was, therefore, successful in obtaining ductile iron. With experience and small adjustments in the melting and casting procedure, the quality of the ductile iron may be increased.

The evaluation of the results of the casting obtained with the EPS pattern is presented in the next section.

5.2 Evaluation of EPS Pattern Casting Results

5.2.1 Microstructure

In order to accurately evaluate the mechanical properties of the samples obtained from the casting with the EPS pattern, the material had to be identified. The mechanical properties of ductile iron greatly depend on the microstructure.

A material sample was obtained from the middle of the casting, just below the sprue. The microstructure of the sample is shown in Figure 5.6.

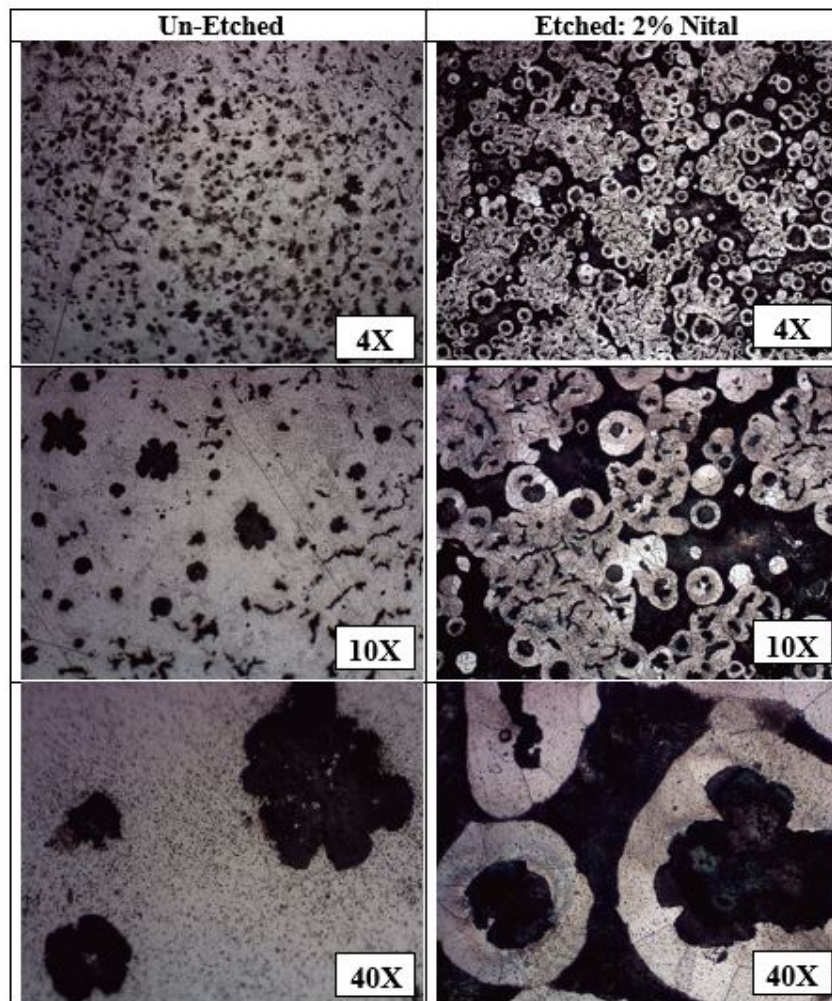


Figure 5.6: Microstructure of a material sample obtained from casting with EPS pattern, under different magnifications indicating the difference between no treatment and etching with 2% nital

Even without etching, a large number of nodules were observed. The effect of the nital etching was very evident in the micrographs of Figure 5.6. The ferrite surrounding the graphite nodules were clearly observed. A ferrite-pearlite matrix structure was identified, which implies that mechanical properties of both a ferritic and a pearlitic matrix structure was expected.

5.2.2 Tensile-Tests

Five standard tensile-test specimens were tension tested to obtain an average ultimate tensile strength and yield strength. Once the tensile strength was known, it could be compared with the values of the intended casting material properties. The ultimate tensile strength of an ASTM A395 Grade 60-40-18, is 414MPa. The tension-test results of the 5 specimens are graphically represented in Figure 5.8 and numerical values are tabulated in Table 5.1.

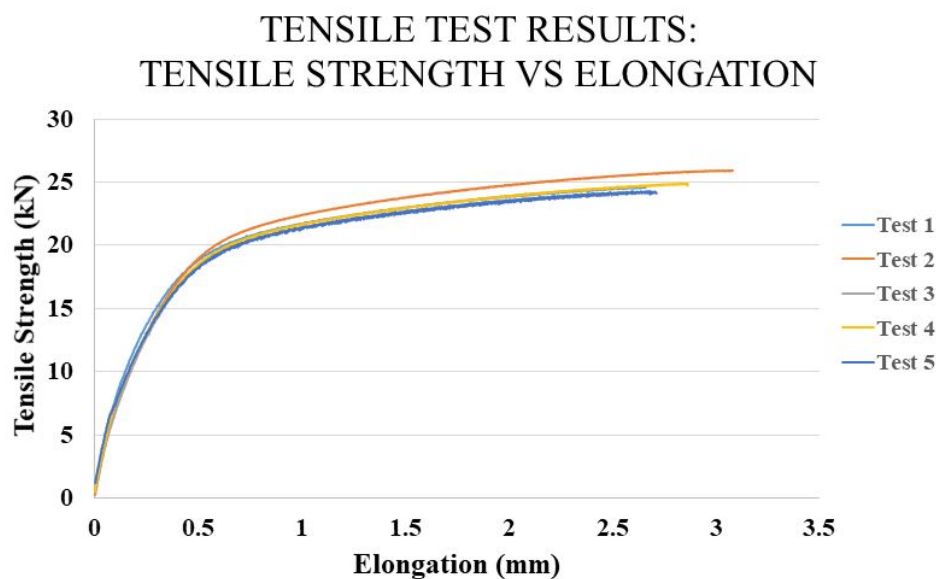


Figure 5.7: A line graph of the tensile strength versus the elongation of five tensile test specimens

Table 5.1: The tensile strength of five tension test specimens obtained from the casting with the EPS pattern

Specimen	Tensile Load [kN]	Ultimate Tensile Strength [MPa]	Yield Load [kN]	Yield Strength [MPa]
1	24.636	387.253	20.718	325.674
2	25.933	407.641	21.502	337.995
3	24.182	380.117	20.707	325.489
4	24.879	391.073	20.930	328.993
5	24.289	381.799	20.783	326.694
Average:	24.783	389.577	20.928	328.969

From Table 5.1 it was observed that the cast material had an ultimate tensile strength that was 25MPa lower than the specified material strength. The average value of the yield strength was very close to the value of the ultimate tensile strength. It was interesting to notice that although the ultimate tensile strength was lower than the specification of the material, the yield strength of the cast sample was higher than the yield strength of the required material.



Figure 5.8: Photo of the test specimens after tension tests were performed

From the evaluation of the microstructure, it was concluded that a ferritic-pearlitic matrix structure of ductile iron was obtained during casting. The quality of the ductile iron nodules were therefore not sufficient to qualify as an A395 Grade 60-40-18. With the results of the tension tests, it was established that a slightly lower grade ductile iron was obtained.

5.2.3 Charpy V-Notch Tests

Three standard Charpy V-Notch test specimens were used to perform Charpy impact tests at room temperature (20°C). The results were compared to the typical impact

energy absorbed by ductile iron specimens with different matrix structures. The graph shown in Figure 5.9 was obtained in Volume 15 of the ASM Handbook, [13].

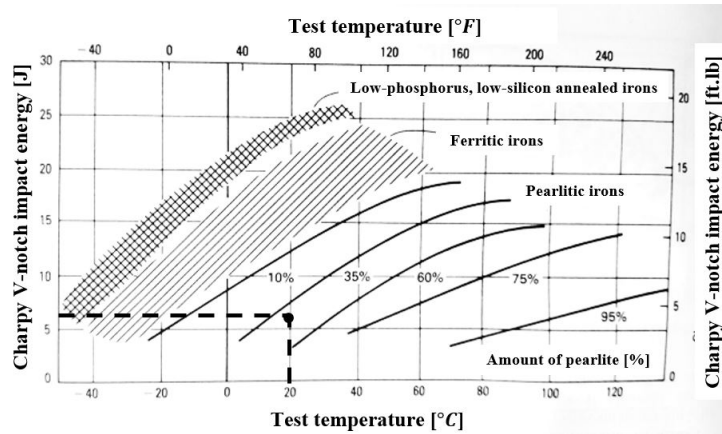


Figure 5.9: Charpy V-notch impact energy absorbed by ductile iron specimens with different matrix structures.

The average impact energy absorbed by the specimens were 6J. When the energy value and the temperature was plotted on the graph, as indicated with the dashed lines, it was observed that the energy absorbed conforms with ductile iron with a pearlite content just above 35%.

The fracture surface indicated a brittle fracture at a low impact energy. No deformation of the specimen was observed, except at the fracture surface. In Figure 5.10 the surface of one of the specimens is shown. All three specimens showed similar fracture surfaces. Figure 5.11 is a representation of the specimen after the Charpy test was performed.

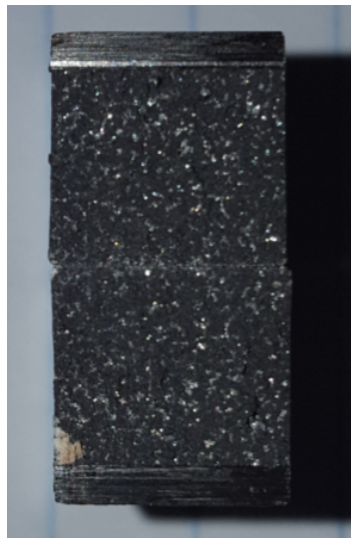


Figure 5.10: The brittle fracture surface of the fracture test performed on the material sample of the casting performed with the EPS pattern

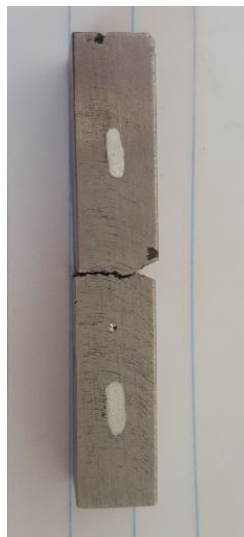


Figure 5.11: The fractured specimen indicating the line of fracture

5.2.4 Hardness

Brinell hardness tests were performed on the same specimens used for the Charpy tests. A 10mm steel ball was used with a load(P) of 1000kg. All three samples had the same diameter indent d . The hardness number was then determined as follows:

$$BHN = \frac{P}{\left(\frac{\pi D}{2}\right)(D - \sqrt{D^2 - d^2})} = \frac{1000}{\left(\frac{\pi 10}{2}\right)(10 - \sqrt{10^2 - 2.7^2})} \therefore BHN = 171.4 \quad (5.1)$$

The value obtained from the hardness tests is well within range of the hardness specified for A395 Grade 60-40-18 which has a BHN between 143 and 187.

5.2.5 Summary

The casting obtained with the EPS pattern may be classified as a successful casting for the purpose of this investigation. A fully filled casting consisting of the desired cast iron type was cast with the magnetic moulding process.

Ductile iron with a ferritic-pearlitic matrix structure was cast. The results obtained from the Charpy impact tests supported this observation by indicating the possibility of a 35% pearlitic matrix structure. Although the majority of the microstructure is ferritic, the presence of pearlite influences the mechanical properties obtained.

The ultimate tensile strength of the cast material was 25MPa lower than desired. The presence of pearlite increases the hardness and decreases the ductility of ductile iron. The observation of a lower tensile strength may be the result of the percentage pearlite present in the matrix structure causing the material to break easier under tension. The effect of pearlite is also evident in the brittle fracture and low impact energy absorbed in the Charpy tests. The high yield strength obtained is desirable and the high ferrite content of the matrix structure contributes to a higher yield strength.

The refractory coating contributed to a dimensionally accurate casting. It also prevented shot-to-metal contact which eliminates the need for finishing processes. The refractory coating does, however, limit the capabilities of the magnetic moulding process. To a certain extent, the refractory coating becomes the mould material and the steel shot serves as support material. The refractory coating creates a thermal barrier that inhibits the full utilisation of thermal characteristics that a steel shot mould offers.

The use of an EPS pattern significantly increases the ease of casting. The rate of pyrolysis is significantly faster when compared to the PMMA pattern. In the evaluation of the microstructure and the mechanical properties of the cast material, no particular influence of the EPS pattern was noticed when compared to the casting with the PMMA pattern.

Chapter 6

Summary, Conclusion and Recommendations

In this final chapter, a concise summary of the preceding chapters is provided. In the conclusion, the outcome of the feasibility of the magnetic moulding process is discussed and recommendations for future studies are presented in the last section of this chapter.

6.1 Summary

In Chapter 1, background on the current status of valve manufacturing and impeding factors experienced in the foundry industry was briefly discussed. Locally manufactured valves are up to 60% more expensive than imported valves due to inefficient manufacturing methods.

Manufacturing processes are placed under scrutiny in Chapter 2 to find methods to use less material, increase the efficiency of production and improve manufacturing techniques to lower the cost of locally manufactured products. The magnetic moulding

process is an extension of the lost-foam casting process and was selected as manufacturing method to establish the feasibility of the application of this method on the casting of a ductile iron valve.

Chapter 3 builds on the literature presented in the previous chapter. Elements of the magnetic moulding process as part of the lost-foam process are discussed in detail and establish the foundation of the process configuration.

The principles introduced in Chapter 3 were implemented in the configuration of the experimental setup in Chapter 4. Simulations performed in FEMM were used to design the electromagnet with specifications to ensure the sufficient cohesion of the mould material. The casting procedure and execution of the casting process are documented within this chapter which leads to the evaluation and discussion of the results.

The results of the castings performed for both the PMMA and EPS pattern were evaluated by means of microstructure analysis and mechanical testing in Chapter 5. The problem experienced with the thermal degradation of the PMMA pattern was summarised. Finally, the evaluation of the results leads to the conclusion where the feasibility of the magnetic moulding process is established and recommendations are proposed for future studies.

6.2 Conclusion

In the process of investigating possible methods to decrease the cost of valve bodies, the magnetic moulding process was identified. The potential of the process attributes to positively enhance the lost-foam manufacturing technique, was argued.

The complexity of the design of valve bodies, requires considerable effort to design and manufacture a mould with an efficient feeding system in traditional manufacturing methods. With the magnetic moulding process, the mould design and manufacturing step are bypassed by this process. Unlike traditional processes where sand is used

as mould material, magnetised steel shot has sufficient cohesion to enable the possibility of multiple orientations of casting positions. The absence of split lines eliminates defects associated with split lines and reduces finishing operations. It is true that steel shot is more expensive than sand used in the traditional lost-foam casting processes, but it comes with the benefits of casting flexibility and quality. When the cost of steel shot is compared to the cost of mould manufacturing equipment and the cost of the die material and design, steel shot is considerably more economical over the process life-cycle. As with sand casting and lost foam-casting, the mould material of magnetic moulding may be recycled and re-used.

The greatest attribute of this process is the ability to vary and control the microstructure of the casting material. With the magnetic moulding process, fine-grained materials may be utilised to adjust the cooling rate in various sections of the casting. Ductile iron was cast with ease with acceptable material properties. Due to the high thermal conductivity of the steel shot, the rate of cooling was favourable to the development of ductile iron.

The implication of the ability to control the microstructure of materials is the fact that castings with improved mechanical properties may be cast with this method. The increase in the mechanical properties may lead to a decrease in material usage. The section sizes may be decreased as the material properties increase.

The control of the microstructure which leads to desirable mechanical properties may result in higher quality castings with fewer defects. This implies that the yield of successful castings is higher, which also reduces material and energy costs.

Currently, the additive manufacturing of a PMMA pattern is not a viable option. The high bulk density of the additive manufactured pattern in combination with the low thermal diffusivity of PMMA contributes to the slow rate of thermal degradation of the pattern.

When considering high production volumes, additive manufacturing of patterns is uneconomical. The equipment costs, material costs, manufacturing costs and manu-

facturing hours will significantly increase the cost of manufactured products. Additive manufacturing cannot yet compete with the speed of contemporary machining equipment.

The magnetic moulding process may be fully automated which may significantly reduce labour costs and increase production volume. However, the industrialisation of the process is questionable. The up-scaling and implementation of an electromagnet suitable for a tree of castings may be very unpractical. The weight of the casting box with the steel shot and the cast components may require specialised machinery for shakeout during de-moulding. A larger electromagnet will require a stronger magnetic flux density. In a factory setup, the influence of a large-scale magnetic field may be dangerous and may complicate the process design. However, it is possible to construct electromagnetic shielding.

The cost of locally manufactured products may be reduced with the magnetic moulding process by:

- reducing the lead time by elimination of the mould design and manufacturing stage.
- reducing lead time by reducing finishing processes due to the absence of split lines.
- eliminating moulding equipment and maintenance on moulding machinery and dies.
- reduce material costs by reducing defects and giving rise to the possibility to enhance the material microstructure which leads to increased mechanical properties.
- full automation resulting in a substantial decrease in labour costs and increase in production volume.
- ease and simplicity of de-moulding increases the production rate.

Ultimately, the magnetic moulding casting process is a feasible manufacturing method with the potential to increase the affordability of locally manufactured valves if a low-density pattern material, such as EPS, is used. The magnetic moulding casting process is a viable manufacturing method with a vast amount of opportunities to increase the competitiveness of local manufacturing.

6.3 Recommendations

Various methods may be implemented to improve the magnetic moulding process. Lack of scientific information on aspects such as the mould material and heat transfer of the process, inhibits the development of this process. The magnetic moulding process has the potential to permit the casting of specialised parts requiring a specific microstructure which may not be obtained by any other manufacturing method.

The mould material which is comprised of steel shot and air is undefined in casting simulation packages. If the mould material can be simulated in software packages such as MAGMASoft®, it will significantly contribute to the development of microstructural design.

The calculation and simulation of the thermodynamic behaviour of the steel shot during the casting process will considerably increase the understanding of the cooling rate of the cast material. If the effect of the thermal conductivity of the spheres as mould material on the casting is understood, the optimal size and quantity steel shot can be determined to ensure the optimal cooling rate to obtain the desired microstructure and therefore the desired mechanical properties.

Spheres with a variation in diameter may strategically be positioned in areas to increase or decrease the cooling rate and therefore "design" of the microstructure may become possible. The use of other materials may be investigated to determine the effect on the cooling rate in the problem areas of castings.

The possibility to control the microstructure provides the opportunity for the development of shape-memory materials. By controlling the cooling rate of the cast material, different phases may coexist in the same part, which may result in shape-memory characteristics.

Exploration and investigation of additive manufacturing technologies and materials may lead to a viable alternative to lost-foam patterns. It is recommended that patterns be printed with less filling material to obtain a lower density pattern. Less material will decrease the material cost and the printing time, resulting in lower overall costs. It may also contribute to a more successful casting as there is less material to decompose and less carbon residue to be formed.

The influence of the orientation and direction of 3D-printing on the thermal degradation of a 3D-printed material, may be investigated. Directional solidification may be manipulated with alignment of the 3D-printing direction with the pouring direction. Various 3D-printing methods of deposition may increase the strength of the pattern in a specific direction. The ease of thermal degradation may be increased if the direction of 3D-printing is orientated in such a way that the strength of the pattern is low enough to speed up thermal degradation, but strong enough to avoid the collapse of the pattern. A skeleton, hollow 3D-printed part may increase the efficiency of thermal degradation and lead to less carbon residue.

A MMC may be obtained with specialised additive manufactured materials. The design of the casting material may include the absorption of fibres embedded in the additive manufacturing material during the thermal degradation of the pattern.

The Replicast manufacturing method where EPS patterns are melted out prior to casting may also be applied to the magnetic moulding process. By melting out the foam pattern prior to casting, carbon residue is reduced. It was observed that the cohesion of the magnetic mould is sufficient to maintain a geometry over a period of time, without a pattern.

Bibliography

- [1] P. Lundall, J. Maree, and S. Godfrey, "Research Report Industrial Structure and Skills in the Metals Beneficiation Sector of South Africa," Department of Labour, Cape Town, Tech. Rep., 2008. [Online]. Available: <http://www.labour.gov.za/DOL/downloads/documents/research-documents/MetalsBenification{-}DoL{-}Report.pdf>
- [2] J. T. Davies, "2nd VAMCOSA FOUNDRIES WORKSHOP," South African Foundry Industry, Tech. Rep., 2015. [Online]. Available: <http://www.foundries.org.za/wp-content/uploads/2015/02/2-John-Davies{-}Vamcosa{-}Workshop{-}20022015.pdf>
- [3] Merchantec Capital, "Industry Supply Analysis: Deliverable 1 Ferrous Metals Downstream Sector," Department of Trade and Industry, Tech. Rep., 2014. [Online]. Available: <https://solidariteit.co.za/wp-content/uploads/2017/03/Steel.Industry.Supply.Analysis.23.09.14.pdf>
- [4] Trade and Industrial Policy Strategies, "The impact of electricity price increases on the competitiveness of selected mining sector and smelting value chains in South Africa," Global Green Growth Institute, Tech. Rep., 2014. [Online]. Available: <http://www.tips.org.za/files/u72/tips{-}for{-}gggi{-}policy{-}paper{-}march{-}2015.pdf>
- [5] B. Crawford, "Power prices hit foundries hardest," *Casting SA*, vol. 13, p. 10, 2013. [Online]. Available: <http://www.metalworkingnews.info/wp-content/uploads/2013/CastingsSAFebruary2013.pdf>

-
- [6] M. Arasu and L. Rogers Jeffrey, "Energy Consumption Studies in Cast Iron Foundries," no. 57, 2009. [Online]. Available: <http://foundryinfo-india.org/images/pdf/57ifctp12.pdf>
- [7] Department of Economic Development, "International Trade Administration Commission of South Africa Amended Export Control Guidelines on the Exportation of Ferrous and Non-Ferrous Waste and Scrap," p. 5, 2014. [Online]. Available: <http://www.itac.org.za/upload/gg37992{-}nn714.pdf>
- [8] Eskom, "Valves Presentation to Industry," Eskom, Tech. Rep., 2012. [Online]. Available: <http://www.foundries.org.za/wp-content/uploads/2012/09/20120912-Valves{-}Presentation-to-VAMCOSA-Localisation-article.pdf>
- [9] Steloy Castings, "Boosting the South African valve industry," p. 24, 2013. [Online]. Available: <https://cld.bz/bookdata/FpoBncr/basic-html/page24.html>
- [10] K. Brown, "Invitation and evaluation of bids based on a stipulated minimum threshold for local production and content for valves products and actuators," Department of National Treasury, Tech. Rep., 2014. [Online]. Available: <http://www.treasury.gov.za/divisions/ocpo/sc/PracticeNotes/Instruction-ValveProductsandActuators.pdf>
- [11] J. Jooste and D. De Beer, "The role of technology and competitiveness," Tech. Rep., 2015. [Online]. Available: <http://www.foundries.org.za/wp-content/uploads/2015/02/8-Jan-Jooste{-}Role{-}of{-}Technology{-}and{-}Competitiveness{-}20022015.pdf>
- [12] J. Davies, "The Impact of IPAP on the Foundry Industry," 2015. [Online]. Available: <https://www.thedti.gov.za/parliament/2015/SAIF.pdf>
- [13] ASM International, *ASM Handbook: Volume 15 Casting*, 3rd ed. ASM International, 2013.
- [14] B. Nesbitt, *Handbook of Valves and Actuators: Valves Manual International*, 1st ed. Elsevier Science, 2007. [Online]. Available: <https://ebookcentral-proquest-com.nwulib.nwu.ac.za/lib/northwu-ebooks/reader.action?docID=330155>

-
- [15] W. Sölken, "Introduction to Valves," 2008. [Online]. Available: www.wermac.org/valves/valves{-}general.html
- [16] J. S. Santner and G. M. Goodrich, "Iron Alloys," *Casting source directory engineered casting solutions*, p. 18, 2006. [Online]. Available: <http://www.afsinc.org/files/images/ironalloys.pdf>
- [17] D. R. Askeland, P. P. Fulay, and W. J. Wright, *The Science and Engineering of Materials*, 6th ed. Stamford: Cengage Learning, 2011.
- [18] ASM International, *Cast Irons*, J. Davis, Ed. ASM International, 1996.
- [19] S. Kalpakjian and S. R. Schmid, *Manufacturing Engineering and Technology*, seven ed. Singapore: Pearson, 2014.
- [20] I. Riposan, M. Chisamera, M. Barstow, and R. L. Naro, "Magnesium-Sulfur Relationships in Ductile and Compacted Graphite Cast Irons as Influenced by Late Sulfur Additions," *AFS Transactions*, vol. 111, no. 03-093, p. 1, 2003. [Online]. Available: <http://asi-alloys.com/pdf/NewadditivesandmethodsfortheManufactureofCGiron.pdf>
- [21] M. Hawryluk, "Review of selected methods of increasing the life of forging tools in hot die forging processes," *Archives of Civil and Mechanical Engineering*, vol. 16, no. 4, pp. 845–866, 2016. [Online]. Available: <http://www.sciencedirect.com.nwulib.nwu.ac.za/science/article/pii/S1644966516300486>
- [22] G. Johnson, "Forgings: Higher Quality with a Cost," 2015. [Online]. Available: <http://www.valvemagazine.com/magazine/sections/beyond-valves/6609-forgings-higher-quality-with-a-cost.html>
- [23] M. Upadhyay, T. Sivarupan, and M. El Mansori, "Optimisation of Additive Manufactured Sand Printed Mould Material for Aluminium Castings," *Procedia Manufacturing*, vol. 11, pp. 457–465, jan 2017. [Online]. Available: <http://www.sciencedirect.com.nwulib.nwu.ac.za/science/article/pii/S2351978917303402>

-
- [24] P.-m. Geffroy, E. Beaunon, M. Lakehal, and J. Go, "Journal of Materials Processing Technology Thermal and mechanical behaviour of grey cast iron and ductile iron castings using magnetic molding and lost foam processes," vol. 209, pp. 4103–4111, 2009.
- [25] J. Goni, "The innovative casting process for the improvement of the competitiveness and working conditions of the European foundries," Tech. Rep., 2004.
- [26] K. J. Suganth, S. Senthilkumaran, S. R. Boopathy, and A. Ramesh, "Theoretical and experimental investigation of mold strength in magnetic molding compacts," *Journal of Materials Processing Technology*, vol. 5, no. 205, pp. 235–242, 2007.
- [27] T. Pacyniak, "The effect of refractory coating permeability on the Lost Foam Process," *Archives of Foundry Engineering*, vol. 8, no. 3, pp. 199–204, 2008.
- [28] C. Mendonsa and V. D. Shenoy, "Additive Manufacturing Technique in Pattern making for Metal Casting using Fused Filament Fabrication Printer," *Journal of Basic and Applied Engineering Research Print*, vol. 1, no. 1, pp. 2350–77, 2014. [Online]. Available: <http://www.krishisanskriti.org/jbaer.html>
- [29] E. Olkhovik, A. A. Butsanets, and A. A. Ageeva, "Use of additive technologies for practical working with complex models for foundry technologies," *IOP Conference Series: Material Science and Engineering*, vol. 140, no. 012013, p. 1, 2016. [Online]. Available: <http://www.krishisanskriti.org/jbaer.html>
- [30] M. Sands and S. Shivkumar, "EPS bead fusion effects on fold defect formation in lost foam casting of aluminum alloys," *Department of Mechanical Engineering, Worcester Polytechnic Institute*, vol. 1, no. 3, pp. 3–2, 2006. [Online]. Available: <https://link.springer.com/content/pdf/10.1007/s10853-006-7077-7.pdf>
- [31] K. Siavashi, "The Effect of Casting Parameters on the Fluidity and Porosity of Aluminium Alloys in the Lost Foam Casting Process," Ph.D. dissertation, University of Birmingham, 2011. [Online]. Available: http://etheses.bham.ac.uk/3525/2/Siavashi_{-}12_{-}PhD.pdf

-
- [32] H. Wenhao, Y. Shengping, and H. Xiaohong, "Development, application and Problem of Ductile Iron in Lost Foam Casting Technology in China," *China Foundry*, p. 315, 2010. [Online]. Available: <http://www.foundryworld.com/uploadfile/2010112329937923.pdf>
- [33] L. Trumbulovic, S. Panic, Z. Acimovic, and I. Belic, "New casting coatings," in *BMC*, no. Figure 1, Belgrade, 2003, pp. 295–299.
- [34] Z. Acimovic-Pavlovic, A. Terzi, L. Andri, and M. Pavlovi, "Comparison of refractory coatings based on talc, cordierite, zircon and mullite fillers for lost foam casting," *Materials and technology*, vol. 49, no. 1, pp. 157–164, 2015.
- [35] C. Sadik, I.-e. E. Amrani, and A. Albizane, "Journal of Asian Ceramic Societies Recent advances in silica-alumina refractory : A review," *Journal of Asian Ceramic Societies*, vol. 2, no. 2, pp. 83–96, 2014. [Online]. Available: <http://dx.doi.org/10.1016/j.jascer.2014.03.001>
- [36] H. Schneider, J. Schreuer, and B. Hildmann, "Structure and properties of mullite A review," *Journal of the European Ceramic Society*, vol. 28, pp. 329–344, 2008.
- [37] B. S. Guru and H. Hiziroglu, *Electric Machinery and Transformers*, 3rd ed. New York: Oxford University Press, 2001.
- [38] S. Louw, "Feasibility of particle reinforcement in the casting of a ductile iron gate valve," North-West University, Potchefstroom, Tech. Rep., 2017.

Appendix A

Cast Irons

The specifications, applications and characteristics of various cast irons [16].

Gray Iron	<p>Standard Specifications</p> <ul style="list-style-type: none"> • ASTM A48: gray iron castings • ASTM A74: cast iron soil & pipe fittings • ASTM A126: gray iron castings for valves, flanges & pipe fittings • ASTM A159: automotive gray iron castings • SAE J431: automotive gray iron castings • ASTM A278 & ASME SA278: gray iron castings for pressure-containing parts for temperatures up to 650F (343C) • ASTM A319: gray iron castings for elevated temperatures for non-pressure-containing parts • ASTM A823: statically cast permanent mold castings • ASTM A834: common requirements for iron castings for general industrial use 	<p>Characteristics</p> <p>Several strength grades; vibration damping; low rate of thermal expansion & resistance to thermal fatigue; lubrication retention; and good machinability.</p>	<p>Applications</p> <p>Automobile engine blocks & heads; manifolds for internal combustion engines; gas burners; machine tool bases; dimensionally stable tooling subjected to temperature variations, such as gear blanks & forming die covers; cylinder liners for internal combustion engines; intake manifolds; soil pipes; counterweights; and enclosures & housings.</p>
Ductile Iron	<p>Standard Specifications</p> <ul style="list-style-type: none"> • ASTM A395 & ASME SA395: ferritic ductile iron pressure-retaining castings for use at elevated temperatures • ASTM A439: austenitic ductile iron castings • ASTM A476 & ASME SA476: ductile iron castings for paper mill dryer rolls • ASTM A536 & SAE J434: ductile iron castings • ASTM A571 & ASME SA571: austenitic ductile iron castings for pressure-containing parts suitable for low-temperature service • ASTM A874: ferritic ductile iron castings suitable for low-temperature service • ASTM A897: austempered ductile iron castings 	<p>Characteristics</p> <p>Several grades for both strength & ductility; high strength, ductility & wear resistance; contact fatigue resistance; ability to withstand thermal cycling; and production of fracture-critical components.</p>	<p>Applications</p> <p>Steering knuckles; plow shares; gears; automotive & truck suspension components; brake components; valves; pumps; linkages; hydraulic components; and wind turbine housings.</p>
CGI	<p>Standard Specifications</p> <ul style="list-style-type: none"> • ASTM A842: CGI castings 	<p>Characteristics</p> <p>A compromise of properties between gray & ductile iron.</p>	<p>Applications</p> <p>Diesel engine blocks & frames; cylinder liners; brake discs for trains; power generators; exhaust manifolds; pump housings; and brackets.</p>
White Iron	<p>Standard Specifications</p> <ul style="list-style-type: none"> • ASTM A532: abrasion-resistant white iron castings 	<p>Characteristics</p> <p>Extremely hard & wear-resistant.</p>	<p>Applications</p> <p>Crushing & grinding applications; and grinding balls.</p>
Malleable Iron	<p>Standard Specifications</p> <ul style="list-style-type: none"> • ASTM A47 & ASME SA47: ferritic malleable iron castings • ASTM A197: cupola malleable iron • ASTM A220: pearlitic malleable iron • ASTM A338: malleable iron flanges, pipe fittings & valve parts for railroad, marine & other heavy-duty service up to 650F (343C) • ASTM A602 & SAE J158: automotive malleable iron castings 	<p>Characteristics</p> <p>Soft & extremely ductile.</p>	<p>Applications</p> <p>Chains; sprockets; tool parts & hardware; connecting rods; drive train & axle components; and spring suspensions.</p>
Alloyed Iron	<p>Standard Specifications</p> <ul style="list-style-type: none"> • ASTM A436: austenitic gray iron castings • ASTM A518: corrosion-resistant high-silicon iron castings 	<p>Characteristics</p> <p>Corrosion resistant; retains strength & dimensions during elevated-temperature exposure; and ability to withstand thermal cycling.</p>	<p>Applications</p> <p>Parts for chemical processing plants; petroleum refining; food handling & marine service; control of corrosive fluids; and pressure valves.</p>

Figure A.1: Specifications and characteristics associated with cast irons

Appendix B

Electromagnet Drawings

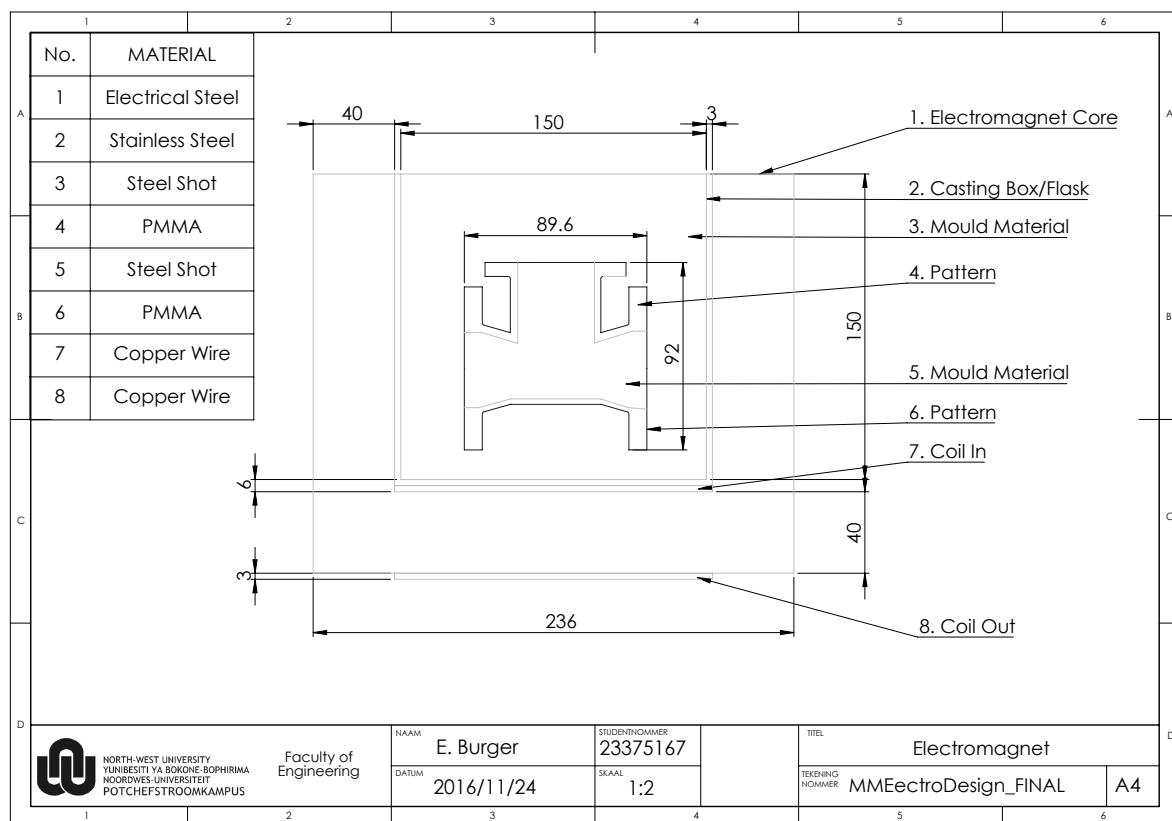


Figure B.1: Dimensions (in mm) and materials used in the final electromagnet FEMM design



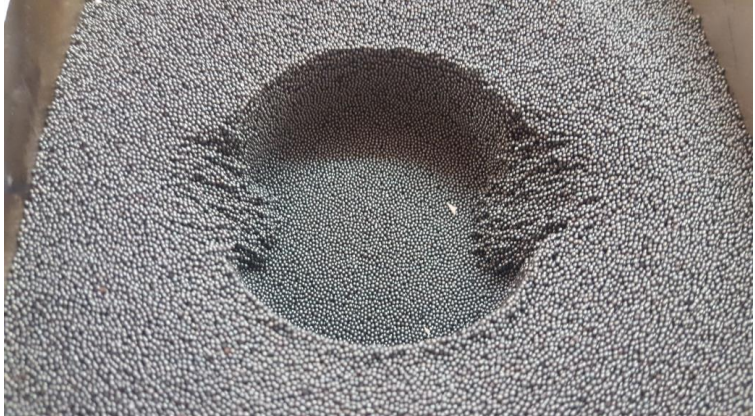
Appendix C




Steel Shot Characteristics


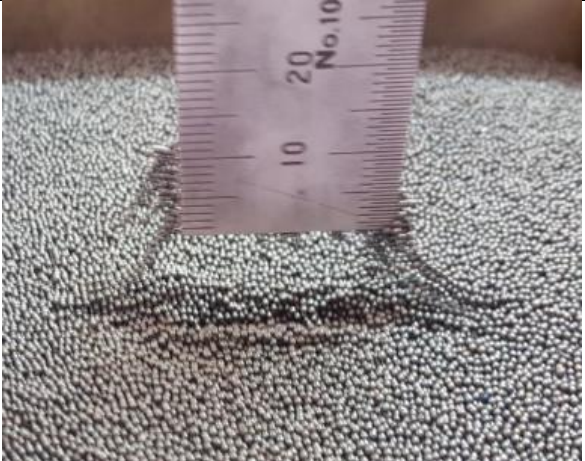
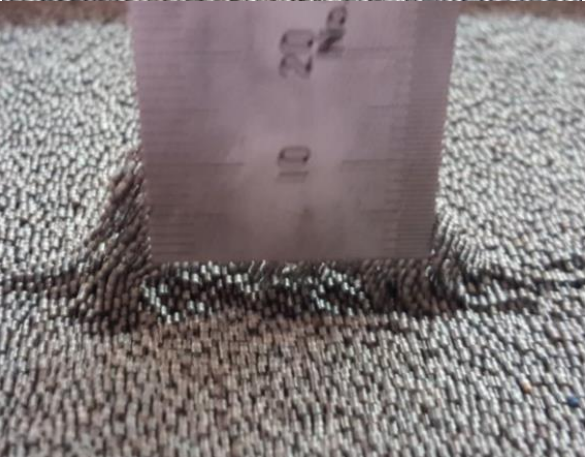
The steel shot cohesion increase with an increase in current. There is a drastic increase in cohesion from 3A to 4A. A teflon cup was placed in the steel shot and the magnetic field was switched on. The electromagnet was then adjusted to a specific current and a photo of the steel shot behaviour was taken. In Figure C.1 the position of the cup is shown. A steel ruler was place in the steel shot and removed slowly to observe the behaviour of the steel shot.



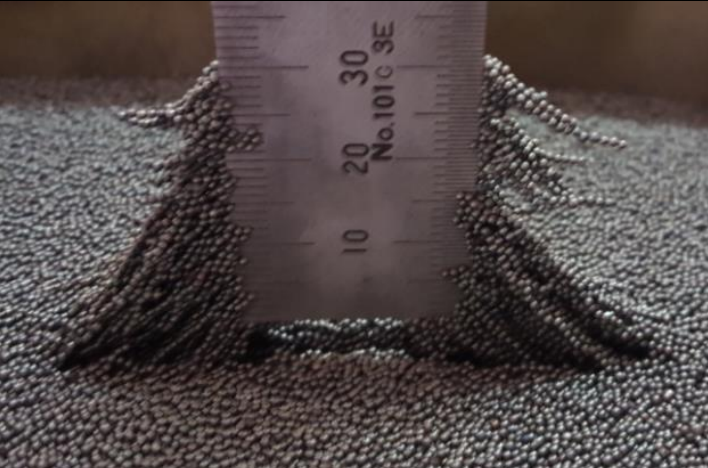


Figure C.1: Position of teflon cup placed in steel shot

Current	Steel Shot Behaviour
1A	 A photograph showing a surface of fine steel shot. A small, shallow, roughly circular crater is visible in the center, with some darker, more compacted material around its edges.
2A	 A photograph showing a surface of fine steel shot. A larger, deeper, and more circular crater is visible in the center, with a distinct rim and a darker, more compacted interior.
3A	 A photograph showing a surface of fine steel shot. A large, deep, and circular crater is visible in the center, with a very distinct rim and a dark, compacted interior.

Current	Steel Shot Behaviour
4A	 A circular steel shot particle is shown against a background of smaller steel shot particles. The particle has a dark, textured surface with some irregularities and a slightly irregular shape.
5A	 A circular steel shot particle is shown against a background of smaller steel shot particles. The particle has a dark, textured surface and a more uniform, spherical shape compared to the 4A particle.
6A	 A circular steel shot particle is shown against a background of smaller steel shot particles. The particle has a dark, textured surface and a very uniform, spherical shape.

Current	Steel Shot Behaviour
1A	 A photograph showing a layer of grey steel shot. A white ruler is placed vertically in the center. The ruler has markings for 10 and 20, and the text 'No. 10' is visible. A very shallow, narrow indentation is visible in the shot directly beneath the ruler's tip.
2A	 A photograph showing a layer of grey steel shot. A white ruler is placed vertically in the center. The ruler has markings for 10 and 20, and the text 'No. 10' is visible. A wider and deeper indentation is visible in the shot directly beneath the ruler's tip compared to the 1A case.
3A	 A photograph showing a layer of grey steel shot. A white ruler is placed vertically in the center. The ruler has markings for 10 and 20, and the text 'No. 10' is visible. A very wide and deep indentation is visible in the shot directly beneath the ruler's tip, showing significant displacement of the shot particles.

Current	Steel Shot Behaviour
4A	 A photograph showing a layer of steel shot on a surface. A ruler is placed vertically over the shot, with the 10, 20, and 30 mm marks visible. The shot is piled up on either side of the ruler, forming a central depression. The ruler is marked "No. 101103".
5A	 A photograph showing a layer of steel shot on a surface. A ruler is placed vertically over the shot, with the 10, 20, and 30 mm marks visible. The shot is piled up on either side of the ruler, forming a central depression. The ruler is marked "No. 101103".
6A	 A photograph showing a layer of steel shot on a surface. A ruler is placed vertically over the shot, with the 10, 20, and 30 mm marks visible. The shot is piled up on either side of the ruler, forming a central depression. The ruler is marked "No. 101103E".

Appendix D

Safety

Electrical Shock

HAZARD	PRECAUTION
<p>The copper coil is covered in a thin layer of isolation material which can handle temperatures up to 160°C. The isolation layer may easily be damaged by sharp edges or objects. Damage of the isolation layer may cause a short within the circuit. If a person is in contact with the wire or the electromagnet, the person may complete the circuit and suffer an electrical shock.</p> <p>Due to the low melting temperature of the isolation material, the isolation material may melt due to high temperatures. High temperature may be caused by currents exceeding the maximum capacity of the copper wire. High temperatures may also be caused by other sources such as molten metal. Once the isolation layer melts, the wires of the coil will come into direct contact with one another and also cause an electrical short within the circuit.</p> <p>The isolation layer at the ends of the coil is removed to ensure contact with the alligator clips. If the power supply is switched on and a person is in contact with the uninsulated wire, a short may occur.</p>	<ul style="list-style-type: none">- Prior to handling any part of the electromagnet, test for shorts within the circuit.- As a general rule, do not touch any part of the electromagnet while the power supply is switched on.- Never exceed a maximum current of 6A for longer than 60 seconds.- Ensure that air flow over one side of the coil is never obstructed.- Keep heat sources away from the copper coil as far as possible.- If heat sources are placed in close proximity of the coil and cannot be prevented, use a fan to cool the coil or lower the room temperature if possible by means of air ventilation or air conditioning.- Do not touch the ends of the coil if the power supply is switched on.

Heavy Objects

HAZARD	PRECAUTION
<p>The electromagnet and coil weigh 30kg. If dropped or if the electromagnet falls it may cause severe damage to human limbs and other objects in the environment it is in.</p>	<ul style="list-style-type: none">- Care should be taken whilst handling the electromagnet to prevent injury or damage to property.- No person with back or knee injuries should carry the electromagnet.- Ensure that there are no obstacles in the way if the electromagnet is carried to another position.- Do not place electromagnet close to an edge where it may fall off or be caused

	to fall due to vibrations of other machines.
--	--

Cuts

HAZARD	PRECAUTION
The electromagnet consists of 300 0.5mm silicon steel plates stacked together in a U-shape. The square edges of the electromagnet are very sharp and may cause severe cuts and bruising.	<ul style="list-style-type: none"> - Use protective gloves when handling the electromagnet. - Avoid touching the edges of the electromagnet.

Burns

HAZARD	PRECAUTION
The ductile cast iron will be cast at 1400°C which is well above most material melting points. The molten metal itself is a burning hazard, but the radiation of the molten metal and the heat of the furnace itself should also be considered. Once the metal is cast, the mould material temperature will also remain high as well as the temperature of the casting box.	<ul style="list-style-type: none"> - Always wear protective clothing when handling the molten metal. - Always ensure that protective trousers cover shoes, in order to prevent molten metal entering the shoe at the ankles. - Always use a ladle with an extension of at least 500mm.

Fumes

HAZARD	PRECAUTION
The molten metal will cause the gasification of the PMMA pattern. The degradation of the PMMA will result in carbon dioxide fumes with a strong, unpleasant smell. It is not listed as a toxic material, but precautionary steps will ensure the health of persons in contact with the fumes.	<ul style="list-style-type: none"> - Ensure that the room where casting takes place is well ventilated. - Wear a gas mask to prevent inhalation of fumes.